NOVEL MIG-7 EXPRESSION INCREASES TUMOR CELL INVASION AND TUMOR

PROGRESSION

By

AARON PETTY

A thesis submitted in partial fulfillment of
the requirements for the degree of

MASTER OF SCIENCE IN GENETICS AND CELL BIOLOGY

WASHINGTON STATE UNIVERSITY
School of Molecular Biosciences
May 2008

To the Faculty of Washington State University:

The members of the Committee appointed to examine the thesis of

AARON PETTY find it satisfactory and recommend that it be accepted.

_____

Chair

_____

_____

_____

ACKNOWLEDGEMENTS

NOVEL MIG-7 EXPRESSION INCREASES TUMOR CELL INVASION AND TUMOR

PROGRESSION

Abstract

By Aaron Petty, M.S.
Washington State University
May 2008

Chair: Kathryn E. Meier

Tumor cell spread by invasion and metastasis is a primary cause of death and post-treatment disease recurrence in cancer and requires complex interactions with the surrounding tumor microenvironment. Therefore, in order to better target cancer spread and mortality, factors specific to these interactions and tumor cell invasion must be identified. We have identified a novel gene expression, Mig-7, which results from the cross-talk between interaction of Hepatocyte growth factor (HGF), a microenvironment growth factor, with c-Met receptor and $\alpha v\beta 5$ integrin signaling. Importantly, Mig-7 expression is specific to cancer cells and tissues in studies to date. The only normal cells to date that express Mig-7 are fetal cytotrophoblast cells (CTBs), which behave similarly to invasive cancer cells. Based on this link, the present studies were undertaken to determine whether Mig-7 expression plays a role in tumor cell invasion, as well as in vasculogenic mimicry and primary tumor growth, processes linked to invasion. Our studies demonstrate that reduction of Mig-7 expression and function by siRNA knockdown in RL95 endometrial carcinoma cells and by antibody treatment in HEC1A endometrial carcinoma cells, respectively, resulted in decreased invasion, as

well as decreased activation of the membrane type-1 matrix metalloproteinase (MT1-MMP). Mig-7 expression knockdown by siRNA also decreased initial primary tumor growth and activation of ERK1/2, Akt, and S6K signaling kinase. In addition, Mig-7 expression, in response to the microenvironment, resulted in increased cleavage of laminin 5 γ2 chain promigratory fragments, important for invasion, as well as in decreased tumor cell adhesion to laminins of the basement membrane. Mig-7 expression in melanoma cells was limited to aggressive cells capable of vasculogenic mimicry, and overexpression in human HT29 colon carcinoma cells resulted in formation of vessel-like structures in 3D cultures. Mouse models revealed that Mig-7 expression colocalized with endothelial cell markers to small, abnormal vessel-like structures in lymph nodes of nude mice injected with human RL95 and HEC1A cell lines. Taken together, these results suggest that Mig-7 expression plays an important role in tumor cell invasion in a tumor microenvironment-dependent manner, and may be involved in primary tumor growth and the process of vasculogenic mimicry.

TABLE OF CONTENTS

3. TARGETING MIG-7 INHIBITS CARCINOMA CELL INVASION, PRIMARY TUMOR GROWTH, AND STIMULATES KILLING OF BREAST CARCINOMA CELLS……………………………………………………………85

4. CONCLUSIONS AND FUTURE DIRECTIONS

LIST OF TABLES

CHAPTER TWO

LIST OF FIGURES

CHAPTER TWO

CHAPTER THREE

ATTRIBUTIONS

Chapter two is in the format of the *American Journal of Pathology*, as this is where it was published. The majority of the writing was done by Dr. J. Suzanne Lindsey, with assistance from myself. All of the data from analyses with RL95 siRNA expressing cells and melanoma cells was produced by myself, as well as the placenta basal plate Mig-7 Western blot. Kiera Garman produced all of the immunohistochemistry data in the paper. Virginia Winn provided the placenta samples and produced the mRNA and protein expression data with the cytotrophoblast cells on Matrigel. Celee Spidel produced the Mig-7 Northern blot data of RL95 cells treated with HGF and EGF. The remaining data were produced by Dr. J. Suzanne Lindsey.

Chapter three is in the format of the journal *Molecular Cancer Therapeutics*, as this is where it was submitted. The manuscript was written mainly by myself, with assistance from my adviser, Dr. J. Suzanne Lindsey. Data from analyses with RL95 siRNA expressing cells, as well as the flow cytometry data, were produced by myself. Michelle Yenderrozos produced the data from invasion analysis with HEC1A cells. Drs. Stephen Wright and Kathleen Rewers-Felkins produced the data from the analysis of monocyte killing of MCF-7 cells. Dr. Beth Vorderstrasse provided a great deal of assistance to me in collection and analysis of my flow cytometry data. The remaining data were produced by Dr. J. Suzanne Lindsey.

Chapter 1

INTRODUCTION

1.1 Tumor progression and the microenvironment

Cancer is currently one of the leading causes of death in the U.S. and is a very complex disease. The major cause of death is the spread of primary tumor cells to distant secondary sites through the lymphatic system or the bloodstream, a process called metastasis. Although previous work has uncovered broad mechanisms for cancer cell invasion leading to tumor progression and spread, more work must be done to further determine tumor cell-specific mechanisms if better, more effective therapies are to be developed.

The metastatic process is very complex and is considered to consist of four main steps (reviewed in [1]). First, in epithelial derived cancers, cells from the primary tumor detach and invade through their anchoring basement membrane, primarily comprised of laminins. Based on different theories, carcinoma cells either acquire or already inherently possess the capability to degrade and recognize revealed epitopes on extracellular matrix (ECM) proteins in concert with surrounding stroma cells. This leads to carcinoma cell invasion locally and into the blood as well as lymphatic vessels, a process termed intravasation. In the second step, carcinoma cells travel through the bloodstream or lymphatics, during which they survive shear force and lack of contact with ECM, to distant sites. The third step is thought to comprise of attachment or entrapment by formation of an emboli of tumor cells in the vessel and invasion into the

nearby tissue, termed extravasation. Finally, the tumor cells must survive at the new site and begin growing, resulting in a secondary tumor. Each of these stages results from known and unknown signaling pathway crosstalk and carcinoma cell-cell, as well as cell-ECM, interactions, which need to be further elucidated so that we can make a significant therapeutic impact on this disease.

One of the limiting steps to the metastatic process is the initial invasion of primary tumor cells through their surrounding tissue and into the blood and lymphatics. Local invasion may also contribute to primary tumor growth by expanding the area of growth until the tumor reaches a size beyond the capacity of its vasculature. Cellular invasion results from a complex set of interactions with the local tumor microenvironment, which consists of multiple tissue and cell types, including ECM proteins, stromal fibroblasts, and endothelial as well as immune cells [2]. Interactions with stromal cells and the surrounding tissue result in the transition of cells to a more invasive, metastatic phenotype, termed the epithelial-to-mesenchymal transition (EMT) (reviewed in [3,4]). However, there is debate as to whether these changes are transiently effected by these interactions, or specific subpopulations already exist in the primary tumor that are capable of metastasis, termed clonal selection [5,6]. The newer cancer stem cell theory posits that "plastic" tumor cells exist from tumor conception that are capable of metastasis, unlimited growth and differentiation [7]. Furthermore, some tumor cells that are invasive can mimic fibroblast cells, a process called epithelial-to-mesenchymal transition [8], or endothelial cells, a process called vasculogenic mimicry [9]. Due to the involvement of these processes with growth factors, ECM, and metalloproteinases, tumor microenvironment research for cancer treatment and

2

metastasis suppression is underway [2]. A major set of interactions involved in this process are those of various growth factors with their corresponding receptors. Some of the well-studied growth factors in this process include hepatocyte growth factor (HGF), insulin-like growth factor (IGF), epidermal growth factor (EGF), and fibroblast growth factor (FGF), among others. The binding of these various factors to their corresponding receptor tyrosine kinases (RTKs) on the tumor cells results in signaling leading to pleiotropic effects, such as differentiation, migration, invasion, proliferation, and survival [10-13]. In addition, growth factors and cytokines, such as interleukins and interferons, can be secreted by the tumor cells and bind receptors on surrounding stromal cells, resulting in their activation. Stromal cells can then secrete proteases and factors that act on tumor cells to stimulate their migration and invasion [14]. Thus, tumor cells can cooperate with and depend on the microenvironment for escape from the primary site.

Another set of interactions involved in tumor cell migration and invasion are those of the integrin class of adhesion molecules (reviewed in [15-17]). These molecules are heterodimeric membrane glycoproteins that each consist of an alpha and beta subunit, which combine to form 24 different known integrins. Integrins interact with the ECM and send signals into the cell, resulting in changes in the cytoskeleton, adhesion, proliferation, and survival [16]. Integrins can also be activated from within the cell, usually by downstream RTK signaling, causing a conformational change resulting in recognition of various components of the ECM [18-21]. Upon activation, these integrins form clusters, called focal adhesions, which link the integrins to the cytoskeleton. These focal adhesions can associate with and activate focal adhesion kinase (FAK), which

can, in turn, activate components of other signaling pathways, such as the Ras-ERK and PI3 kinase pathways, resulting in various effects [22]. Integrin-induced changes in tumor cell adhesion and cytoskeletal distribution results in increased migration of the cell.

The interactions of RTK and integrin signaling pathways are important for migration and invasion. Signaling from these components can converge downstream into a single pathway, such as the Ras-Raf-ERK pathway [23]. Thus, signaling from one component may require signaling from the other. An example of this convergent signaling can be seen in embryonic and fetal cytotrophoblast cells (CTBs). These cells have been compared to cancer cells in their behaviors for over one hundred years [24,25] because they invade into the maternal decidua and remodel the maternal vessels during placental development. Convergence of signaling from both HGF/SF interaction with its receptor, c-Met, and activation of αvβ5 integrin is required for invasion and remodeling by these cells [26,27]. In addition to this convergence, one signaling system, may also regulate the other by changing its expression or activation. Integrins can alter the expression and phosphorylation of growth factor receptors, while growth factor receptors can, in turn, alter the expression, post-translational modification, and activation of integrin receptors [23].

In order for cancer cells to effectively invade through their surrounding environment, an array of proteases must be activated to digest the surrounding tissue. This also reveals epitopes on extracellular matrix proteins that enhances signaling and invasion [28-31]. In studies to date, some of the most important proteases involved in this process are the matrix metalloproteinases (MMPs), which require zinc binding for

their activity and have been found to be upregulated in most types of cancer (reviewed in [32,33]). These are a family of endopeptidases that can cleave various components of the ECM and basement membranes.   This family of enzymes contains both membrane-bound and secreted proteases. They largely exist as inactive proenzymes, called zymogens, and are held in this inactive state by interaction of a cysteine sulfhydryl group in the prodomain with the Zn^{2+} ion in the catalytic domain.   Disruption of this interaction makes the Zn^{2+} ion readily available for catalysis and can occur by a variety of methods [34].   These methods include activation by proteases, such as trypsin [35], conformational perturbants, such as sodium dodecyl sulfate (SDS) [36], organomercurials [35], oxidants [37], disulfide compounds, such as glutathione [38], sulfhydryl alkylating agents [39], and free thiol groups [40].

Cleavage of ECM components by MMPs results in various cell behaviors related to cancer, including altered cell growth, migration, invasion, apoptosis, as well as tumor angiogenesis [32,33].   ECM and basement membrane digestion by MMPs not only creates a path for the cell to escape from the primary site, but the resulting cleaved ECM proteins can also alter signalling in the cancer cells, resulting in different behaviors most likely due to the different integrins involved and their resulting signaling pathways. Cleaved ECM proteins can be recognized by integrins on the cell surface, causing activation and changes in adhesion and migration, as well as other behaviors [17].   In some cases, MMPs can cleave ECM proteins that are bound to latent growth factors, such as EGF and TGFβ [41], thereby releasing these growth factors that allows binding to their receptors and signaling. MMPs can also cleave adhesion molecules, such as E-cadherin, resulting in release of cell-cell and cell-matrix contacts causing resulting

signaling, such as β-catenin nuclear localization [42-44]. Finally, digestion of these ECM proteins can result in new functional fragments [28,29,31,45]. One common example of this is the cleavage of laminin 5, an abundant component of the basement membrane and ECM that exists as a heterotrimer consisting of α3, β3, and γ2 subunits. MMP-2 is initially activated by a protein complex consisting of membrane-type 1 MMP (MT1-MMP), tissue inhibitor of matrix metalloproteinase-2 (TIMP-2) and MMP-2 [46-48]. Laminin 5 interacts with this complex and both MMP-2 and MT1-MMP can cleave the γ2 chain into promigratory fragments containing cryptic sites [49-51]. One new cysteine-rich fragment, the domain III (DIII) fragment, contains EGF-like repeats and can bind the EGF receptor, stimulating migration and invasion of the cell [52].

While all of these processes and interactions are important for cancer cell migration and invasion, they also are known to play roles in normal cell functions as well. MMPs, while overexpressed and deregulated in cancer cells, are known to play roles in normal wound healing, morphogenesis, and tissue remodeling [33]. Similarly, growth factors and RTKs, such as HGF/SF and c-Met, are overexpressed in cancer cells, but play roles in normal cell functions as well [53-56]. Therefore, in order to effectively target invasion and metastasis, new cancer cell-specific molecules that are involved in these processes must be identified and validated.

1.2 Vasculogenic mimicry

Aggressive, highly invasive tumor cells, also have the ability to form vessel-like structures both *in vitro and in* vivo, a process termed vasculogenic mimicry [9,57]. This process has been observed in multiple types of tumors, including ovarian carcinoma,

Ewing sarcoma, uveal melanoma, and hepatocarcinoma [9,58-60], but has been well characterized in melanoma cells *in vitro* and *in vivo*. Vessels rich in ECM, particularly laminins, are lined predominately by tumor, rather than endothelial, cells in the interior, more hypoxic, region of the tumor [9,61]. Formation of these structures also seems to correlate with poor patient outcome [57,58], and these vessels seem to be resistant to current anti-angiogenic [62] and anti-proliferation [63] therapies. Tumor cells undergoing this process are plastic and form these tubular patterns that are capable of conducting plasma and red blood cells. Genetic dysregulation of these cells results in their dedifferentiation into a phenotype similar to embryonic stem cells, resulting in expression of genes specific to a variety of cell types, including markers common to endothelial cells that line blood vessels [64,65]. Similarly, CTBs also have the ability to invade, remodel the maternal vasculature, and mimic endothelial cells during placenta development, a process that is termed pseudovasculogenesis [25,26]. Both vessels formed during vasculogenic mimicry and pseudovasculogenesis allow perfusion of blood and nutrients to the tumor and fetus, respectively [26,66].

The process of vasculogenic mimicry involves multiple factors. The protease complex containing MT1-MMP and MMP-2 is involved in this process and facilitates cleavage of laminin 5-γ2 into promigratory fragments important for migration during vessel formation [61,67]. The receptor EphA2, or epithelial cell kinase (Eck), a receptor tyrosine kinase, is present in the membrane of cells capable of vasculogenic mimicry and is important for vasculogenic mimicry [61,68]. In addition, tumor cell expression of vascular endothelial-cadherin (VE-cadherin) is required for this process [69], including one mechanism by which it might facilitate interaction of EphA2 with its ligand and

subsequent activation [70]. Signaling molecules PI3K and focal adhesion kinase (FAK), as well as activation of their downstream targets Akt and ERK1/2, also increase matrix metalloprotease activity during vasculogenic mimicry [71,72].

Although the mechanisms that result in the process of vasculogenic mimicry have been partially elucidated, factors involved also play important roles in normal cells. For instance, the formation of laminin 5-γ2 promigratory fragments enhances invasion of normal epithelial cells [73]. FAK and PI3K also play major roles in a number of other signaling pathways resulting in normal cellular processes [22,74]. Therefore, new molecules and mechanisms specific to this process in tumor cells must be determined in order to better target disease progression.

1.3 Mig-7 Expression and Translation

The interaction of tumor microenvironment components with primary tumor cells is important for the adoption of an invasive phenotype and tumor progression. Complex signaling resulting from these interactions, including receptor tyrosine kinase (RTK) activation and integrin binding to ECM components, alters the behaviors of tumor cells, and this signaling is still not completely understood. Because aggressive, invasive tumor cells show differential migration and adhesion compared to normal cells, it will be important to determine these mechanisms which distinguish tumor cells from normal cells in order to develop more specific therapies targeting disease progression.

One of the best characterized of the microenvironment growth factors is HGF/SF, which is overexpressed, along with its receptor c-Met, in most cancers. Interaction of HGF/SF with c-Met, has been shown to result in multiple behaviors. These include

increased migration and invasion, as well as altered morphogenesis and increased proliferation [10,13,75-77]. These different phenotypes are mainly determined by the differentiation state of the cell [10-13], as well as by different integrins, their activation and resultant signaling [78,79]. Our lab identified a novel gene expression, called Migration inducting gene 7 (Mig-7) that is upregulated by HGF/SF treatment and activation of c-Met. In addition, well characterized blocking antibody to $\alpha v \beta 5$ integrin inhibits induction of Mig-7 by HGF/SF suggesting that cross-talk between HGF/SF and $\alpha v \beta 5$ signaling upregulates Mig-7 expression. This increased expression occurs early after 6 hours of HGF treatment [80]. Upregulation of Mig-7 expression was also seen upon treatment with epidermal growth factor [81]. Interestingly, the Mig-7 sequence shows 99% homology specifically to ESTs from early placenta [80], at which stage CTBs are involved in invasion and remodeling maternal vessels. These CTBs also require convergent signaling from HGF/SF interaction with c-Met and $\alpha v \beta 5$ integrin [26], implying a potential link between Mig-7 expression, invasion, and vascular mimicry.

Translation of Mig-7 protein appears to be atypical, based on the cDNA sequence and protein product. Mig-7 protein is cysteine-rich, with the majority of cysteines located in an internal valine-cysteine repeat region [80]. The only other protein in the database containing this repeat is the "hypothetical" protein Q300 (X52164), which is predicted to be a membrane protein in this repeat region. This valine-cysteine repeat region is predicted to be the transmembrane portion of Mig-7 as well, based on Kyte-Doolittle hydrophobicity plots [80]. Consistent with this prediction, Mig-7 protein localizes primarily to membrane, and less to cytosolic, fractions of cell lysates by immunoblotting [80].

1.4 Tumor cell-specific Mig-7

Previous studies to date demonstrate that Mig-7 is expressed in primary metastatic tumors, secondary metastatic sites, and tissue surrounding tumors (n=300) [80,82]. This expression is detected in a variety of metastatic tumor tissues, including endometrial, ovarian, oral and lung squamous cell and colon carcinomas. However, Mig-7 is not found to be expressed in cells of normal tissue samples from various tissues (n=6 each: brain, heart, kidney, spleen, liver, colon, lung, small intestine, muscle, stomach, testis, term placenta, salivary gland, thyroid, adrenal, pancreas, ovary, uterus, prostate, skin, leukocytes, bone marrow, fetal brain, and fetal liver) [80]. In fact, the only normal tissue found to express Mig-7 is early placental tissue, which consists of highly invasive CTBs. In addition, the induction of Mig-7 expression by HGF/SF seen in endometrial carcinoma cells does not occur in normal primary endometrial epithelial cells stimulated with HGF/SF [80], consistent with the altered differentiation state and integrin expression of carcinoma cells compared to primary epithelial cells. Previous data also demonstrates that Mig-7 is expressed in blood from untreated cancer patients and not in normal or treated patients' blood [82]. These results demonstrate that Mig-7 appears to be expressed in a tumor cell and placenta-specific manner.

1.5 Effects of Mig-7 expression

Mig-7 was initially found to be upregulated early by HGF/SF treatment in RL95 and HEC1A endometrial carcinoma cells [80] before scattering, and both of these cell lines have been shown to invade and migrate toward HGF/SF *in vitro* [75]. Thus, it was

hypothesized that Mig-7 expression is involved in invasion and migration of these cell lines. Mig-7-specific antisense oligodeoxynucleotides (ODNs) cause a significant decrease in migration of RL95 endometrial carcinoma cells [80], indicating its involvement in cancer cell migration. Mig-7 is also expressed in lymph node metastases in nude mice injected with human HEC1A or RL95 endometrial carcinoma cell lines [82], implying its involvement with invasion *in vivo*.

Based on these collective data, it is hypothesized that Mig-7 plays a role in the invasive behavior of multiple types of tumor cells and modulation of its expression may be used to better determine the mechanisms and signaling resulting in the altered behavior of invasive cancer cells compared to normal cells. The current studies focused on analyses of Mig-7 expression, its effects and potential mechanisms by which they occur in a variety of carcinoma cells, as well as melanoma cells, *in vitro* and *in vivo*. Specifically, modulation of Mig-7 expression and function by antibody treatment, siRNA expression, and overexpression was utilized to test these effects and potential mechanisms.

Chapter 2

OVEREXPRESSION OF CARCINOMA AND EMBRYONIC CYTOTROPHOBLAST

CELL-SPECIFIC MIG-7 INDUCES INVASION AND VESSEL-LIKE STRUCTURE

FORMATION

Overexpression of carcinoma and embryonic cytotrophoblast cell-specific Mig-7 induces invasion and vessel-like structure formation

Aaron P. Petty[2], Kiera L. Garman[1], Virginia D. Winn[5], Celee M. Spidel[6] and J. Suzanne Lindsey[1,2,3,4]

[1]*Department of Pharmaceutical Sciences at College of Pharmacy;* [2]*School of Molecular Biosciences;* [3]*Center for Reproductive Biology;* [4]*Cancer Prevention and Research Center, Washington State University, Pullman;* [5]*Department of Obstetrics and Gynecology Sections of Maternal-Fetal Medicine and Reproductive Sciences, University of Colorado Health Sciences Center, Denver;* [6]*Department of Pharmaceutical Sciences at the School of Pharmacy Texas Tech University Health Sciences Center, Amarillo*

Running title: Mig-7 expression and vasculogenic mimicry

Key words: vasculogenic mimicry, 3D culture, EGF, laminin, γ2 chain fragments, Factor VIII associated antigen, VE-cadherin

Request for reprints: J. Suzanne Lindsey, Washington State University, College of Pharmacy, Department of Pharmaceutical Sciences, Wegner Hall, Pullman, Washington, 99164-6534 Tel: 509 335-4689, Fax: 509 335-5902; E-mail address: lindseys@wsu.edu

Abstract

Molecular requirements for carcinoma cell interactions with the microenvironment are critical for disease progression but poorly understood. Integrin αvβ5, which senses the extracellular matrix, is important for carcinoma cell dissemination *in vivo*. αvβ5 signaling induces Mig-7, a novel, human, apparently carcinoma-specific gene product. We hypothesize that Mig-7 expression facilitates tumor cell dissemination by increasing invasion and vasculogenic mimicry. Results show that embryonic cytotrophoblasts upregulate Mig-7 expression as they acquire an invasive phenotype capable of pseudovasculogenesis. Mig-7 protein primarily co-localizes with vasculogenic mimicry markers Factor VIII associated antigen, VE-cadherin, and laminin 5 γ2 chain domain III fragment in lymph node metastases. Overexpression of Mig-7 increases γ2 chain domain III fragments known to contain EGF-like repeats that can activate EGF receptor. Interestingly, EGF also induces Mig-7 expression. Carcinoma cell adhesion to laminins is significantly reduced by Mig-7 expression. Remarkably, in 2D and 3D Matrigel cultures, Mig-7 expression causes invasion and vessel-like structures. Melanoma cells, which were previously characterized to invade aggressively and to undergo vasculogenic mimicry, express Mig-7. Taken together, these data suggest that Mig-7 expression allows cells to sense their environment, to invade, and to form vessel-like structures through a novel relationship with laminin 5 γ2 chain domain III fragments.

Introduction

For over one hundred years, researchers have proposed that embryonic cytotrophoblast cells and cancer cells are one and the same.[1;2] While they may not be the exact same cells, embryonic cytotrophoblast cells (CTBs) are similar to cancer cells. They invade maternal tissues from the site of embryo implantation during placenta development. In addition, CTBs remodel maternal vasculature, a process known as vascular mimicry or pseudovasculogenesis, creating leaky vessels[3] similar to those found in tumors.[4] Invasion of these two cells types is initiated by receptor tyrosine kinase (RTK) and αvβ5 signaling crosstalk.[5-8]

Data suggest that highly invasive cancer cells can form conduits in tumors, a process some researchers call vasculogenic mimicry.[9-11] Publications before use of this terminology have described tumor cells lining the lumen of irregular and leaky tumor vessels (see[12] for a review). These tumor cells that form vessel-like structures and CTBs can masquerade as endothelial cells by expressing vascular endothelial (VE)-cadherin and Factor VIII associated antigen (FVIII assoc:ag) as well as other endothelial markers.[10;11;13;14] Laminin 5 γ2 chain promigratory fragments contribute to cell motility, invasion[15-19] and to this vessel-like structure formation by tumor cells.[9] Invasive melanoma cells capable of forming vessels express significantly higher levels of laminin 5, a basement membrane component that is a heterotrimer of alpha3, beta3, and γ2 chains. Metalloproteinase-2 and membrane type 1 (MT-1) MMP cooperate to cleave γ2 chain into fragments that cause melanoma cell invasion leading to vasculogenic mimicry.[9] *In vivo*, predominantly tumor cells rather than endothelial cells form vessels in the interior, more hypoxic regions of tumors and are thought to provide new blood flow

to the tumor causing renewed growth and dissemination.[20] This formation of tumor cell-lined vessels appears to be resistant to antiangiogenic therapies.[21] In addition, invading tumor cells are resistant to current therapies.[22] Because no specific marker expressed by tumor cells that invade or mimic endothelial cells has previously been discovered, these cells can evade detection. Understanding the regulation of tumor cell invasion and vessel formation is therefore of considerable importance for development of more efficient and effective targeted tumor cell detection as well as therapies.

Mig-7 is a cysteine-rich protein found in carcinoma cell membrane and cytoplasm protein lysate fractions by immunoblotting. Expression of Mig-7 appears to be restricted to carcinoma cells and putatively to early placenta, based on homology with expressed sequence tags (ESTs) isolated from this tissue. Human malignant tumors, blood, and metastatic sites from over 200 cancer patients express Mig-7 regardless of tissue origin. Notably, Mig-7 is not detected in 25 different normal human tissues or in blood from normal subjects.[6;23] Signaling that initiates CTBs and tumor cell invasion from RTK c-Met, the hepatocyte growth factor/scatter factor (HGF/SF) receptor, and $\alpha v \beta 5$ integrin, induce Mig-7 expression.[6;8;24]

Based on these data, we hypothesize that Mig-7 expression plays a role in behaviors in common between CTBs and carcinoma cells, namely invasion and vascular cell mimicry. To test this hypothesis, Mig-7 expression by human CTBs was examined *in vitro* and *in vivo*. Tumor microenvironment extracellular matrix (ECM) and its growth factors important for these behaviors were used with endogenous Mig-7 and siRNA stable knockdown cell lines, as well as overexpressed Mig-7 in two-dimensional (2D) and three-dimensional (3D) cultures, to determine Mig-7 biological relevance.

Immunohistochemistry of lymph nodes from our nude mouse model of tumor cell invasion determined localization of Mig-7 expression and topographical relationships *in situ* with VE-cadherin, laminin 5 γ2 chain domain III fragments, and FVIII assoc:ag. Adhesion assays were also used to elucidate mechanisms by which Mig-7 expression contributes to tumor cell invasion and its potential role in vessel-like structure formation.

Materials and Methods

Cell cultures

Human CTBs were isolated from second trimester placentas under IRB approval as described previously.[25] CTBs were cultured on an extracellular matrix, Matrigel (BD Biosystems), which initiates their differentiation along the invasive pathway.[26] HEC1A, RL95-2 (RL95) endometrial carcinoma and HT29 colon carcinoma cell lines (all from ATCC) were cultured as described previously.[6;23] Epidermal growth factor (EGF, Calbiochem) or HGF/SF (R&D Systems) treatment (each at 20 ng/ml) were incubated for the indicated time with RL95 cells that had been serum-starved for 12 hours. Melanoma cell lines, MUM-2B, MUM-2C, C918, C8161, and A375P, were maintained in RPMI 1640 (Gibco, Invitrogen) supplemented with 10% fetal bovine serum (Gibco, Invitrogen), 20 mM HEPES, and 0.1% gentamicin sulfate. Cultures, invasive phenotypes, and ability to undergo vasculogenic mimicry are well characterized for melanoma cell lines.[9;10;14;20;27;28] All cultures were maintained in a humidified incubator at 37°C in 5% CO_2 air.

For 2D cultures, HT29, HEC1A or RL95 cells were plated on Matrigel containing growth factors (GF+ Matrigel) or growth factor reduced Matrigel (GFR Matrigel, >10

mg/ml lots, BD Biosciences) ~ 0.2mm thick from 80% confluent cultures for indicated times prior to collecting protein lysates. 3D cultures were performed using 50 µl domes of GF+ Matrigel (no dilution) allowed to polymerize for 30 minutes at 37°C in a humidified, 5% CO_2 incubator. Cells were removed from their plates non-enzymatically (2 mM EGTA); 2 µl of single cell suspensions (7.5 X 10^4) were injected into the dome of Matrigel.   Images of 2D and 3D cultures were taken using a Nikon Diaphot inverted microscope and Retiga 2000R digital CCD camera with QCapture 5.1 software (QImaging).

Xenograft mouse model

The nude mouse model was utilized as described previously[23] under Institutional Animal Care and Use Committee approval. Briefly, 1 X 10^5 HEC1A or RL95 viable cells in 250 µl media were combined with 250 µl of GF+ Matrigel and injected subcutaneously into the dorsal neck region of nu/nu athymic mice. Negative controls were mice injected with Matrigel alone (i.e. no cells). Five animals per group were injected. After six weeks, animals were euthanized. Brachial and axillary lymph nodes were harvested, flash frozen in OCT (Miles Labs), and stored at -80° C until cryosectioned.

Expression of Mig-7 FLAG-tagged protein and Mig-7 specific siRNA

Selection of transfected pooled clones (n=3 each construct), as well as expression of 3XFLAG CMV Mig-7, were described previously.[6]

Endogenous Mig-7 expression was reduced with siRNA. Briefly, four Mig-7 specific siRNAs sequences (see Table I) were designed by Ambion with BamHI and HindIII

restriction enzyme sites at each 5' and 3', respectively for directional cloning. No significant homology was found to any human sequence other than Mig-7 (accession DQ080207). Double stranded DNA oligonucliotides that encode each Mig-7 siRNA were synthesized by Invitrogen, resuspended, quantified, annealed, cut with BamHI and Hind III restriction enzymes and ligated into the pSilencer vector (pSilencer 3.1-H1 neo) cut with the same enzymes according to manufacturer's instructions (Ambion). After one optimal concentration of G418 for RL95 cell killing was determined, RL95 cells were transfected in triplicate for each construct at a ratio of 1 μg plasmid to 3 μl of FuGene 6 (Roche). After G418 selection at 600 μg/ml, levels of Mig-7 protein expression were determined for each pooled, transfected cell line by immunoblotting and densitometry using β-tubulin as a normalizing gene expression.

Immunohistochemistry (IHC)

Detection of Mig-7 protein was performed using Mig-7 specific affinity purified antibody produced in rabbits immunized with KLH-conjugated Mig-7 peptide (MAASRCSGL) representing the first nine amino acids of Mig-7 protein, as previously described.[6] Briefly, cryostat sections (10 μm) of fresh frozen lymph node from five HEC1A, four RL95, and five control (Matrigel-alone) injected nude mice on Superfrost plus slides were washed two times in D-PBS (Hyclone), then treated with 50 mM NH_4CL (Sigma) for 10 minutes at room temperature. Slides were washed two times in D-PBS and then permeabilized with 0.01% digitonin (Aldrich Chemical Company) in PBS at room temperature for 30 minutes. After washing two times in D-PBS, slides were blocked in 10% horse serum (Gibco) in D-PBS for 30 minutes at room temperature. Primary

antibodies, polyclonal rabbit, anti-human Mig-7, monoclonal mouse, human-specific anti-γ2 domain III (Chemicon, clone D4B5), polyclonal rabbit anti-VE-cadherin (Cayman Chemical), and polyclonal rabbit, FVIII assoc:ag (Dako) were diluted 1:50 and incubated on the tissue for 2 hours at room temperature and overnight at 4 ºC. Slides were washed two times in D-PBS then incubated for 20 minutes in 3% H_2O_2 in methanol. Slides were washed two times in D-PBS and then incubated for 30 minutes in 1:200 dilution of goat anti-rabbit IgG-horseradish peroxidase (HRP) or goat anti-mouse IgG-HRP labeled antibody (Santa Cruz Biotechnology) relevant to the primary antibody used in D-PBS containing 0.5% bovine serum albumin (BSA, Fisher Scientific, Fair Lawn, NJ, Cat # BP1600-100). Slides were washed two times in D-PBS and then developed using 3,3'-diaminobenzidine (DAB) substrate (to detect HRP-labeled secondary antibodies) kit (Vector Laboratories) until brown specific staining was detected by microscopy (less than 3 minutes). After washing in water for 5 minutes, slides were counterstained in Hematoxylin QS (Vector Laboratories). Slides were dehydrated in two incubations for 3 minute each of 75%, 95% and absolute ethanol, air dried, and mounted in DPX mounting medium (BDH Laboratory Supplies). Controls included sections without primary or secondary antibodies, as well as staining of normal (vehicle injected animal) lymph node sections with each primary antibody.

Ten percent formalin fixed, paraffin embedded, 5 μm sections were used for basal plate placenta analyses. After deparaffinization with xylene for 10 minutes, rehydration through 100%, 95% and 70% ethanol, and antigen retrieval for 2 seconds on ice in a microwave oven, these sections were processed as described above to

20

detect Mig-7 or cytokeratin 7 (CK7).   Mouse anti-human antibody for CK7 (Dako) was used at 1:100.

Images from low (40X) to high (1000X) magnifications were taken on a Nikon Microphot microscope with a Retiga 2000R digital CCD camera and analyzed with QCapture 5.1 software program (both QImaging) and Canvas 8.0 (Deneba Systems Inc). Measurement of vessels in lymph nodes invaded by HEC1A and RL95 cells was performed with the QCapture software program calibrated with a micrometer. At least four different tumors from four mice of each cell line (HEC1A or RL95) injected or Matrigel alone were analyzed.

Western blot analyses

Western blot analyses were performed as described previously with the following modifications.[6] Cells grown on plastic or 2D Matrigel (10 mg/ml lot) were homogenized in lysis buffer [2% SDS, 100 mM DTT, 0.01% bromophenol blue, 60 mM Tris, 10% glycerol, 2X protease inhibitor (Complete™, Roche)] and quantitated using RC/DC Protein Assay (Bio-Rad). Equal amounts of protein were loaded onto a 12% polyacrylamide gel and run at constant 200 V for 30-40 minutes. Gels were semi-dry transferred (Boekel) to polyvinylidene fluoride membranes and blocked in TBS containing Tween-20 detergent (TBST, 0.1 %) and 5% dry milk for one hour at room temperature. Endogenous or FLAG-tagged Mig-7 protein was detected using human-specific, affinity purified Mig-7 antibody (1:2,000) or the M2-peroxidase anti-FLAG antibody (1:100, Sigma), respectively. Mouse anti-β-tubulin monoclonal antibody (Upstate, clone AA2) or mouse anti-β-actin (Sigma, clone AC-40) served as loading

controls. Antibody to laminin 5 γ2 chain domain III was described in Methods for IHC.

After washing in TBST, a horseradish peroxidase-labeled secondary anti-rabbit IgG

antibody at a dilution of 1:40,000 was used to detect the Mig-7 antibody or goat anti-

mouse IgG-HRP labeled antibody (Santa Cruz Biotechnology) to detect the β-tubulin,

actin, or laminin 5 γ2 chain domain III antibodies. Chemiluminescence Plus Reagent

(Amersham) allowed detection of HRP-labeled antibodies once exposed to film.

Densitometry was performed using the Bio-Rad imager and Quantity One analysis

software program and comparing each protein of interest band intensity to its respective

β-tubulin or actin band intensity. All raw signal intensities were corrected for

background. Data analyses were performed with GraphPad Prism 3.0 statistical

software.

RNA isolation, Relative RT-PCR and Northern blot analyses

Total RNA isolation and relative RT-PCR, including optimization of cycle number to

achieve mid-linear range, were performed as described previously.[6] Placental RNA was

obtained, with patient consent and IRB approval, as described previously.[29] PCR

products were confirmed by Southern blot (Mig-7 specific cDNA probe) or by subcloning

and sequencing. Northern blots were performed as described previously.[6]

Quantitative Real-time RT-PCR (Q-PCR)

Reverse transcription of RNA was performed using the TaqMan Gold RT-PCR kit as

described by the manufacturer (Applied Biosystems). Q-PCR, employed the Applied

Biosystems 9700HT sequence detection system. Each target was amplified in triplicate

with a Mig-7 specific primer probe set (forward = 5' CAC CTG CCT CTG GTC GTT

AGG 3'; reverse = 5' TAC TGG ATT CCT CTA GCT TTG GTG TT 3'; probe =

AAACTCTCAGTGATCTCT) or 18S primer probe set (Applied Biosystems).   Primer

pairs for HLA-G and integrin α1 were as previously published.[8;30] Briefly, 5 μL of cDNA

target was added to a 20μL mix of 1X TaqMan universal PCR master containing

Amperase UNG and 1μL of primer/probe.   Reactions were incubated at 50° C for 2

minutes, then at 95° C for 10 minutes followed by 40 cycles of 95° C for 15 s and 60° C

for 1 minute.   A five-fold titration of control template was included along with both RT

negative and no template controls.   Relative mRNA levels were then calculated using

the standard curve method (ABI User Bulletin #2) using 18S as the endogenous control

and 0 hour as the calibrator.

Adhesion Assays

Adhesion of stably transfected FLAG-Mig7 expressing, pooled clones, or empty vector

HT29 colon carcinoma cells to laminins, fibronectin, vitronectin, collagen I or collagen IV

was tested using the CytoMatrix™(5) Screen kit (Chemicon) according to the

manufacturer's instructions.   Briefly, after counting with a hemacytometer in the

presence of trypan blue, one thousand viable cells of each cell line in 100 μl of single

cell suspensions per well were plated as indicated in 6 coated wells per ECM

component plus six wells coated with BSA as control and incubated in a humidified CO_2

incubator at 37°C for one hour. After washing the plate 3 times with 200 μl/well of PBS

containing Ca^{2+} and Mg^{2+}, cells were stained and fixed in 100 μl of 0.2% crystal violet in

10% ethanol for 5 minutes at room temperature.   After washing 3 times to remove the

stain with 300 µl/well PBS, 100 µl/well of a 50:50 mix containing 0.1 M NaH_2PO, pH 4.5 and 50% ethanol to solubilize and release the cell-bound stain was added with 5 minutes gentle shaking at room temperature. Absorbance readings were taken at 550 nm on a microplate reader (BioRad). Median BSA readings (background) for each cell line were subtracted from ECM readings and resulting data were analyzed using GraphPad Prism 3.0.

Statistical Analyses

All experiments were performed 2-4 times as indicated in figure legends. Student's t-test when comparing two experimental groups or one-way analysis of variance (ANOVA) with Tukey-Kramer Multiple comparisons post test for multiple group comparisons were used for statistical analyses in the GraphPad Prism statistical analyses software. A $p < 0.05$ was considered significant.

Results

Temporal expression of Mig-7 in placental tissue and during invasive CTBs differentiation.

Mig-7 cDNA (accession DQ080207) is homologous to ESTs (N41315 and AI18969) isolated from 10 week gestation placenta.[6] Even though our previous report suggests that Mig-7 is carcinoma cell-specific, this homology indicated that Mig-7 may be expressed by early placenta cells. Therefore, Mig-7 expression in placenta needed to be verified because behaviors of cancer cells have been compared to embryonic

trophoblast cells,[1;2] yet gene expression specific to these two cell types remains obscure.

Relative RT-PCR analyses of total, DNased RNA from early and late gestation placenta detected Mig-7 expression strictly in early gestational tissue (Figure 1a). Human CTBs invade maternal decidua and vasculature during early placental development, with peak invasion and vascular remodeling occurring between 14 and 22 weeks of gestation. This invasive capacity is greatly reduced by term.[2;25] Therefore, placental basal plate tissue, the location of cytotrophoblast invasion and vascular remodeling, was isolated from first, second, and third trimester as well as term placentas. Mig-7 mRNA expression was highest in the second trimester samples prior to 22 weeks gestation, was reduced at 23 weeks, and was absent at term (Figure 1b). Immunoblot analysis of Mig-7 protein in lysates from basal plates of the indicated stage in gestation is shown in Figure 1c. Densitometry analyses (Figure 1d) show a 10 fold decrease in 38 week basal plate expression of Mig-7 protein relative to β-tubulin compared to that of first trimester basal plate.

Isolated embryonic CTBs plated on GF+ Matrigel differentiate in a manner that recapitulates that of invasive basal plate CTBs (reviewed in[3]). Therefore, we analyzed Mig-7 expression in isolated human CTBs cultured on GF+ Matrigel. Mig-7 mRNA expression increased 6-15 fold by 12 hours after plating on Matrigel (Figure 1e). To confirm that the primary CTBs differentiated down the invasive pathway, mRNA levels of CTB invasive markers HLA-G[30] 1 and integrin [8] were also measured and found to increase at least 15 fold by 12 hours on Matrigel as expected (Figure 1f).

Immunoblot analyses demonstrated that the upregulation of Mig-7 protein also occurred by 3 hours and peaked at 12 hours. The previously reported 23 kD Mig-7 band when carcinoma cells were plated on plastic[6] was detected along with a novel ~46 kD sized band (Figure 1d). Lysates from platelets that served as negative controls lacked detectable Mig-7 protein (Figure 1d). Immunohistochemistry of basal plates from first, second or third trimester (n=2 each stage) using CTB-specific cytokeratin-7[31] (CK7) antibody (Figure 1h) or antibody to Mig-7 (Figure 1i) were performed. In serial sections, cells stained for Mig-7 were in the same areas that stained for CK7.

Tumor microenvironment growth factors induce expression of Mig-7 that leads to laminin 5 γ2 chain fragmentation in carcinoma cells.

Mig-7 is detected in tumor cells from all types of solid cancers and is induced by RTK c-Met activation. Preincubation of serum-starved endometrial carcinoma cells with well-characterized blocking antibodies to αvβ6, β1 or αvβ5 integrins prior to HGF treatment has demonstrated that αvβ5 ligation is required in cross-talk signaling with RTK c-Met to initiate Mig-7 expression.[6] EGF-induced invasion of another αvβ5 positive cell line, FG pancreatic carcinoma cells, as well as CTBs, also requires this cross-talk signaling.[7;32] Therefore, we tested whether EGF can induce Mig-7 in αvβ5-positive RL95 endometrial carcinoma cell line from which we originally isolated Mig-7.[6]

After serum starvation for 12 hours, RL95 endometrial carcinoma cells were treated with 20 ng/ml of either HGF or EGF. By Northern blot analyses, Mig-7 mRNA was increased 2.5 hours after treatment with HGF, consistent with our previous findings with this growth factor.[6] EGF also induced Mig-7 mRNA levels 2.5 hours after treatment

(Figure 2a).   Densitometry analyses revealed a 3-fold (HGF) and 3.5-fold (EGF)

increase at 2.5 hours of growth factor treatment over 12 hour serum starved RL95 cells

(Figure 2b).

To further explore effects of tumor microenvironment growth factors, we utilized

plating of endogenous Mig-7 expressing human cell lines, RL-95 and HEC1A

endometrial epithelial carcinoma[6], on GF+ or GFR Matrigel.   The RL95 cell line is

isolated from a moderately differentiated adenosquamous carcinoma of the

endometrium.[33] HEC1A cells were isolated from a stage IA endometrial cancer.[34] Both

cell lines are invasive *in vitro*[35] and *in vivo*.[23] Matrigel is a commercially available

basement membrane isolated from Engelbreth-Holm-Swarm mouse tumor whose major

matrix components are laminins (56%), collagen IV (31%) and entactin (8%).[36;37].

Greater than 10 mg/ml GF+ Matrigel ECM contains approximate concentrations of EGF

1.3 ng, basic fibroblast growth factor 0.2 pg, nerve growth factor 0.2 ng, platelet derived

growth factor 48 pg, insulin-like growth factor-I 24 ng, and transforming growth factor-β

4.7 ng (all per ml).[36;37]

Immunoblot analyses detected Mig-7 at the known 23 kD and a more

predominant, novel ~63kD sized protein in lysates from RL95 or HEC1A cells plated on

GF+ Matrigel but not from cells plated on GFR Matrigel (Figure 2c).   Lysates from

Matrigel alone cultures do not possess these bands (data not shown). Densitometry of

these immunoblots comparing intensities of Mig-7 to β-actin bands revealed that levels

of this upper 63 kD Mig-7 band in HEC1A cells were significantly 40% greater than the

63 kD bands in RL95 cells while the levels of the 23 kD Mig-7 band were not

significantly different (Figure 2d).   Plating endometrial carcinoma cell lines on GF+

Matrigel also induced production of laminin 5 γ2 fragments that were different from those found from cells plated on GFR Matrigel. A ~63 kD γ2 chain domain III fragment was detectable in the GF+ Matrigel plated cells and not in the GFR Matrigel plated cells (Figure 2e).

To confirm the Mig-7 ~63 kD band and the γ2 chain fragment of 63 kD, we used our 3XFLAG CMV Mig-7 or empty vector stably transfected, pooled clones of a cell line that does not endogenously express Mig-7, HT-29 colon carcinoma.[6] HT-29 cells are from a human stage I colon tumor. On plastic, we previously detected 26 kD (an increase of ~3 kD is due to the 3XFLAG of 24 amino acids) Mig-7 bands from each pooled clones A, B, and C[6]; these bands were not detected in vector alone cells plated on GF+ Matrigel (Figure 2f). However, plating HT29 transfectants on GF+ Matrigel revealed, by immunoblotting with anti-FLAG antibody, the additional ~66 kD form (again, an increase of ~3 kD is due to the 3XFLAG of 24 amino acids) Mig-7 band (Figure 2f). Fragmentation of γ2 chain was predominantly detected at the same size, ~66 kD, as the upper band of Mig-7 only in the HT29 cell lines expressing Mig-7 (Figure 2f). This upper band was previously seen in cells endogenously expressing Mig-7 (Figure 2e). No 80 kD sized γ2 chain fragment and very low levels of ~66 kD as well as 40 kD sizes were seen by immunoblotting of lysates from empty vector cells plated on GF+Matrigel, even though equal levels of protein were loaded as determined by protein assays and by β-tubulin antibody (Figure 2f).

Mig-7 expression causes cell spreading on two-dimensional GF+ Matrigel.

Laminin 5 γ2 chain fragmentation is required for carcinoma cell invasion[19;38] and for vasculogenic mimicy.[9;20] Domain III γ2 chain fragments, detected by the γ2 antibody used in the previous immunoblots, activate the EGF receptor.[39;40] Because we detected different Mig-7- and γ2 chain-specific bands when either endogenous or FLAG-Mig-7 HT29 cells were cultured on GF+ Matrigel compared to when cultured on plastic, we examined morphology of these cell lines on plastic to those cultured in 2D and in 3D GF+ Matrigel cultures. When cultured on a thick layer (no dilution) GF+ Matrigel, FLAG-Mig-7 expressing cells were found to be similar in morphology to vector alone cells (Figures 3a & d) after 17 hours plating. In contrast, after 10 days in culture, Mig-7 expressing HT29 cells were predominantly spread out over the Matrigel (Figure 3b) whereas cells transfected with empty vector remained primarily in colonies comprised of densely piled cells (Figure 3e). On tissue culture plastic (no Matrigel), the morphology of FLAG-Mig-7 expressing HT29 cells (Figure 3c) was indistinguishable from that of HT29 cells transfected with empty vector (Figure 3f).

Invasion and vessel-like structure formation in three-dimensional GF+ Matrigel is caused by Mig-7 overexpression in HT29 cells.

Cells cultured in 3D matrices can more accurately recapitulate the *in vivo* microenvironment, based on different morphologies, signal transduction and microfilaments than the same cells plated on rigid substrates or plastic.[41-45] Therefore, we employed a GF+ Matrigel 3D culture system to determine effects of Mig-7 expression on cell behavior via interaction with this microenvironment.

Domes of 50 µl GF+ Matrigel can be formed on plastic because polymerization initiates as soon as the cold Matrigel comes in contact with room temperature plastic, thereby building up Matrigel instead of it spreading over the surface. Media was added to the dish to cover the dome of Matrigel. No other cells were co-cultured with the transfected HT29 cells in these 3D domes. After injection, the single cells started to coalesce during days 1 and 2. Empty vector HT29 cells formed colonies by days 4 and 5. Over 10 days of culture, equal numbers of HT29 empty vector stably transfected cells formed discrete, dense colonies in 3D cultures (Figure 4a). In stark contrast, Mig-7 overexpressing HT29 cells invaded and formed vessel-like structures in the Matrigel domes (Figure 4b & c). Photomicroscopy through four planes of view (z-dimension) demonstrated that cords of invading cells were formed by Mig-7 expressing HT29 (Supplemental data images were taken through 3D Matrigel. Due to the branching morphology, cells that were in that plane are in focus; the rest are out of focus.

To further examine the possibility that Mig-7 expression leads to vasculogenic mimicry, we obtained melanoma cell lines previously characterized to invade aggressively and to undergo vasculogenic mimicry (C918, C8161, MUM2B), as well as melanoma cell lines that do not possess these behaviors (A375P, MUM2C, generously provided by Dr. Mary Hendrix, Northwestern University). The MUM-2B and MUM-2C cell lines were derived from a metastatic uveal melanoma explant within the liver from the MUM-2 heterogeneous cell strain.[28] C8161 cells are a cutaneous melanoma cell line from a metastatic site, whereas C918 (uveal) and A375P (cutaneous) are from primary sites. (for a review of these cell lines see [10]). As determined by immunoblotting of lysates from these melanoma cell lines plated on plastic, Mig-7 protein 23 kD

expression was limited to melanoma cell lines C918, C8161, MUM2B. In contrast, A375P, MUM2C did not express Mig-7 (Figure 4d).

Decrease of endogenous Mig-7 causes colony formation and less invasion in 3D cultures.

Because the behaviors of empty vector and Mig-7 transfected HT29 cell lines were so strikingly different, we developed Mig-7-specific siRNA stably transfected RL95 cell lines to validate these differences. Sequences for each siRNA construct are shown in Table I. In Figure 5a, immunoblotting revealed that two out of three siRNA constructs efficiently decreased levels of Mig-7 protein. Densitometry comparing band intensities of Mig-7 to β-tubulin bands for each sample confirmed a 3.8-fold reduction in Mig-7 protein levels in the 1-3A and 2-3B cell lines, whereas the 3-1A siRNA cell line showed no reduction in Mig-7 protein as compared to parental RL95 cells (Figure 5b).

Morphologies of RL95 siRNA cell lines 1-3A, 3-1A, and parental were not discernibly different when plated on tissue culture plastic with no Matrigel (Figures 5c-e). However, when equal numbers of cells were grown for 10 days in 3D GF+ Matrigel, the RL95 parental cell line and the 3-1A siRNA cell line that express endogenous levels of Mig-7 were similar in invasive behavior with no dense colony formations observed (Figure 5f & h). In contrast, the siRNA Mig-7 knockdown expressing 3.8-fold less Mig-7 protein formed dense colonies (Figure 5g).

Mig-7 expression causes decreased adhesion to tissue culture plastic and to laminins.

Laminin 5 γ2 fragments allow migration and invasion, apparently through less stable adhesion to basement membrane and upregulation of matrix metalloproteinase-2 (MMP-2).[15;46]   During selection of stable 3XFLAGCMVMig-7 HT29 cells and before pooling clones, we noticed that Mig-7 expressing cell colonies but not empty vector colonies could be suctioned off during media aspiration (Figure 6a). Various cell types are known to lay down laminin 5 and fragment γ2 chains differently, due to the type of protease they produce that can cleave γ2. Some cells form less stable adhesions to basement membrane of which laminin is a major component. [9;15;17-19]   Therefore, we performed adhesion assays with HT29 transfected cell lines. Mig-7 expressing HT29 cells were significantly less adherent to laminin coated wells. In contrast, adhesion to other ECM components (fibronectin, vitronectin, collagen I, or collagen IV) was not significantly affected by Mig-7 expression (Figure 6b).

Mig-7 protein and FVIII assoc:ag co-localize to vessel-like structures in lymph node

Carcinoma cells use vessels to travel and metastasize to distant sites. Once at the distant site, tumor cells must acclimate or die. Mig-7 has been detected at primary and secondary sites, as well as in the blood of cancer patients, but not in cells of or blood from normal subjects.[6;23]   To determine HEC1A and RL95 cell fate in brachial and axillary lymph nodes to which these human endometrial carcinoma cells had invaded in a xenograft nude mouse model, we performed IHC to detect Mig-7 and FVIIIassoc:ag, an endothelial cell marker that is also found in plasma.[47]   In serial sections, areas of Mig-7 staining co-localized with areas of staining for FVIII assoc:ag in vessel-like

structures that are irregular in shape and sometimes adjacent to one another in lymph nodes from HEC1A injected nude mice (Figures 7a-f) or RL95 injected nude mice (Figures 7g-l). Staining for FVIII assoc:ag appeared to be more blurred and outside of vessel-like structures than Mig-7 staining (Figures 7a-l). Overlays of FVIII assoc:ag stained sections onto Mig-7 serial sections using Canvas 8.0 imaging software revealed that the staining patterns for both antigens were in the same regions (data not shown). No similar staining above background or vessel-like structures were observed in sections from normal lymph nodes stained for Mig-7 (Figures 7m-o) or for FVIII assoc:ag (Figures 7p-r). Controls also included no primary antibody processed sections of lymph nodes from HEC1A injected animals and no specific brown staining was detected (Figures 7s-u).

Because HEC1A cells are known to be more invasive *in vitro* than RL95 cells,[35] the number of vessel-like structure "hot spots", arbitrarily defined as >3 vessel-like structures per area positive for Mig-7, were quantitated and statistically analyzed. At least four lymph nodes from four different nude mice injected with either cell line were analyzed. There was a significant 4-fold increase in vessel-like "hot spots" in lymph nodes from HEC1A injected animals as compared to lymph nodes from RL95 injected animals (Figure 7v).

Tumor vessels, and especially those that are lined by tumor cells, are small in diameter.[4;13] QCapture imaging program calibrated to a micrometer was used to measure the diameter of these Mig-7 positive vessel-like structures. Median diameter size was not significantly different between vessels lined with RL95 cells or HEC1A cells

as determined by human Mig-7 staining; median diameters ranged from 9-13 microns (Figure 7w).

Mig-7 and FVIII assoc:ag positive vessel-like structures in lymph node stain for γ2 chain domain III fragment as well as VE-cadherin.

To extend our studies of the possible biological relevance of Mig-7 expression in tumors[6;23], we examined expression of Mig-7 and known vasculogenic mimicry associated proteins, FVIII assoc:ag, VE-cadherin, and laminin 5 γ2 chain domain III fragment at high magnification (1000X). All of these markers were found in vessel-like structures.   At high magnification, Mig-7-positive cells lining vessel-like structures appeared flattened and spindle shaped rather than endometrial epithelial cuboidal in shape (Figure 8a and e).

In lymph nodes from RL95 injected nude mice, Mig-7 and FVIII assoc:ag co-localized predominantly to cells lining vessel-like structures in both the membrane and cytoplasm (Figures 8a & b, arrows). Again, FVIII assoc:ag staining appeared to spread away from the vessel like structures (Figure 8b, stars). Laminin 5 γ2 chain domain III also localized to cells lining vessel-like structures, mostly in the cytoplasm (Figure 8c, arrows).   VE-cadherin specific staining was observed in membranes of cells lining vessel-like structures (Figure 8d, arrows).   As shown in Figures 8 a-d, vessel-like structures are located adjacent to one another, or as single structures that also contain cytoplasmic projections or membranous extensions that appear to cross the lumen.

In lymph nodes from HEC1A injected nude mice, when slides were processed in parallel, IHC staining for Mig-7 and FVIII assoc:ag appeared to be more intense than

those found in RL95 vessel-like structures. Mig-7 staining was both membrane and cytoplasm localized in cells lining vessel-like structures (Figure 8e, arrows). FVIII assoc:ag was localized to cells lining vessel-like structures (arrows) and other sites (stars) near these vessels (Figure 8f). In Figure 8f, laminin 5 γ2 chain domain III staining appeared predominantly membrane localized with some residual cytoplasmic staining mostly in cells of vessel-like regions. VE-cadherin staining was specific for the membranes of cells lining these vessels (Figure 8g, arrows). Again, in HEC1A injected animal lymph nodes, vessel-like structures are located adjacent to one another or as single structures that also contain cytoplasmic projections or membranous extensions that appeared to cross the lumen (Figures 8e-h) like those observed in RL95 cell injected animal lymph nodes (Figures 8a-d).

No specific staining was detected in sections processed in parallel with no primary antibody (Figure 8i). Staining of Mig-7, FVIII assoc:ag, γ2 chain, or VE-cadherin in normal lymph nodes from was not specific above background and no vessel-like structures were observed (Figures 8j-m).

Discussion

The present study sought to determine the biological relevance and related mechanisms of Mig-7 during invasion by using overexpression and expression knockdown, cell culture and *in vivo* analyses. Specificity of Mig-7 antibody in these studies is established by immunoblot, immunohistochemistry, and detection of RNAi specific knockdown of Mig-7 protein. Detection of same sized bands with anti-FLAG antibody also supports that our Mig-7 antibody is specific. Confirmation of CTBs Mig-7

expression by RT-PCR, immunoblot and immunohistochemistry is important because these embryonic cells possess aggressive invasion and vessel remodeling capabilities found in carcinoma cells that metastasize and can undergo vasculogenic mimicry. In addition, because normal tissues previously studied do not express Mig-7[6;23], it is important that cells of a normal physiologic process express Mig-7.

We found that expression of Mig-7 affected the invasiveness of carcinoma cells and cleavage of laminin 5 γ2 chain fragments. These effects appeared to be dependent on extracellular matrix, modification and attachment to laminins, as well as the availability of growth factors. Human, Mig-7 expressing endometrial carcinoma cells injected into nude mice localized to vessel-like structures to which these cells invaded. FVIII assoc:ag staining in and around these vessels co-localized and spread away from the vessels, suggesting that these are leaky vessels typically found in tumors and in the spiral arteries that CTBs remodel. The morphology of these vessel-like structures support that they are the leaky vessels previously described by Hashizume and co-workers.   Specifically, the vessels are adjacent to one another, unlike normal vessels, are of small diameter, and contain cytoplasmic projections or membranous extensions that appear to cross the lumen.[17] Other endothelial cell markers localized to these vessel-like structures suggest that these human endometrial epithelial carcinoma cells are masquerading as endothelial cells.

Biological relevance of Mig-7 in CTBs and carcinoma cell functions

CTBs and carcinoma cells require αvβ5 ligation for induction of their invasive and vessel modification behaviors.[5-8]   Plating carcinoma cells or CTBs on GF+ Matrigel

induces Mig-7 expression. Whereas lysates from platelets, that served as negative control, lack detectable Mig-7 protein consistent with our previous reports that platelets lack detectable Mig-7 mRNA even with sensitive RT-PCR.[6;23] Mig-7, HLA-G and integrin α1 expression decrease between 12 and 36 hours on GF+ Matrigel. These data are consistent with a depletion of Matrigel growth factors because Mig-7 mRNA decreases with a single dose of HGF in serum deprived endometrial carcinoma cell line cultures.[6]

We detected the previously reported Mig-7 23 kD band in common between these carcinoma and cytotrophoblast cell types but different sized larger bands of Mig-7 between CTBs (~46 kD) and carcinoma cells (~63 kD) when lysates were from cells plated on Matrigel. This finding is not unusual because other cysteine-rich proteins form dimers or migrate aberrantly in reducing gels.[46;48;49] Mig-7 protein possesses 10% cysteine residues in the first 91 amino acids (accession DQ080207). In addition, there may be a difference in protease expression between carcinomas and CTBs plated on Matrigel.[31] Importantly, in carcinoma cells the larger sized band is detected with either Mig-7, γ2 domain III, or FLAG antibody strongly suggesting that Mig-7 is interacting with itself or with another protein depending on the cell type and presence of ECM.

Regardless, these data strongly suggest that invading CTBs from early placenta express Mig-7. This novel finding is significant because invasion and vascular remodeling are behaviors in common between CTBs and carcinoma cells. Our data suggest that Mig-7 plays a role in the plasticity of carcinoma cells to invade and to mimic endothelial cells.

Importance of the tumor microenvironment in Mig-7 effects

Our data show that the tumor microenvironment growth factors, HGF/SF[6] and EGF, as well as GF+ Matrigel, induce carcinoma-specific Mig-7 in αvβ5 integrin-positive cells. This redundancy suggests that Mig-7 expression is important for the invasive capabilities of tumor cells. It is well known that these growth factors promote tumor progression and metastasis. The FG pancreatic carcinoma cell line requires signaling from αvβ5 in conjunction with EGF receptor activation for migration on vitronectin [7]. Interestingly, EGF also acts as a chemoattractant for tumor cell intravasation into blood vessels, a process required for tumor metastasis.[22] αvβ5 integrin ligation is also required for cytotrophoblast invasion[8] as well as for tumor dissemination *in vivo*.[5;7] These results, indicating that multiple tumor-microenvironment growth factors induce Mig-7, may account for its expression in virtually all cancer samples (n > 200) irrespective of tissue of origin [6;23].

Laminin 5 γ2 promigratory fragments are involved in tumor cell invasion and vasculogenic mimicry.[9;19;38] Intriguingly, cleavage of laminin 5 γ2 chain releases domain III consisting of several EGF-like repeats that activate EGF receptor stimulating downstream signaling (e.g. Erk activation), MMP-2 gene expression, and cell migration.[15;46] Another link to γ2 fragments and invasion is provided by our data that show carcinoma cells expressing Mig-7 fragment γ2 differently than cells that do not express Mig-7 when plated on Matrigel. It is tempting to speculate that Mig-7 and γ2 domain III fragments, which range in size from 20-40 kD, interact in a non-reducible manner due to both Mig-7 (accession DQ080207) as well as domain III possessing 10% cysteine residues. In support of these two cysteine-rich proteins interacting, we

observed that Mig-7 expressing cells were significantly less adherent to a mix of laminins but not to other ECM components. In addition, recombinant γ2 domain III fragments form dimers on reducing gels.[46] Because carcinoma cells consistently invaded when Mig-7 was expressed, these data are consistent with a novel relationship between Mig-7, γ2 fragments, invasion, and vasculogenic mimicry.

Overexpression of Mig-7 in HT29 colon carcinoma cells in GF+ Matrigel causes invasion, branching and cords of cells with a vessel-like appearance. In stark contrast, empty vector HT29 cell morphology is comprised of well defined colonies with no visible invasion. These are the same differences in morphology found by Folberg and colleagues when aggressive melanoma cells were compared to their non aggressive counterparts. In addition, these differences in morphology are detected solely on thick or 3D Matrigel not on tissue culture plastic.[50] Our findings show that carcinoma cells expressing Mig-7 invade and form vessel-like structures in the context of ECM that mimics the tumor microenvironment but not when plated on plastic.

Since 3D cultures were initiated with same number of cells and cultured for the same duration of time, it appears that Mig-7 expressing HT29 were more invasive than proliferative. This is consistent with recent data demonstrating that growth arrest of keratinocytes occurs after initiation of hypermotility in a migration on γ2 chain-dependent manner.[51] It has long been noted that the cells leading re-epithelialization to close a wound are less mitotically active than those behind them.[52] Importantly, melanoma cells that undergo vasculogenic mimicry decrease expression of proliferation-related genes GDF15 and p21.[50]

A role for Mig-7 in vasculogenic mimicry

Vasculogenic mimicry has been reported in other tumors such as ovarian, Ewing sarcoma, uveal melanoma and hepato-carcinomas.[10;11;13;53;54] Plasticity of tumor cells that form vessel-like structures has been termed vasculogenic mimicry and correlates with poor patient outcome.[53] These vessels are capable of being perfused and can carry blood to tumors.[55]

The formation of laminin 5 γ2 promigratory fragments is important for the process of vasculogenic mimicry.[20] Laminin 5 is the only laminin that contains the γ2 chain. As previously discussed, when cleaved into promigratory fragments the domain III region which contains EGF repeats causes EGF-like effects, including upregulation of MMP-2, a protease shown to be important in vasculogenic mimicry via γ2 chain fragmentation.[9] As we have shown in this report, Mig-7 mRNA is induced by EGF.

As determined by immunoblotting, Mig-7 protein expression was limited to melanoma cells that aggressively invade and undergo vasculogenic mimicry (C918, C8161, MUM2B[10]). In contrast, melanoma cell lines that are poorly invasive and fail to form vessel-like structures (A375P, MUM2C[10]) do not express Mig-7. These data further support a role for Mig-7 in carcinoma cell-specific behaviors of aggressive invasion and vasculogenic mimicry.

Mig-7 protein is localized to CTBs and carcinoma cells as well as to cells of vessel-like structures in lymph nodes to which human carcinoma cells had spread in nude mice. Mig-7 protein co-localizes with endothelial markers FVIII assoc:ag, VE-cadherin and γ2 chain domain III fragment by IHC analyses. VE-cadherin is expressed by the same aggressively invasive melanoma cell lines that can undergo vasculogenic

mimicry and that express Mig-7.[56] Taken together with Mig-7 induction of invasion and vessel-like structure formation in 3D cultures, as well as Mig-7 expression in melanoma cells that undergo vasculogenic mimicry, these data strongly suggest that Mig-7 plays an important role in these processes.

Identity of cells lining vessel-like structures

Endothelial markers such as FVIII assoc:ag (also known as von Willebrand factor), have been previously localized to tumor vessels.[47] FVIII assoc:ag is a plasma protein produced by endothelial cells and platelets.[57] In serial sections, areas of Mig-7 staining co-localized with areas of staining for FVIII assoc:ag in vessel-like structures that are irregular in shape found with tumor cell formed vessels during vasculogenic mimicry.[13;55] These vessel-like structures are adjacent to one another, unlike normal vessels, are of small diameter and contain cytoplasmic projections or membranous extensions that appear to cross the lumen as previously described for leaky tumor vessels.[4] Frequently, Mig-7 expressing tumor cells that line vessel-like structures are more spindle shaped. This morphology is consistent with melanoma cells undergoing vasculogenic mimicry changing to a spindle shape.[50] Because CTBs form leaky vessels in the maternal vasculature of the placenta,[3] and because we did not detect vessel-like structures or Mig-7 in nude mice normal lymph nodes, these data strongly suggest that these vessels are formed by Mig-7 expressing tumor cells that were injected.

Our data suggest that Mig-7 expression affects tumor cell interaction with the tumor microenvironment in a growth factor-dependent manner. Mig-7 expression

41

causes invasion and vasculogenic mimicry. It has been proposed that finding a protein specific to vasculogenic mimicry would be an excellent anti-cancer target because this process does not occur in any normal tissue in children or adults. Vasculogenic mimicry is prognostic of a poor patient outcome[13] and is not reduced by anti-angiogenic therapies.[21] Additionally, invading cancer cells are resistant to cancer therapies that typically target cell growth.[22] Therefore, therapies directed specifically to invading cancer cells are needed. Mig-7 may be a carcinoma-specific target to inhibit invasion and vasculogenic mimicry *in vivo* thereby preventing growth of tumors and dissemination of tumor cells.

Reference List

1. Beard J: Embryological aspects and etiology of carcinoma. The Lancet 1902, 1758-1761

2. Soundararajan R and Rao AJ: Trophoblast 'pseudo-tumorigenesis': Significance and contributory factors. Reproductive Biology and Endocrinology 2004, 2: 15

3. Red-Horse K, Zhou Y, Genbacev O, Prakobphol A, Foulk R, McMaster MT, and Fisher SJ: Trophoblast differentiation during embryo implantation and formation of the maternal-fetal interface. Journal of Clinical Investigation 2004, 114: 744-754

4. Hashizume H, Baluk P, Morikawa S, McLean JW, Thurston G, Roberge S, Jain RK, and McDonald DM: Openings between defective endothelial cells explain tumor vessel leakiness. Am J Pathol 2000, 156: 1363-1380

5. Brooks PC, Klemke RL, Schon S, Lewis JM, Schwartz MA, and Cheresh DA: Insulin-like growth factor receptor cooperates with integrin alpha v beta 5 to promote tumor cell dissemination in vivo. Journal of Clinical Investigation 1997, 99: 1390-1398

6. Crouch S, Spidel CS, and Lindsey JS: HGF and ligation of avb5 integrin induce a novel, cancer cell-specific gene expression required for cell scattering. Experimental Cell Research 2004, 292: 274-287

7. Klemke RL, Yebra M, Bayna EM, and Cheresh DA: Receptor tyrosine kinase signaling required for integrin alpha v beta 5-directed cell motility but not adhesion on vitronectin. Journal of Cell Biology 1994, 127: 859-866

8. Zhou Y, Fisher SJ, Janatpour M, Genbacev O, Dejana E, Wheelock M, and Damsky CH: Human cytotrophoblasts adopt a vascular phenotype as they differentiate. Journal of Clinical Investigation 1997, 99: 2139-2151

9. Seftor REB, Seftor EA, Koshikawa N, Meltzer PS, Gardner LMG, Bilban M, Stetler-Stevenson WG, Quanranta V, and Hendrix MJC: Cooperative interactions of Laminin 5 g2 Chain, Matrix Metalloproteinase-2, and Membrane Type-1 Matrix/Metalloproteinase are required for mimicry of embryonic vasculogenesis by aggressive melanoma. Cancer Res 2001, 61: 6322-6327

10. Hess AR, Postovit L-M, Margaryan NV, Seftor EA, Schneider GB, Seftor REB, Nickoloff BJ, and Hendrix MJC: Focal Adhesion Kinase promotes the aggressive melanoma phenotype. Cancer Res 2005, 65: 9851-9860

11. van der Schaft DWJ, Hillen F, Pauwels P, Kirschmann DA, Castermans K, oude Egbrink MGA, Tran MGB, Sciot R, Hauben E, Hogendoorn PCW, Delattre O, Maxwell PH, Hendrix MJC, and Griffioen AW: Tumor cell plasticity in Ewing sarcoma, an alternative circulatory system stimulated by hypoxia. Cancer Res 2005, 65: 11520-11528

12. McDonald DM, Munn L, and Jain RK: Vasculogenic mimicry: How convincing, how novel, and how significant? Am J Pathol 2000, 156: 383-388

13. Folberg R, Hendrix MJC, and Maniotis AJ: Vasculogenic mimicry and tumor angiogenesis. Am J Pathol 2000, 156: 361-381

14. Hess AR, Seftor EA, Gardner LMG, Carles-Kinch K, Schneider GB, Seftor REB, Kinch MS, and Hendrix MJC: Molecular regulation of tumor cell vasculogenic mimicry by tyrosine phosphorylation: Role of epithelial cell kinase (Eck/EphA2). Cancer Res 2001, 61: 3250-3255

15. Hintermann E and Quaranta V: Epithelial cell motility on laminin-5: regulation by matrix assembly, proteolysis, integrins and erbB receptors. Matrix Biology 2004, 23: 75-85

16. Hornebeck W and Maquart FX: Proteolyzed matrix as a template for the regulation of tumor progression. Biomedecine & Pharmacotherapy 2003, 57: 223-230

17. Miyazaki K, Kikkawa Y, Nakamura A, Yasumitsu H, and Umeda M: A large cell-adhesive scatter factor secreted by human gastric carcinoma cells. Proceedings of the National Academy of Sciences of the United States of America 1993, 90: 11767-11771

18. Pirila E, Sharabi A, Salo T, Quaranta V, Tu H, Heljasvaara R, Koshikawa N, Sorsa T, and Maisi P: Matrix metalloproteinases process the laminin-5 [gamma]2-chain and regulate epithelial cell migration. Biochemical and Biophysical Research Communications 2003, 303: 1012-1017

19. Pyke C, Romer J, Kallunki P, Lund LR, Ralfkiaer F, Dano K, and Tryggvason K: The gamma 2 chain of kalinin/laminin 5 is preferentially expressed in invading malignant cells in human cancers. The American Journal of Pathology 1994, 145: 782-791

20. Hendrix MJC, Seftor EA, Kirschmann DA, Quaranta V, and Seftor REB: Remodeling of the microenvironment by aggressive melanoma tumor cells. Ann NY Acad Sci 2003, 995: 151-161

21. van der Schaft DWJ, Seftor REB, Seftor EA, Hess AR, Gruman LM, Kirschmann DA, Yokoyama Y, Griffioen AW, and Hendrix MJC: Effects of angiogenesis inhibitors on vascular network formation by human endothelial and melanoma Cells. J Natl Cancer Inst 2004, 96: 1473-1477

22. Condeelis J, Singer RH, and Segall JE: The great escape: When cancer cells hijack the genes for chemotaxis and motility. Annual Review of Cell and Developmental Biology 2005, 21: 695-718

23. Phillips TM and Lindsey JS: Carcinoma cell-specific Mig-7: A new potential marker for circulating and migrating cancer cells. Oncology Reports 2005, 13: 37-44

24. Dokras A, Gardner LMG, Seftor EA, and Hendrix MJC: Regulation of human cytotrophoblast morphogenesis hepatocyte growth factor/scatter factor. Biol Reprod 2001, 65: 1278-1288

25. Fisher SJ, Cui TY, Zhang L, Hartman L, Grahl K, Zhang GY, Tarpey J, and Damsky CH: Adhesive and degradative properties of human placental cytotrophoblast cells in vitro. J Cell Biol 1989, 109: 891-902

26. Librach CL, Werb Z, Fitzgerald ML, Chiu K, Corwin NM, Esteves RA, Grobelny D, Galardy R, Damsky CH, and Fisher SJ: 92-kD type IV collagenase mediates invasion of human cytotrophoblasts. J Cell Biol 1991, 113: 437-449

27. Hess AR, Seftor EA, Seftor REB, and Hendrix MJC: Phosphoinositide 3-kinase regulates membrane type 1-Matrix Metalloproteinase (MMP) and MMP-2 activity during melanoma cell vasculogenic mimicry. Cancer Res 2003, 63: 4757-4762

28. Seftor REB, Seftor EA, and Hendrix MJC: Molecular roles for integrins in human melanoma invasion. Cancer Metastasis Reviews 1999, 18: 359-375

29. Haimov-Kochman R, Fisher SJ, and Winn VD: Modification of the standard Trizol-based technique improves the integrity of RNA isolated from RNase-rich placental tissue. Clin Chem 2006, 52: 159-160

30. McMaster MT, Librach CL, Zhou Y, Lim KH, Janatpour MJ, DeMars R, Kovats S, Damsky C, and Fisher SJ: Human placental HLA-G expression is restricted to differentiated cytotrophoblasts. J Immunol 1995, 154: 3771-3778

31. Tarrade A, Goffin F, Munaut C, Lai-Kuen R, Tricottet V, Foidart JM, Vidaud M, Frankenne F, and Evain-Brion D: Effect of Matrigel on human extravillous trophoblasts differentiation: Modulation of protease pattern gene expression. Biol Reprod 2002, 67: 1628-1637

32. Qiu Q, Yang M, Tsang BK, and Gruslin A: Both mitogen-activated protein kinase and phosphatidylinositol 3-kinase signalling are required in epidermal growth factor-induced human trophoblast migration. Mol Hum Reprod 2004, 10: 677-684

33. Way DL, Grosso DS, Davis JR, Surwit EA, and Christian DD: Characterization of a new human endometrial carcinoma (RL95-2) established in tissue culture. In Vitro 1983, 19: 147-158

34. Kuramoto H: Studies of the growth and cytogenetic properties of human endometrial adenocarcinoma in culture and its development into an established line. Acta Obstetrica et Gynaecologica Japonica 1972, 19: 47-58

35. Bae-Jump V, Segreti EM, Vandermolen D, and Kauma S: Hepatocyte growth factor (HGF) induces invasion of endometrial carcinoma cell lines in vitro. Gynecologic Oncology 1999, 73: 265-272

36. Kleinman HK, McGarvey ML, Liotta LA, Robey PG, Tryggvason T, and Martin GR: Isolation and characterization of type IV procollagen, laminin, and heparan sulfate proteoglycan from the EHS sarcoma. Biochemistry 1982, 21: 6188-6193

37. Kleinman HK, McGarvey ML, Hassell GR, Star VL, Cannon FB, Laurie GW, and Martin GR: Basement membrane complexes with biological activity. Biochemistry 1986, 25: 312-318

38. Givant-Horwitz V, Davidson B, and Reich R: Laminin-induced signaling in tumor cells. Cancer Letters 2005, 223: 1-10

39. Koshikawa N, Minegishi T, Sharabi A, Quaranta V, and Seiki M: Membrane-type Matrix Metalloproteinase-1 (MT1-MMP) is a processing enzyme for human laminin {gamma}2 chain. J Biol Chem 2005, 280: 88-93

40. Oku N, Sasabe E, Ueta E, Yamamoto T, and Osaki T: Tight junction protein claudin-1 enhances the invasive activity of oral squamous cell carcinoma cells by promoting cleavage of laminin-5 {gamma}2 chain via Matrix Metalloproteinase (MMP)-2 and Membrane-Type MMP-1. Cancer Res 2006, 66: 5251-5257

41. Discher DE, Janmey P, and Wang Y-L: Tissue cells feel and respond to the stiffness of their substrate. Science 2005, 310: 1139-1143

42. Walker-Daniels J, Hess AR, Hendrix MJC, and Kinch MS: Differential regulation of EphA2 in normal and malignant cells. Am J Pathol 2003, 162: 1037-1042

43. Cukierman E, Pankov R, Stevens DR, and Yamada KM: Taking cell-matrix adhesions to the third dimension. Science 2001, 294: 1708-1712

44. Debnath J and Brugge JS: Modeling glandular epithelial cancers in three-dimensional cultures. Nat Rev Cancer 2005, 5: 675-688

45. Weaver VM, Fischer AH, Peterson OW, and Bissell MJ: The importance of the microenvironment in breast cancer progression: recapitulation of mammary tumorigenesis using a unique human mammary epithelial cell model and a three-dimensional culture assay. Biochemistry and Cell Biology 1996, 74: 833-851

46. Schenk S, Hintermann E, Bilban M, Koshikawa N, Hojilla C, Khokha R, and Quaranta V: Binding to EGF receptor of a laminin-5 EGF-like fragment liberated during MMP-dependent mammary gland involution. J Cell Biol 2003, 161: 197-209

47. Frangou E, Lawson J, and Kanthan R: Angiogenesis in male breast cancer. World Journal of Surgical Oncology 2005, 3: 16

48. Mayer U, Nischt R, Poschl E, Mann K, Fukuda K, Gerl M, Yamada Y, and Timpl R: A single EGF-like repeat-like motif of laminin is responsible for high affinity nidogen binding. EMBO Journal 1993, 12: 1879-1885

49. Lucia-Ortega L, De los Ríos V, Martínez-Ruiz A, Oñaderra M, Lacadena J, and Gavilanes JG: Anomalous electrophoretic behavior of a very acidic protein: Ribonuclease U2. Electrophoresis 2005, 26: 3407-3413

50. Folberg R, Arbieva Z, Moses J, Hayee A, Sandal T, Kadkol S, Lin AY, Valyi-Nagy K, Setty S, Leach L, Chevez-Barrios P, Larsen P, Majumdar D, Pe'er J, and Maniotis AJ: Tumor cell plasticity in uveal melanoma: Microenvironment directed dampening of the invasive and metastatic genotype and phenotype accompanies the generation of vasculogenic mimicry patterns. Am J Pathol 2006, 169: 1376-1389

51. Natarajan E, Omobono JD, II, Guo Z, Hopkinson S, Lazar AJF, Brenn T, Jones JC, and Rheinwald JG: A keratinocyte hypermotility/growth-arrest response

involving laminin 5 and p16INK4A activated in wound healing and senescence. Am J Pathol 2006, 168: 1821-1837

52. Garlick JA and Talchman LB: Fate of human keratinocytes during reepithelialization in an organotypic culture model. Laboratory Investigation 1994, 70: 916-924

53. Sood AK, Seftor EA, Fletcher MS, Gardner LMG, Heidger PM, Buller RE, Seftor REB, and Hendrix MJC: Molecular determinants of ovarian cancer plasticity. Am J Pathol 2001, 158: 1279-1288

54. Sun B, Zhang S, Zhang D, Du J, Guo H, Zhao X, Zhang W, and Hao X: Vasculogenic mimicry is associated with high tumor grade, invasion and metastasis, and short survival in patients with hepatocellular carcinoma. Oncology Reports 2006, 16: 693-698

55. Chang YS, di Tomaso E, McDonald DM, Jones R, Jain RK, and Munn LL: Mosaic blood vessels in tumors: Frequency of cancer cells in contact with flowing blood. PNAS 2000, 97: 14608-14613

56. Hendrix MJC, Seftor EA, Meltzer PS, Gardner LMG, Hess AR, Kirschmann DA, Schatteman GC, and Seftor REB: Expression and functional significance of VE-cadherin in aggressive human melanoma cells: Role in vasculogenic mimicry. PNAS 2001, 98: 8018-8023

57. Sadler JE: Biochemistry and genetics of von Willebrand factor. Annual Reviews in Biochemistry 1998, 67: 395-424

Table I. siRNA sequences specific to Mig-7

Sequence antisense-loop-sense	Location in Mig-7 sequence (accession: DQ080207) in base pairs	Pooled clones number
AAAGTTTCATTCTTCGACTTCAAGAGA GTCGAAGAAATGAAACTTT	379 - 398	1-3A
AGATTTCCTGTGATTTAAGTTCAAGAGA CTTAAATCACAGGAAATCT	728 - 746	2-3B
CATGATCTGGATTTGAATCTTCAAGAGA GATTCAAATCCAGATCATG	1275 - 1293	3-1A

Figure 1. Early gestation human placental tissue and invasive embryonic cytotrophoblasts express Mig-7. **a:** Representative relative RT-PCR analysis of Mig-7 mRNA expression in early and late gestation placenta. Mig-7 amplicon (501 bp) is present in early gestation placenta (7 weeks) but not in term placenta (38 weeks, term). Ribosomal 18S RNA amplicon (324 bp) served as loading control. RNA isolation and relative RT-PCR including optimization of cycle number to achieve mid-linear range were performed as described previously [80]. **b:** RT-PCR of human placental basal plate RNA from second trimester and term shows expression of Mig-7 highest prior to 22 weeks gestation (16, 19.5 weeks), reduced at 23 weeks and undetectable at term. RL95 cells served as positive control and ribosomal 18S RNA served as loading control. **c:** Immunoblot of Mig-7 protein from cells of first second and third trimester placenta basal plate. Tubulin probe was used as a loading control. **d:** Densitometry of immunoblot in c. Note decrease of Mig-7 protein consistent with a decrease in Mig-7 protein mRNA shown in a and b. Ten basal plate placenta samples, 2 first trimester, 2 second trimester, 2 third trimester and 2 term, were used. **e:** Quantitative (Q)-PCR analysis of Mig-7 mRNA in triplicate on reversed transcribed total RNA isolated from human cytotrophoblasts prior to and 3, 12 and 36 hours after plating on Matrigel from 4 separate cytotrophoblast isolations (○=13weeks, ●=13+15weeks, △=15+18weeks, ▲=14.5+19weeks). Data are presented as mean ± SE. The mean 12 hour time point for all experiments was significantly different compared to 0 hour (p=0.001) using the Student's t-test. **f:** Representative quantitative (Q)-PCR analysis of HLA-G and integrin α1 mRNA in triplicate on reversed transcribed total RNA isolated from human cytotrophoblasts (13 weeks) prior to and 3, 12 and 36 hours after plating on Matrigel

(○=integrin α1, ■=HLA-G).   Data are presented as mean ± SE. **g:** Representative Western blot analysis of Mig-7 in 2nd trimester isolated CTBs plated on Matrigel for the indicated times. Human platelet (plt) lysate served as a negative control. Note that Mig-7 antibody detects a 46 kD sized band from CTBs plated on Matrigel in addition to the previously published 23kD from carcinoma cells plated on plastic. **h:** Representative immunohistochemistry of a section (10% formalin fixed, paraffin embedded, 5 µm) of 19 week gestation basal plate using cytokeratin 7 (CK7), an antigen specific to CTB, antibody. **i:** Representative immunohistochemistry of cells in the basal plate (19 weeks gestation) expressing Mig-7. Note that areas of staining (brown) are the same for both antigens (h and i) in these serial sections. Two different basal plates were examined from each of first, second and third trimester placentas for each protein. CK7 and Mig-7 demonstrated the same areas of staining. Bars represent 20 µm. Experiments were repeated at least twice (> 3 times for Q-PCR).
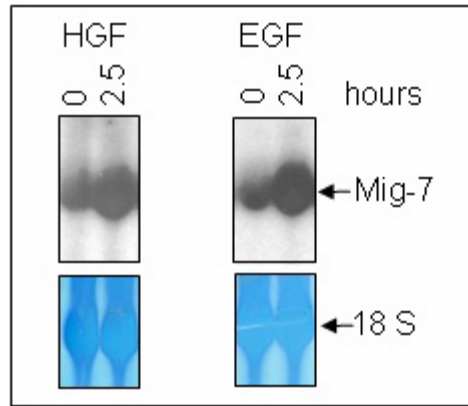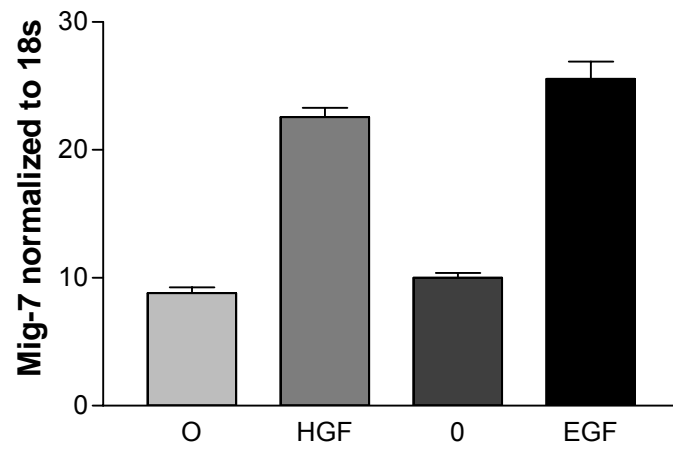
g

h

i
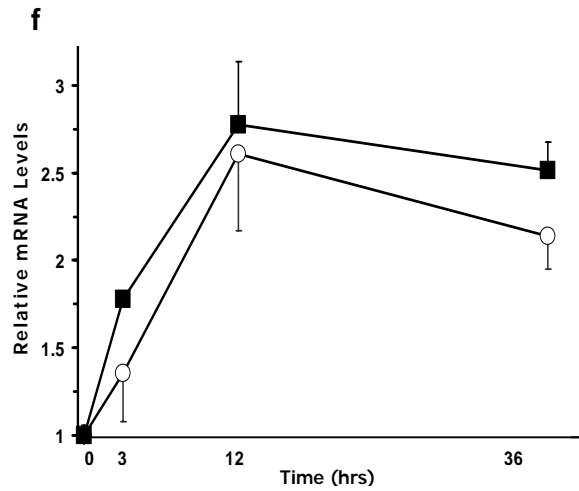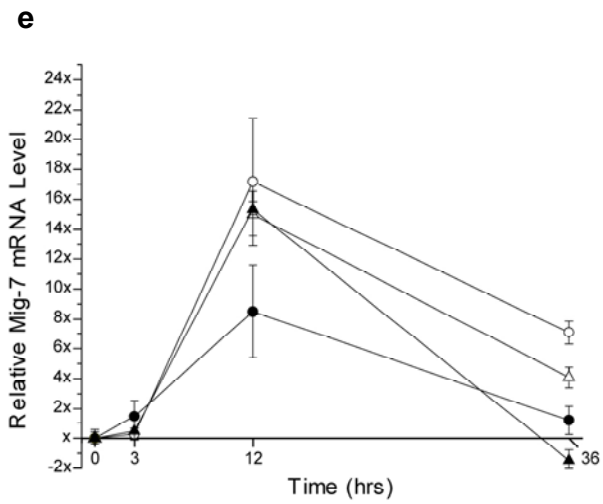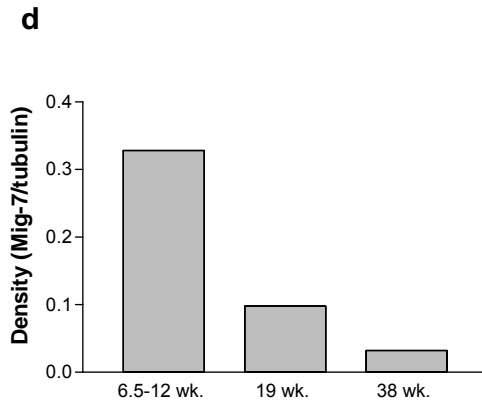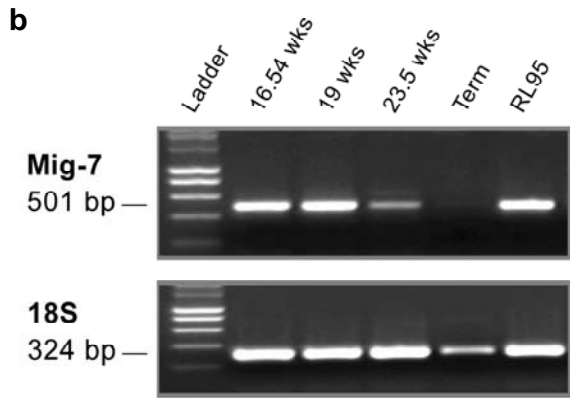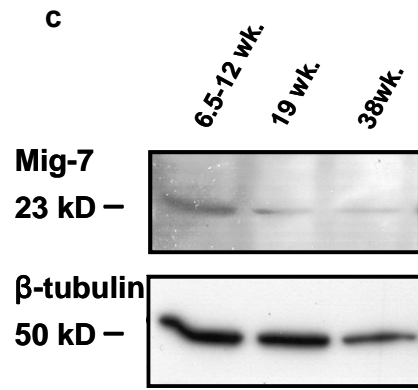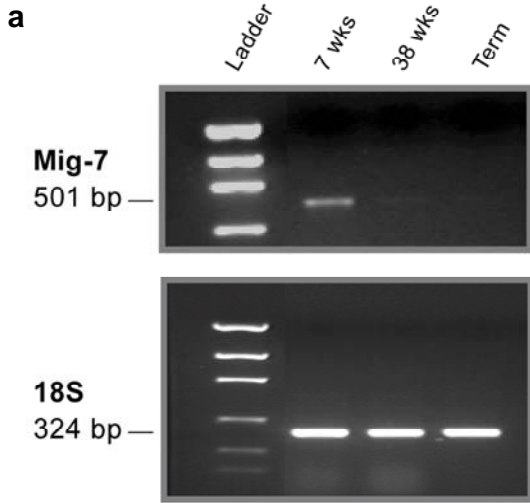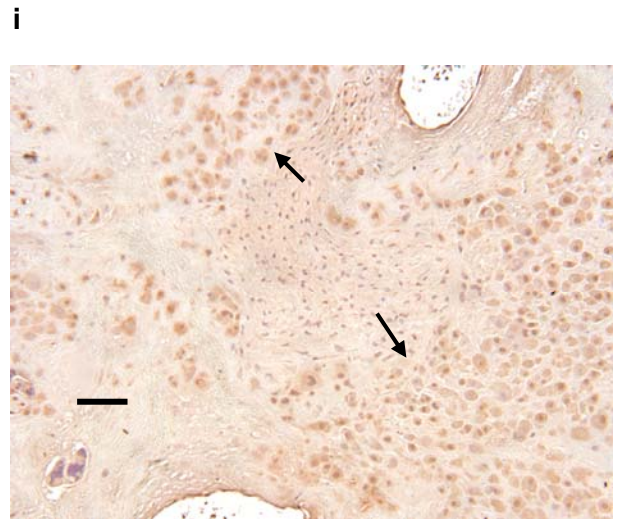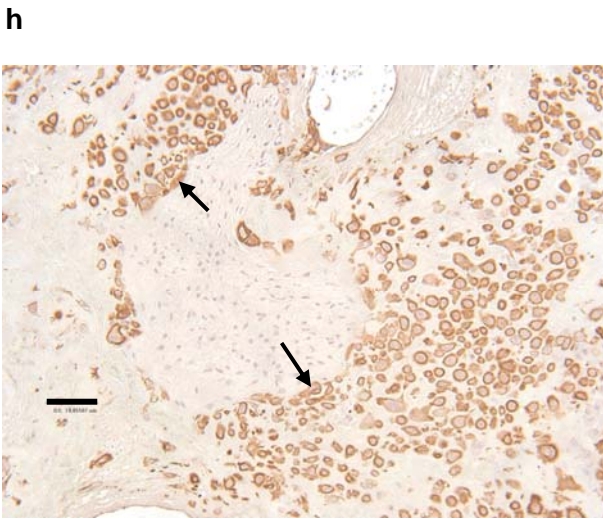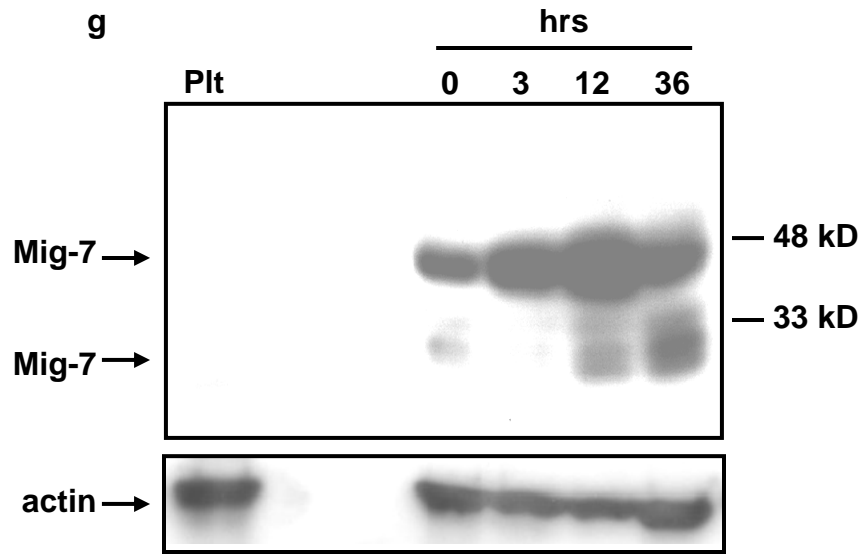
Figure 2. Tumor microenvironment RTK ligands, HGF and EGF induce Mig-7 in RL95 endometrial carcinoma cells. **a:** Representative Northern blot analyses shows that after 12 hours of serum starvation EGF induces Mig-7 as similar to HGF treatment, the growth factor used to isolate Mig-7. **b:** Northern blot densitometry analyses with Mig-7 band intensities normalized to those for respective 18s bands stained with methylene blue revealed that EGF induced Mig-7 mRNA at least if not more so than does HGF. Error bars represent SEM. **c:** Representative immunoblot of serum starved (48 hours) HEC1A and RL95 cells that endogenously express Mig-7 plated on Matrigel that contains growth factors unless indicated as reduced growth factor Matrigel (GFR). Previously reported 23 kD Mig-7 was detected in addition to a higher kD ~63 sized band not seen in lysates from cells plated on plastic. No Mig-7 is detected in lysates from either cell line plated on GFR Matrigel. **d:** Densitometry and statistical analyses of these immunoblots revealed that the larger Mig-7 kD band was significantly greater in HEC1A cells. Error bars represent SEM. **e:** Representative Mig-7 and laminin 5 γ2 chain domain III fragment immunoblot analysis of protein lysates from serum starved (48 hours) RL95 cells plated for 17 h on GF+ or GFR Matrigel. Blots were stripped and reprobed with anti-γ2 domain III antibody or new immunblots run and probed first with anti-γ2 antibody to confirm that this was not residual Mig-7 antibody detection at ~63 kD. Detection of β-actin at the last probing served as loading control. **f:** Representative immunoblot detection of FLAG-Mig-7 and laminin 5 γ2 chain domain III fragments in lysates from three pooled clone, stable transfectants (A, B, and C) and from empty vector transfected HT29 colon carcinoma cells. All cells were plated on GF+ Matrigel. Note predominant γ2 chain fragment ~66 kD bands in Mig-7 expressing HT29 cells.

Detection of β-actin at the last probing of each blot served as loading control. Figure 2 experiments were repeated three times in triplicate.
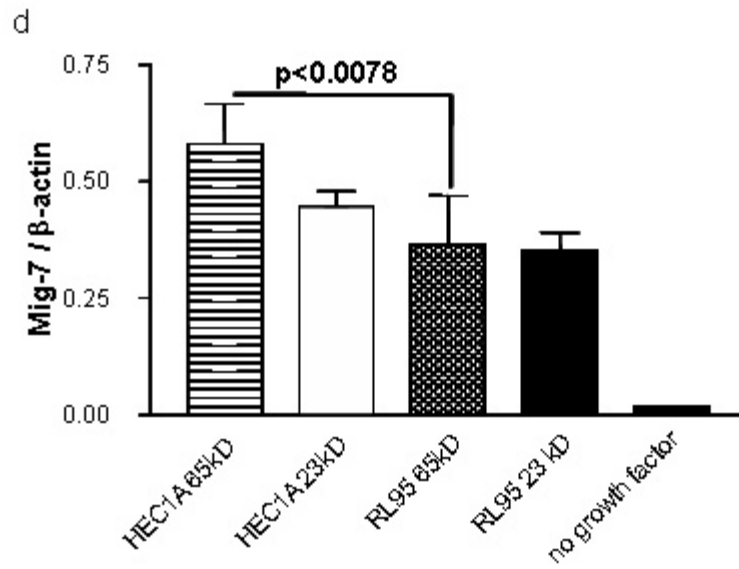
a

b

c

kD

75 —
50 —   HEC1A   GFR   RL95   GFR   All on Matrigel (2D)

← Mig-7

25 —
20 —

← Mig-7

42 —

← β-actin

d

p<0.0078

Mig-7 / β-actin

0.75

0.50

0.25

0.00

HEC1A 65KD   HEC1A 23kD   RL95 65KD   RL95 23 KD   no growth factor

e

17 h 2D GF+ Matrigel

17 H 2D GFR Matrigel

kD

75 —

50 — ← Mig-7

75 — ⎤ γ2 chain domainIII
50 — ⎦ fragments

42 — ← β-actin

f

GF+ Matrigel

3XFLAGCMV Mig-7

A   B   C   vector

75 —
50 —   ← FLAG Mig-7

25 —   ← FLAG Mig-7
20 —

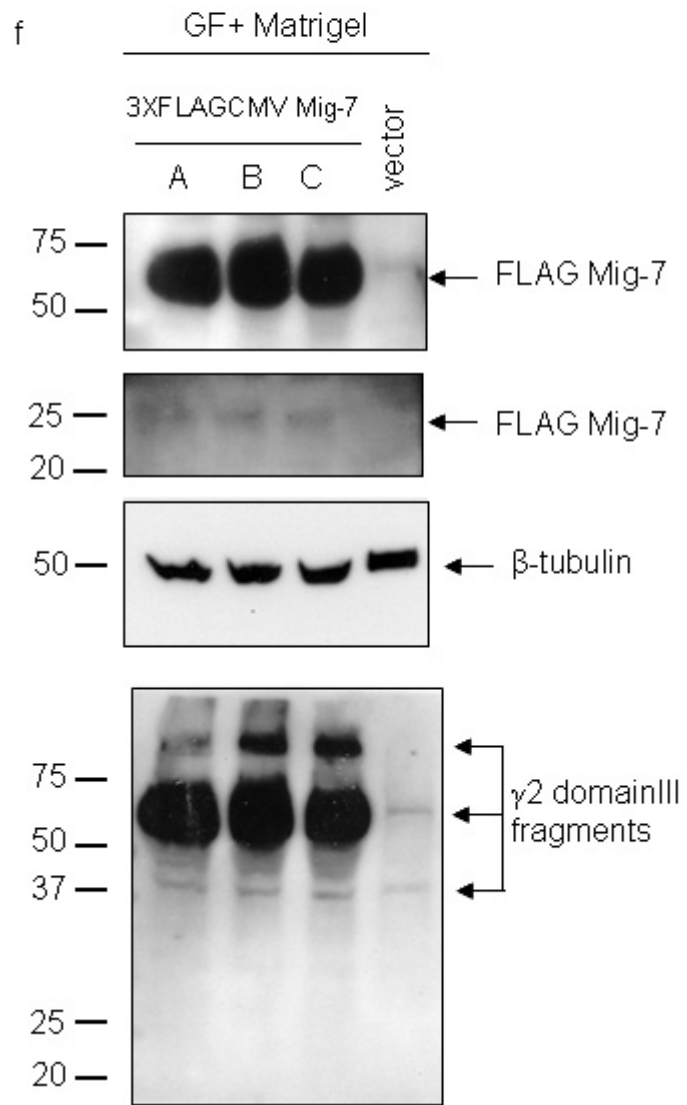50 —   ← β-tubulin

75 —   ← γ2 domainIII
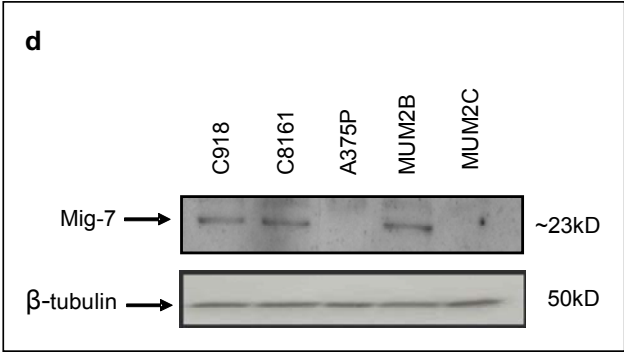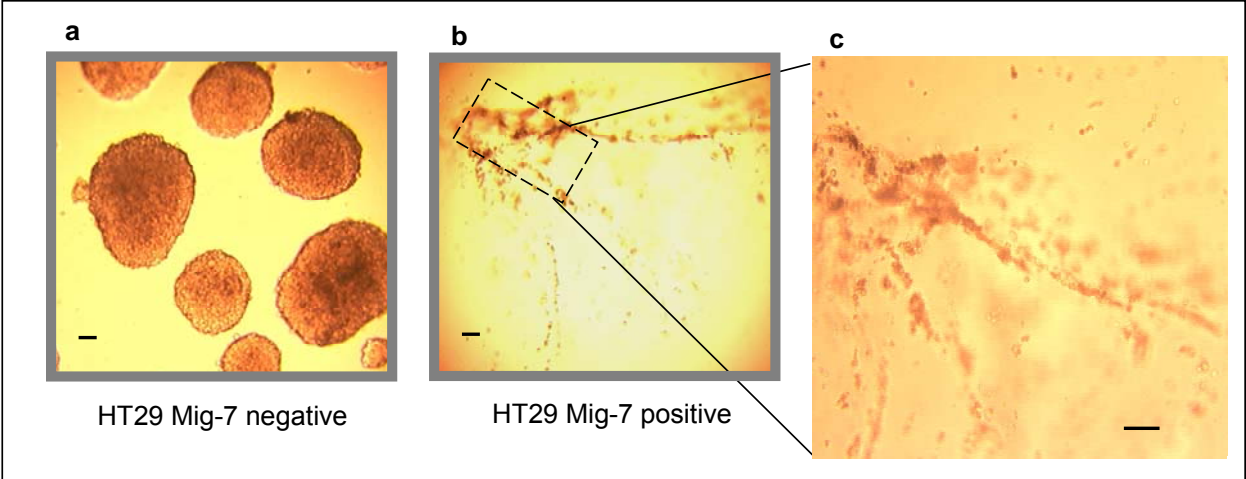50 —   fragments
37 —

25 —
20 —

Figure 3. HT29 Mig-7 overexpression causes cell spreading on GF+ Matrigel but not

on plastic. **a:** HT29 cells overexpressing FLAG-Mig-7 at 17 hours. There is no

morphological difference observed at this time period compared to empty vector HT29

cells (a and d), Bar represents 100 µm. **b:** After 10 days on GF+ Matrigel, HT29 cells

overexpressing FLAG-Mig-7 spread over the matrix in contrast to HT29 non expressing

cells that primarily form colonies and do not spread over the matrix (compare b and e)

Bar represents 150 µm. **c:** HT29 cells overexpressing FLAG-Mig-7 plated on plastic did

not appear different from empty vector HT29 cells on plastic (c and f). Bars represent 20

µm. Empty vector HT29 cells after **d:** 17 hours on GF+ Matrigel. **e:** 10 days on GF+

Matrigel or **f:** on plastic. Figure 3 experiments were repeated 3 times in triplicate.

17 hr on GF+ Matrigel

10 d on GF+ Matrigel

7 d on plastic (no Matrigel)

HT29 FLAG- Mig-7
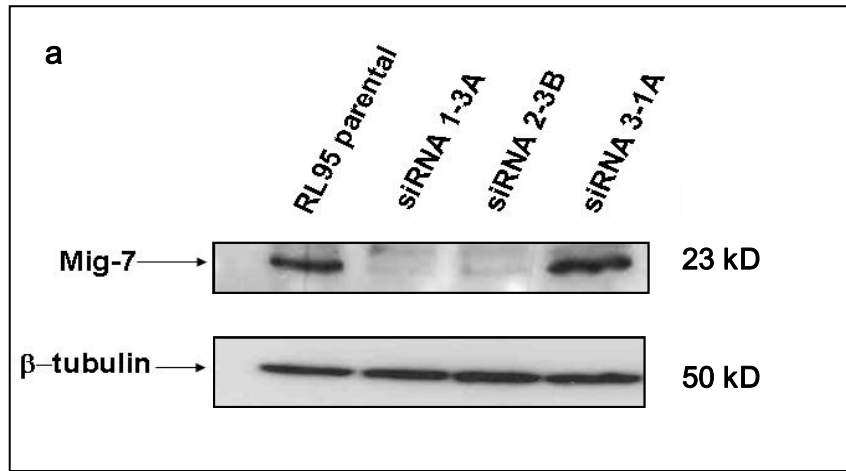
HT29 empty vector

a

b

c

d

e

f
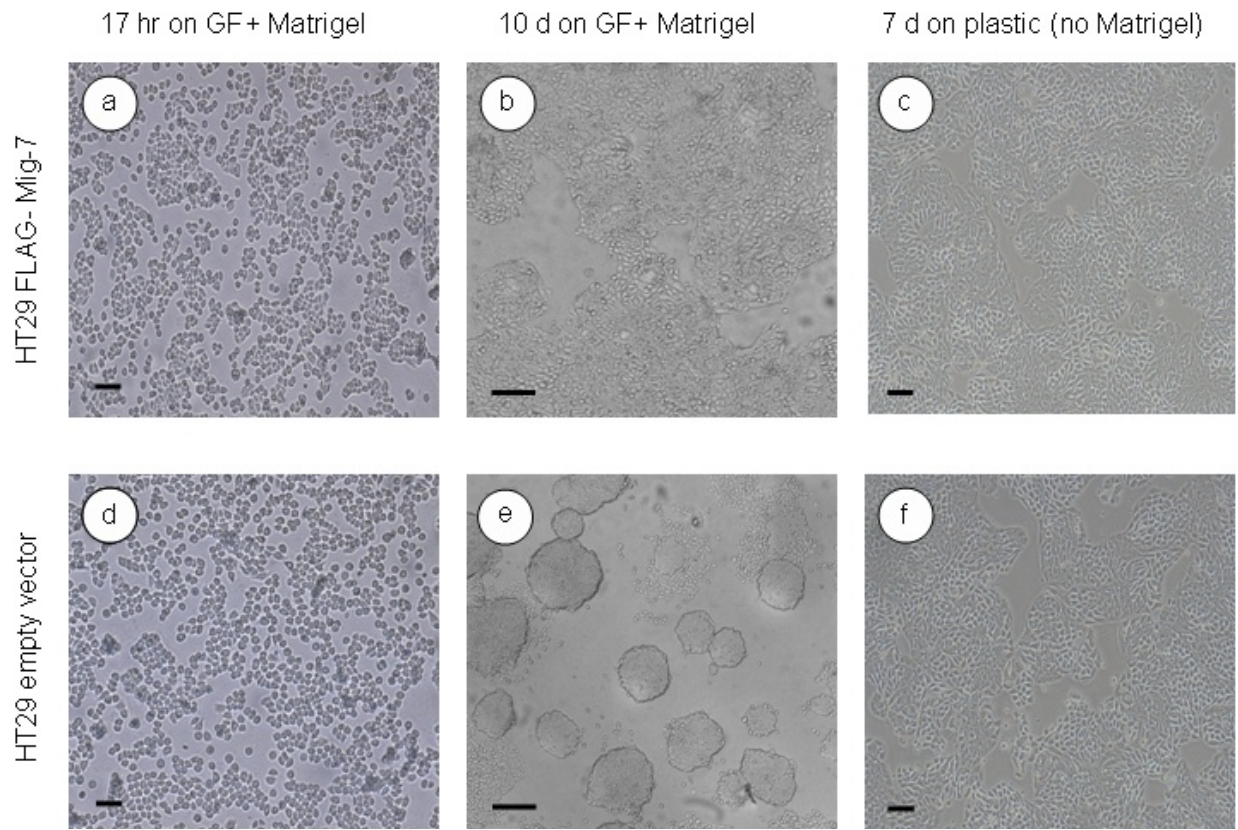
Figure 4. Mig-7 overexpression caused vessel formation in Matrigel 3D cultures. **a:** HT29 cells with empty vector form discrete colonies in 3D GF+ Matrigel cultures. Bar represents 150 µm. **b:** In contrast, HT29 cells overexpressing FLAG Mig-7 invade the 3D Matrigel and appear to form vessel-like structures. Bar represents 150 µm. **c:** Inset from b at higher magnification. Bar represents 100 µm. Supplemental data: Images taken at four different planes through 3D domes of Matrigel in which Mig-7 expressing cells invaded demonstrated cords of cells with vessel-like appearance. Images taken in z-dimension have cells in focus and out of focus (i.e. not in that focal plane). **d:** Representative immunoblot analysis of Mig-7 expression in melanoma cells that aggressively invade and undergo vasculogenic mimicry (C918, C8161, MUM2B). A lack of Mig-7 protein is found in melanoma cell lines that are poorly invasive and fail to form vessel-like structures (A375P, MUM2C). Stripping and reprobing with β-tubulin antibody was used to confirm equal amounts of protein loaded for each cell lysate. Experiments in figure 3 were repeated 3 times in triplicate (3D cultures) or with each cell line (d).

a

HT29 Mig-7 negative

b

HT29 Mig-7 positive

c

d

Mig-7 ➔

β-tubulin ➔

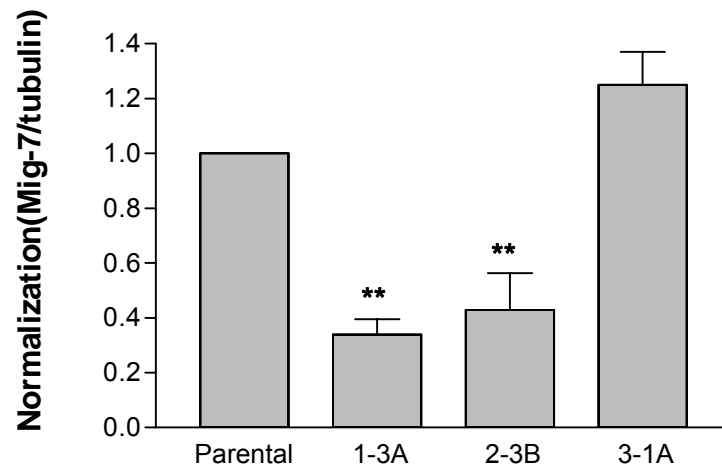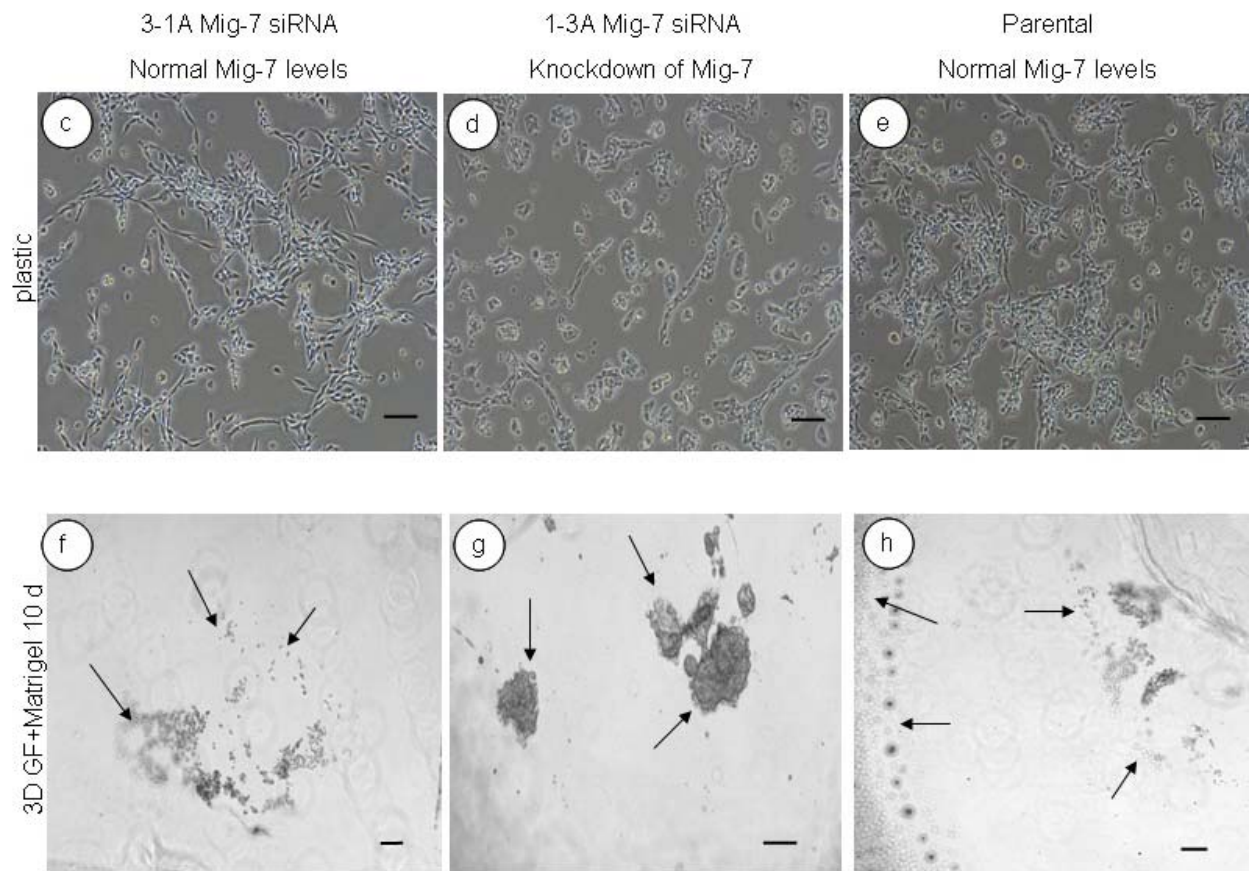C918 C8161 A375P MUM2B MUM2C

~23kD

50kD

Figure 5. Mig-7 siRNA reduces Mig-7 protein levels and invasion. **a:** Representative immunoblot analysis of parental and Mig-7-specific siRNA stably transfected, pooled clones RL95 cell lines 1-3A, 2-3B, and 3-1A. Cells were grown for 4 days before harvesting cell lysates. Stripping and reprobing with β-tubulin confirmed equal loading and transfer of 20 μg protein each sample. **b:** Densitometry analyses demonstrated a consistent 3.5-3.8 fold, statistically significant ($p < 0.01$) reduction of Mig-7 protein in RL95 1-3A and 2-3B siRNA stably transfected cells. Experiments were repeated three times. Error bars represent SEM. **c:** Stably tranfected RL95 siRNA 3-1A on plastic. **d:** Stably transfected RL95 siRNA 1-3A on plastic. **e:** Parental (no transfection) RL95 on plastic. No difference in morphology was observed on plastic in normal growth media (compare c, d, and e). **f:** RL95 cells stably transfected with 3-1A Mig7 siRNA invaded (**arrows**) GF+ Matrigel and did not form dense colonies (**arrow**) after 10 days. **g:** In contrast, RL95 cells stably transfected with 1-3A Mig-7 siRNA, that reduced levels of Mig-7 by 3.8 fold, predominantly formed dense colonies (**arrows**) after 10 days. **h:** Parental RL95 cells that expressed the same level of Mig-7 protein as those transfected with 3-1A construct invaded and did not form dense colonies (**arrows**) in GF+ Matrigel after 10 days. All bars represent 100 μm.

a

	RL95 parental	siRNA 1-3A	siRNA 2-3B	siRNA 3-1A	
Mig-7 →					23 kD
β−tubulin →					50 kD

b

3-1A Mig-7 siRNA	1-3A Mig-7 siRNA	Parental
Normal Mig-7 levels	Knockdown of Mig-7	Normal Mig-7 levels

69

Figure 6. Mig-7 expression causes decreased adhesion to tissue culture plastic and to laminin. **a:** Image of selected colonies in which the top well contained empty vector transfected HT29 cells and the bottom well contained 3XFLAG cytomegalovirus (CMV) promoter vector containing Mig-7 encoding region transfected cells. Note the area denuded **(dotted line)** after suctioning off media in Mig-7 expressing cells. **b:** HT29 Mig-7 expressing cells (**black columns**) were >30% less adherent than HT29 cells transfected with empty vector (**grey columns**) to a mix of laminins 1, 2, 3, 6, 8 & 10 in a statistically significant manner ($p < 0.001$). Experiments were performed three times in replicates of six well per matrix component and BSA as control. One-way analysis of variance (ANOVA) was used in the GraphPad Prism statistical analyses software. $P < 0.05$ was considered significant. Error bars represent SEM. Experiments in this figure were repeated three times.
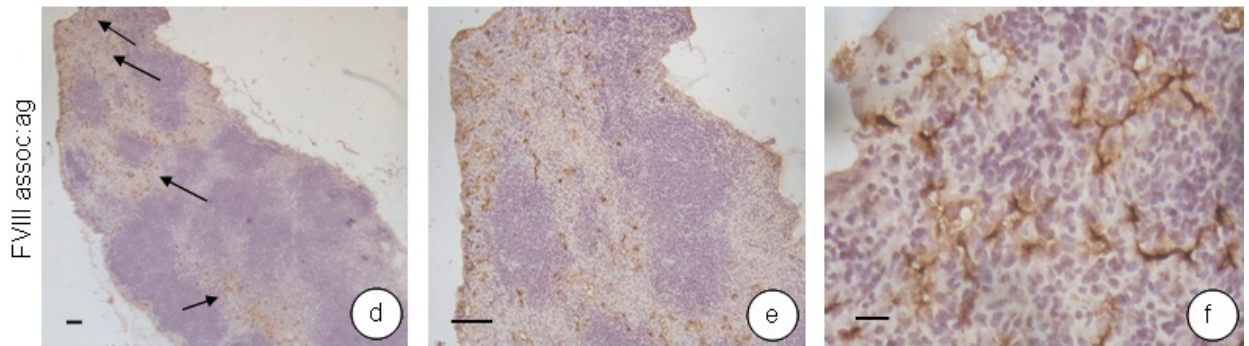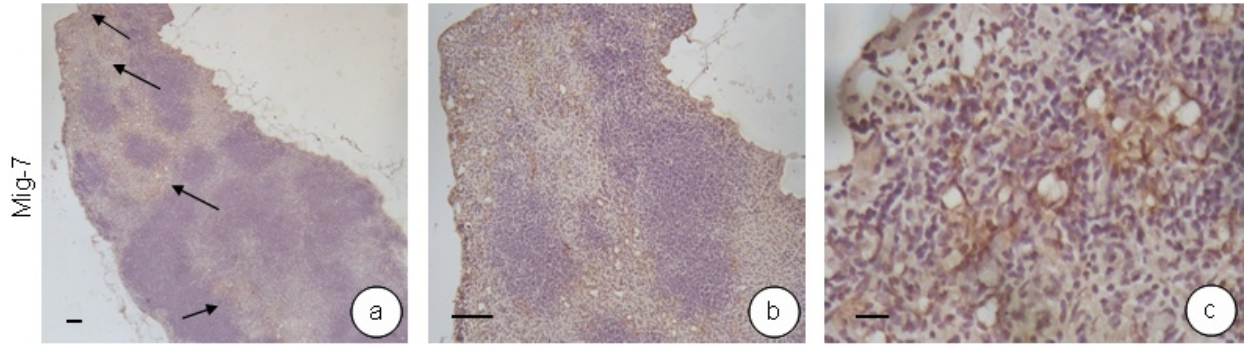
a

b

OD 550 nm

p<0.001

fibronectin
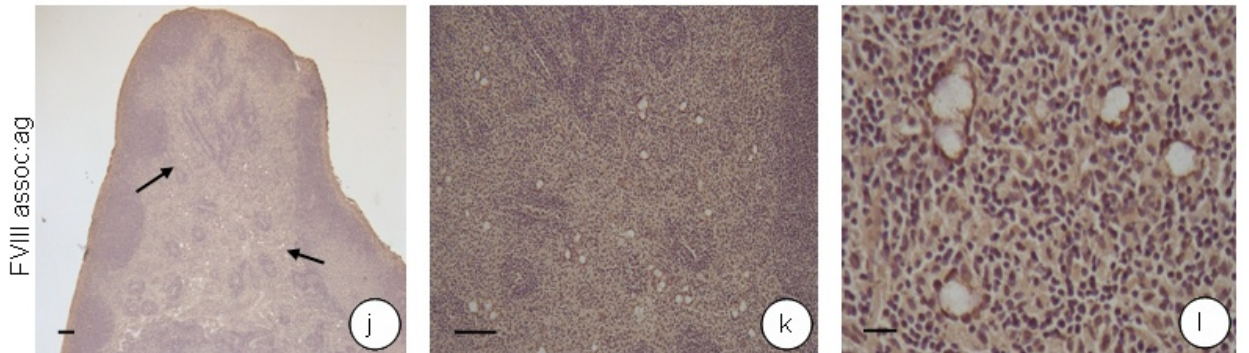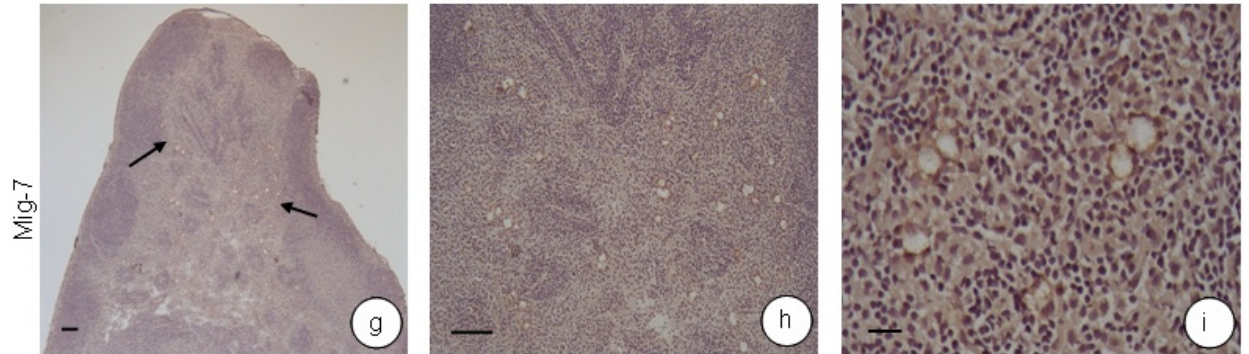vitronectin
laminin
collagen I
collagen IV
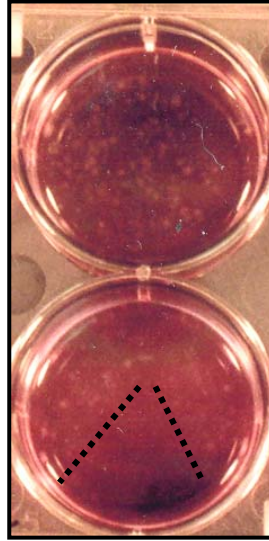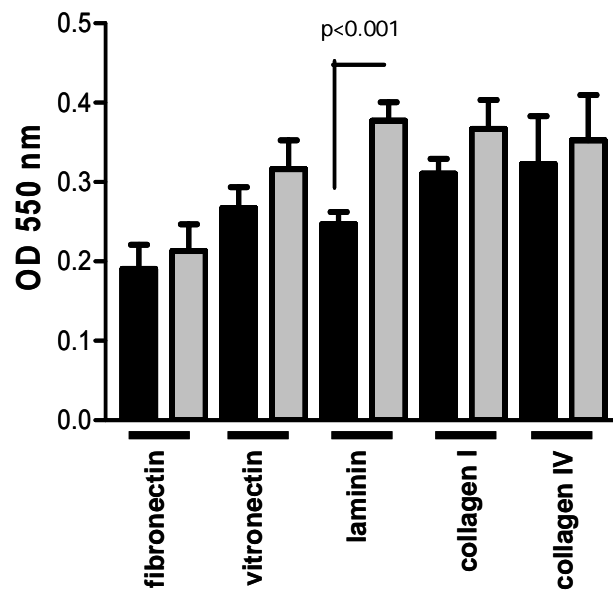
Figure 7. *In situ*, Mig-7 protein co-localized primarily to vessel-like structures in lymph nodes from xenograft nude mouse models of metastasis. Representative IHC of lymph nodes from HEC-1A cell injected nude mice detecting Mig-7 protein localization (DAB, brown stain) at **a:** low (40X) magnification, arrows show representative "hot spots" of vessel like structures **b:** 100X magnification and **c:** 400X magnification. Representative IHC of lymph nodes from HEC-1A cell injected nude mice detecting FVIII assoc:ag protein localization (DAB, brown stain) at **d:** low (40X) magnification arrows show representative "hot spots" of vessel like structures, **e:** 100X magnification and **f:** 400X magnification. Representative IHC of lymph nodes from RL95 cell injected nude mice detecting Mig-7 protein localization (DAB, brown stain) at **g:** low (40X) magnification, arrows show representative "hot spots" of vessel like structures, **h:** 100X magnification and **i:** 400X magnification. Representative IHC of lymph nodes from RL95 cell injected nude mice detecting FVIII assoc:ag protein localization (DAB, brown stain) at **j:** low (40X) magnification, arrows show representative "hot spots" of vessel like structures, **k:** 100X magnification and **l:** 400X magnification. Representative IHC of normal lymph nodes from nude mice to detect Mig-7 protein at **m:** low (40X) magnification, **n:** 100X magnification and **0:** 400X magnification. Note that no vessel-like structures or specific DAB staining was observed. Representative IHC of normal lymph nodes to detect FVIII assoc:ag at **p:** low (40X) magnification, **q:** 100X magnification and **r:** 400X magnification. Note that no vessel-like structures or specific DAB staining was observed. Representative no primary antibody IHC of HEC-1A cell injected nude mice. at **s:** low (40X) magnification, **t:** 100X magnification and **u:** 400X magnification. Note that no specific DAB staining was observed. Bars in 40X and 100X images represent

72

100 μm and in 400X images represent 20 μm. Experiments were repeated four times with 4-5 animals per treatment group. Counterstain was hematoxylin. **v:** Median number of vessel-like "hot spots" in lymph nodes from HEC1A or RL95 cell line injected nude mice. P < 0.05 was considered significant. Error bars represent SEM. **w:** Median diameter of vessel-like structures in lymph nodes from HEC1A or RL95 cell line injected nude mice. Error bars represent SEM.

HEC1A invaded lymph nodes

RL95 invaded lymph nodes

74

normal lymph nodes

Mig-7

FVIII assoc·ag

No primary antibody

HEC1A invaded lymph nodes

p < 0.0238

number of Mig-7 hot spots

HEC1A   RL95

vessel diameter (μm)

HEC1A   RL95
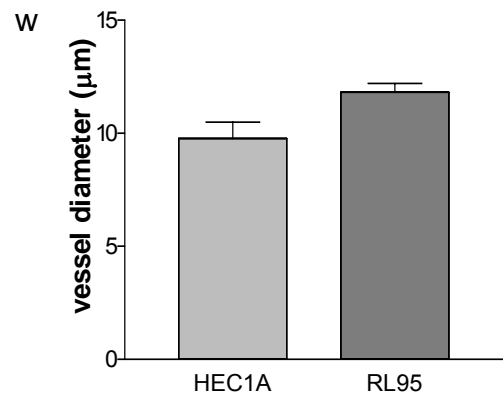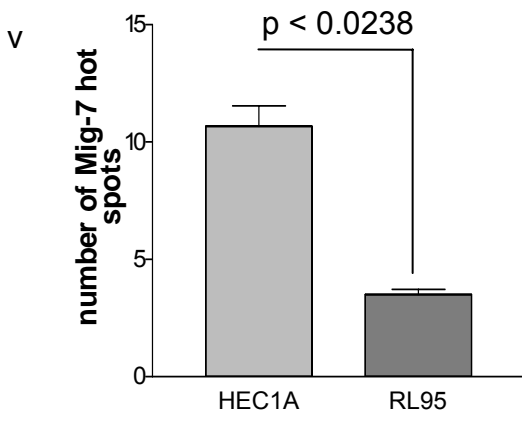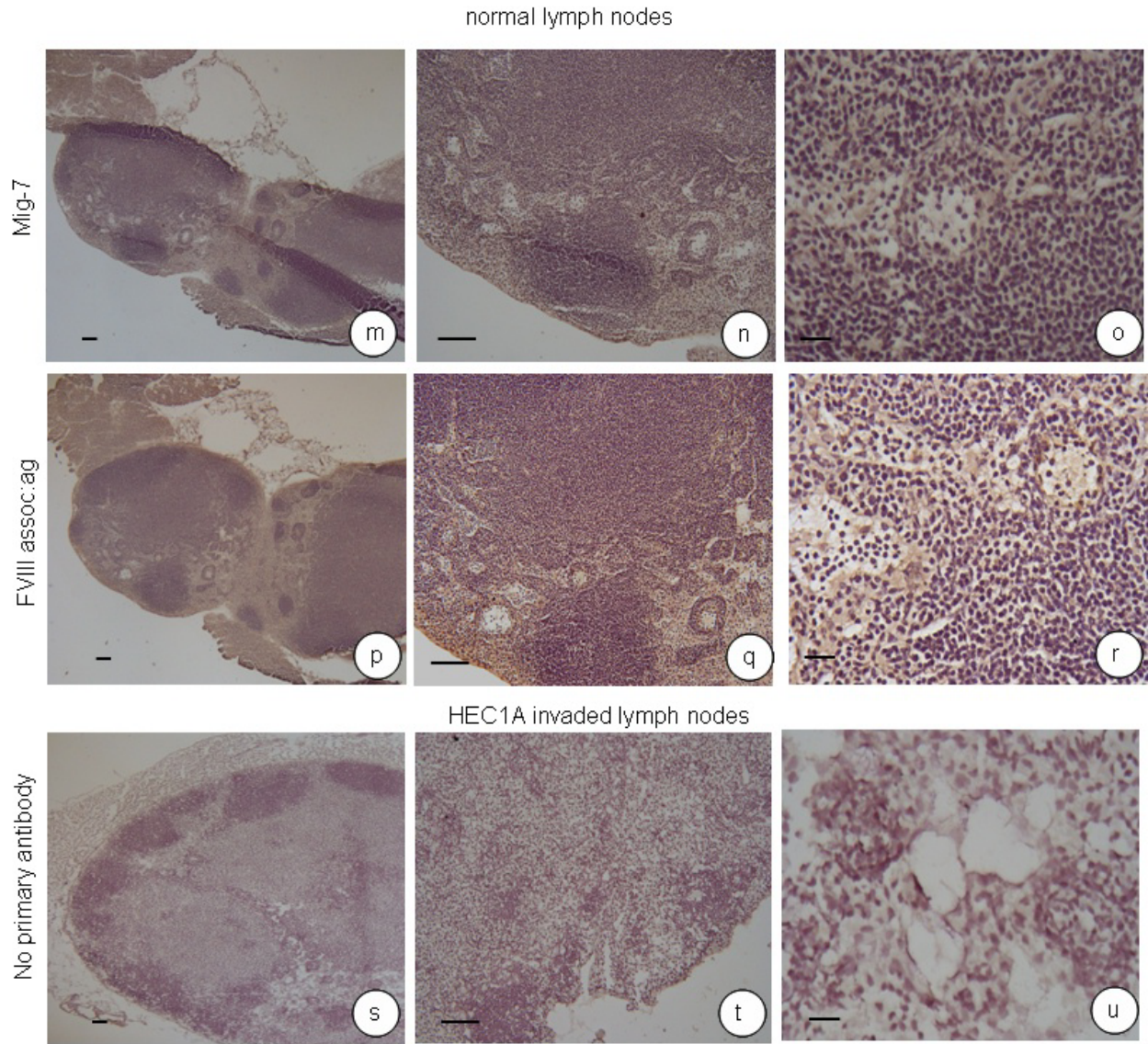
Figure 8. Localization of endothelial markers and laminin 5 γ2 to cells lining vessel-like structures in lymph nodes of RL95 or HEC1A cell line injected nude mice. In lymph nodes from RL95 cell line injected nude mice **a:** Mig-7 specific staining in vessel-like structure (arrows) **b:** FVIII assoc:ag specific staining in vessel-like structures (**arrows**) and at sites (**stars**) outside these structures, **c:** laminin 5 γ2 chain staining (**arrows**) in vessel-like structures, and **d:** VE-cadherin specific staining (**arrows**) in vessel-like structure. In lymph nodes from HEC1A cell line injected nude mice **e:** Mig-7 specific staining in vessel-like structure (arrows) **f:** FVIII assoc:ag specific staining in vessel-like structures (**arrows**) and at sites (**stars**) outside these structures, **g:** laminin 5 γ2 chain staining (**arrows**) in vessel-like structures, and **h:** VE-cadherin specific staining (**arrows**) in vessel-like structure. **i:** No specific staining was observed in no primary antibody processed lymph nodes from carcinoma cell injected nude mice. Vessel-like structures or positive staining for **j:** Mig-7, **k:** FVIII assoc:ag, **l:** laminin 5 γ2 chain domain III fragment or **m:** VE-cadherin was detected in normal lymph nods fro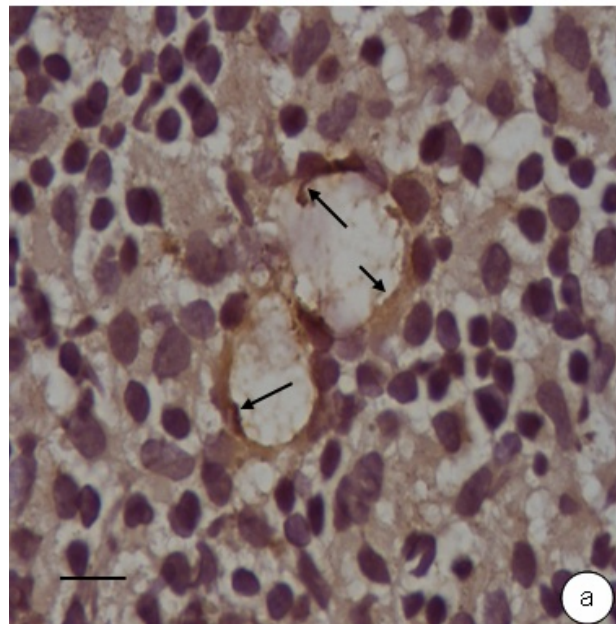m nude mice. Experiments were repeated four times with 4-5 animals per treatment group. Counterstain was hematoxylin. Bars represent 10 µm.

Mig-7

FVIII assoc:ag
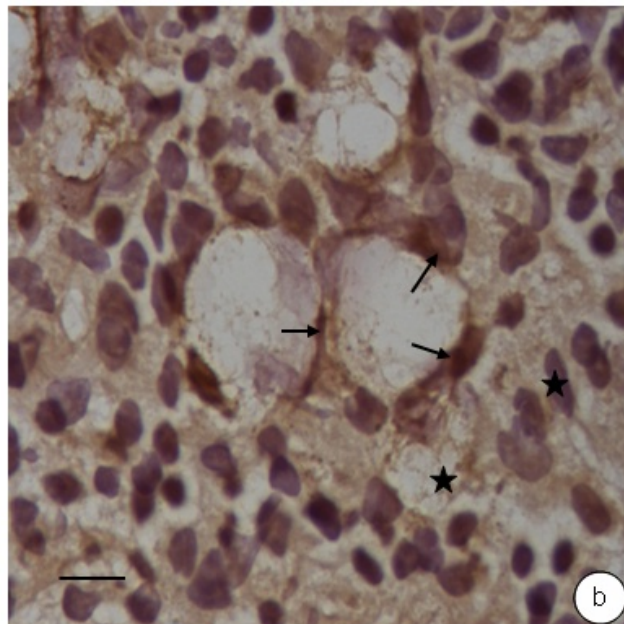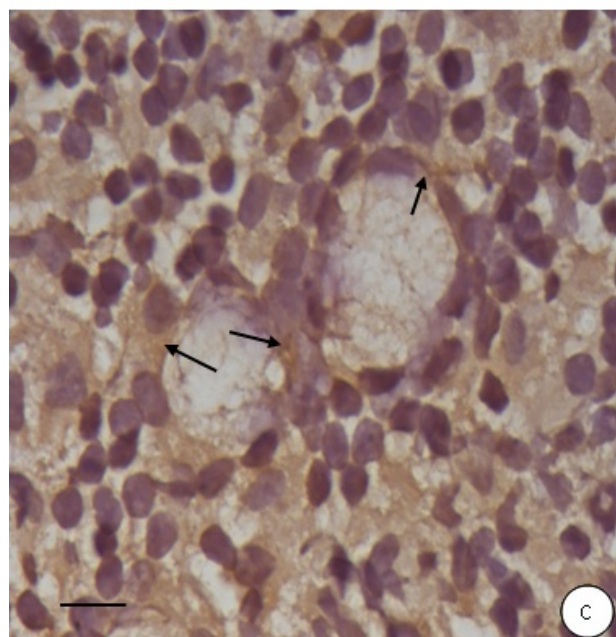
γ2 chain domain III
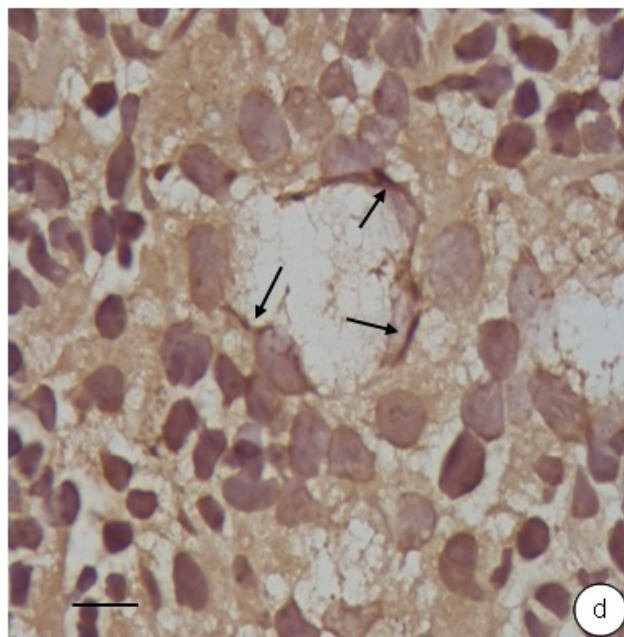
VE-cadherin

Mig-7
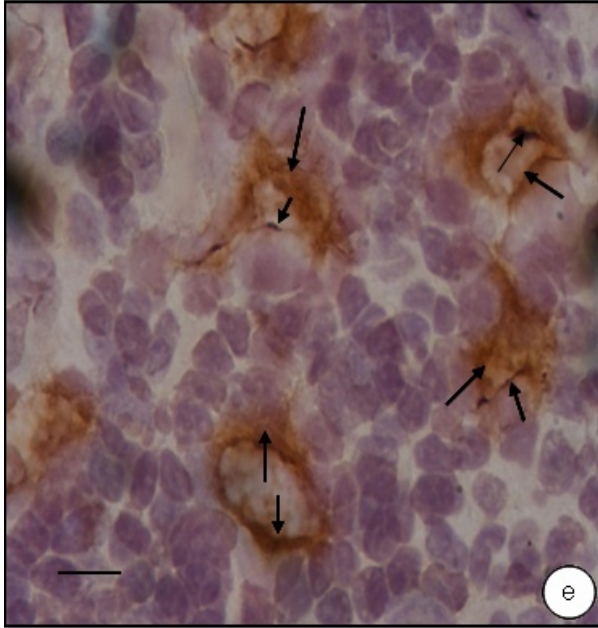
FVIII assoc:ag
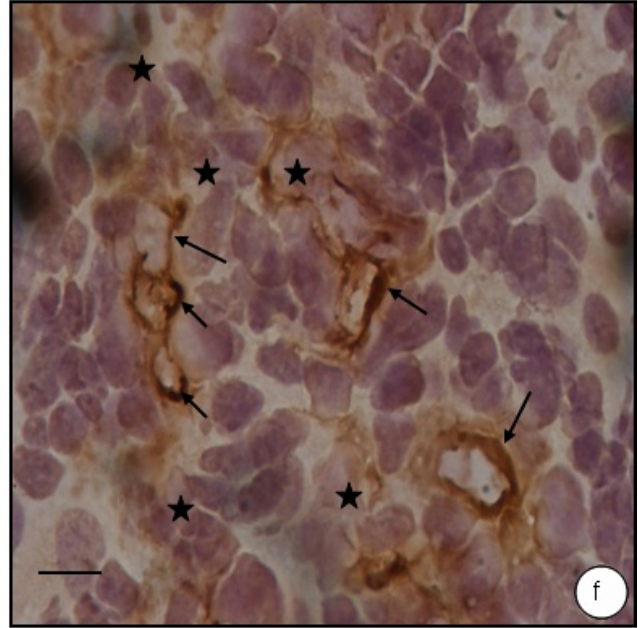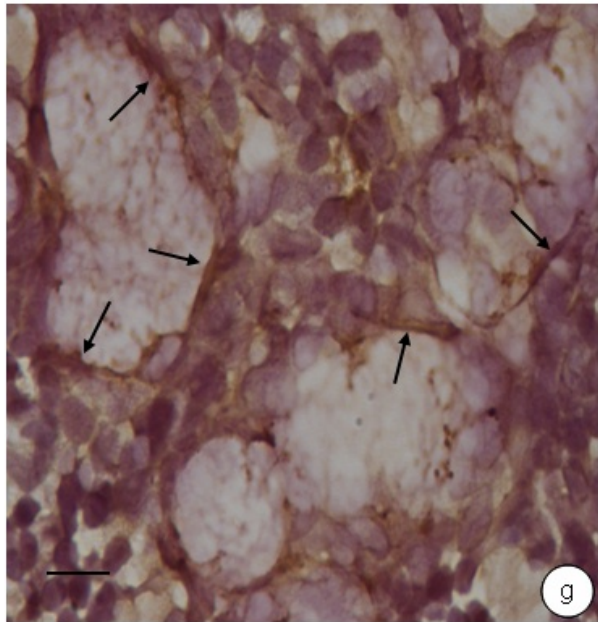
γ2 chain domain III
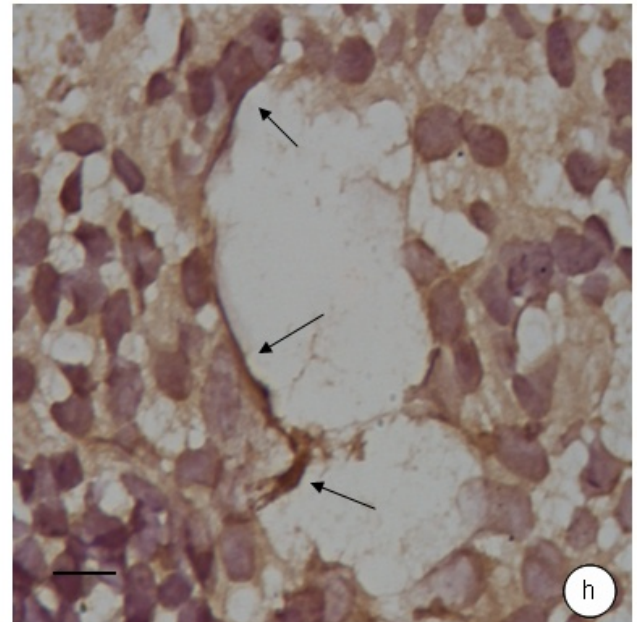
VE cadherin

2EN2 no primary
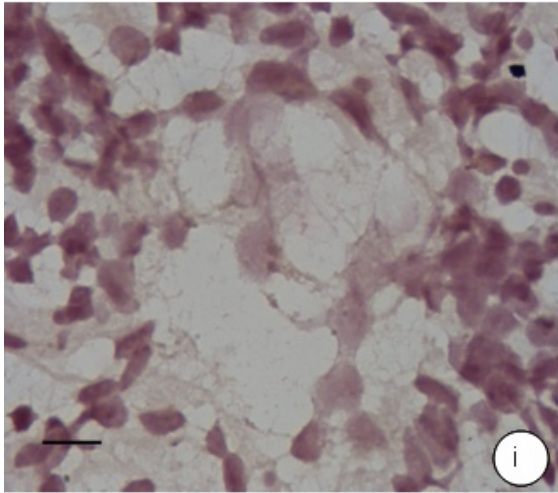
Normal LN Mig-7
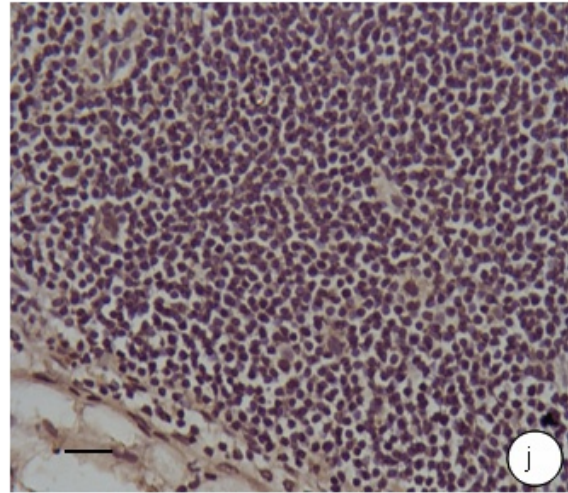
Normal LN FVIII assoc:ag
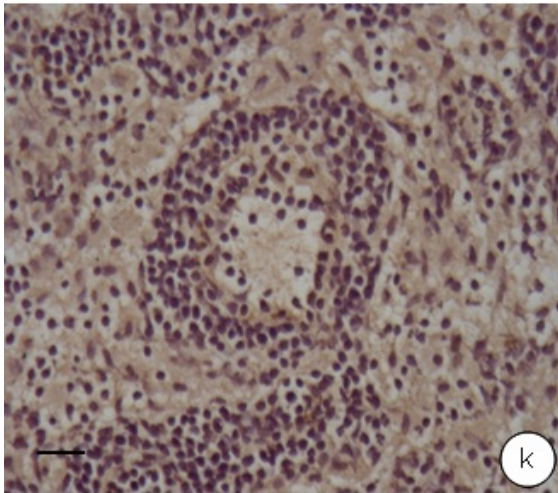
Normal LN γ2 chain domain III
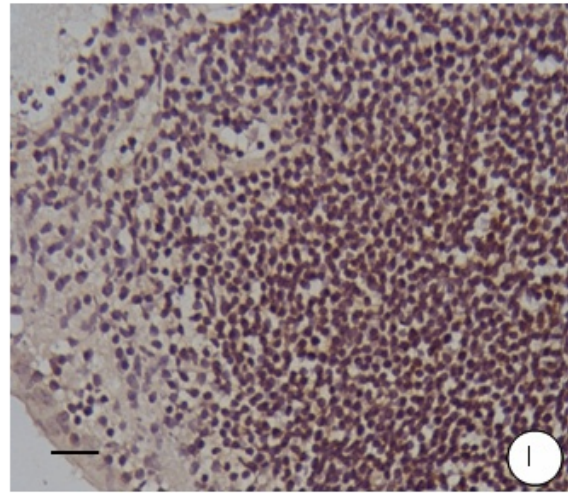
Normal LN VE-cadherin
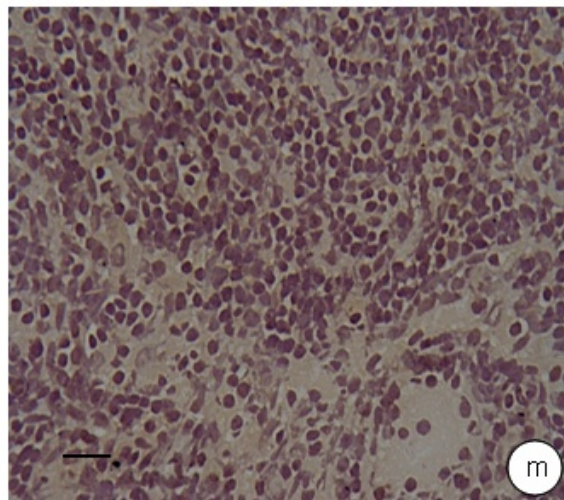
Supplemental data. Overexpression of Mig-7 causes vessel-like structure formation in 3D domes of Matrigel. Images were taken sequentially through four planes of view in the z-dimension of a representative dome of Matrigel (3D culture) shown in figures 4b and c. Photomicroscopy demonstrated that cords of invading cells were formed by HT29 cells overexpressing FLAG tagged Mig-7 Due to the branching morphology, cells that were in that plane are in focus; the rest are out of focus. Images are at the same magnification as in Figure 4c.

Supplemental 1
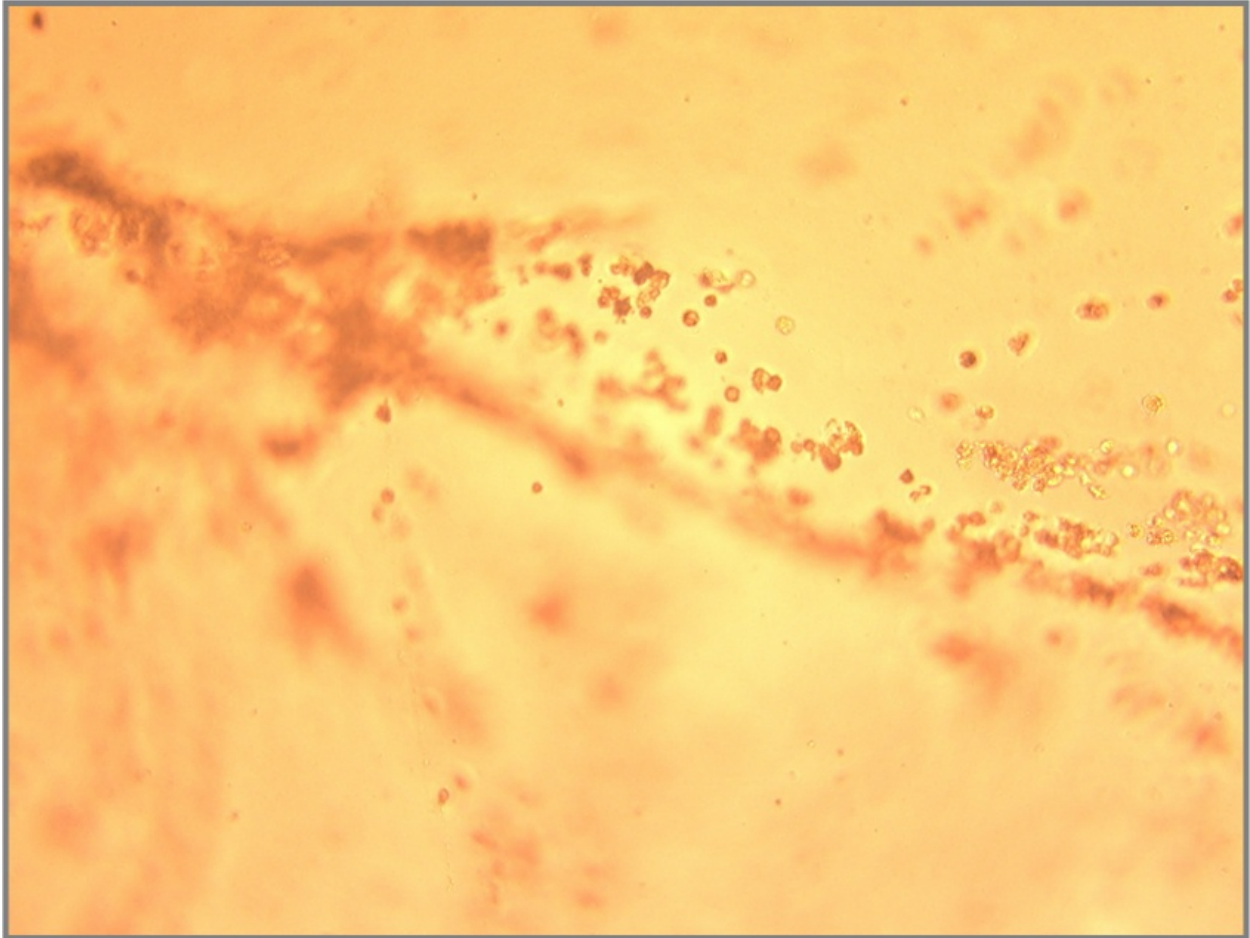
Supplemental 2
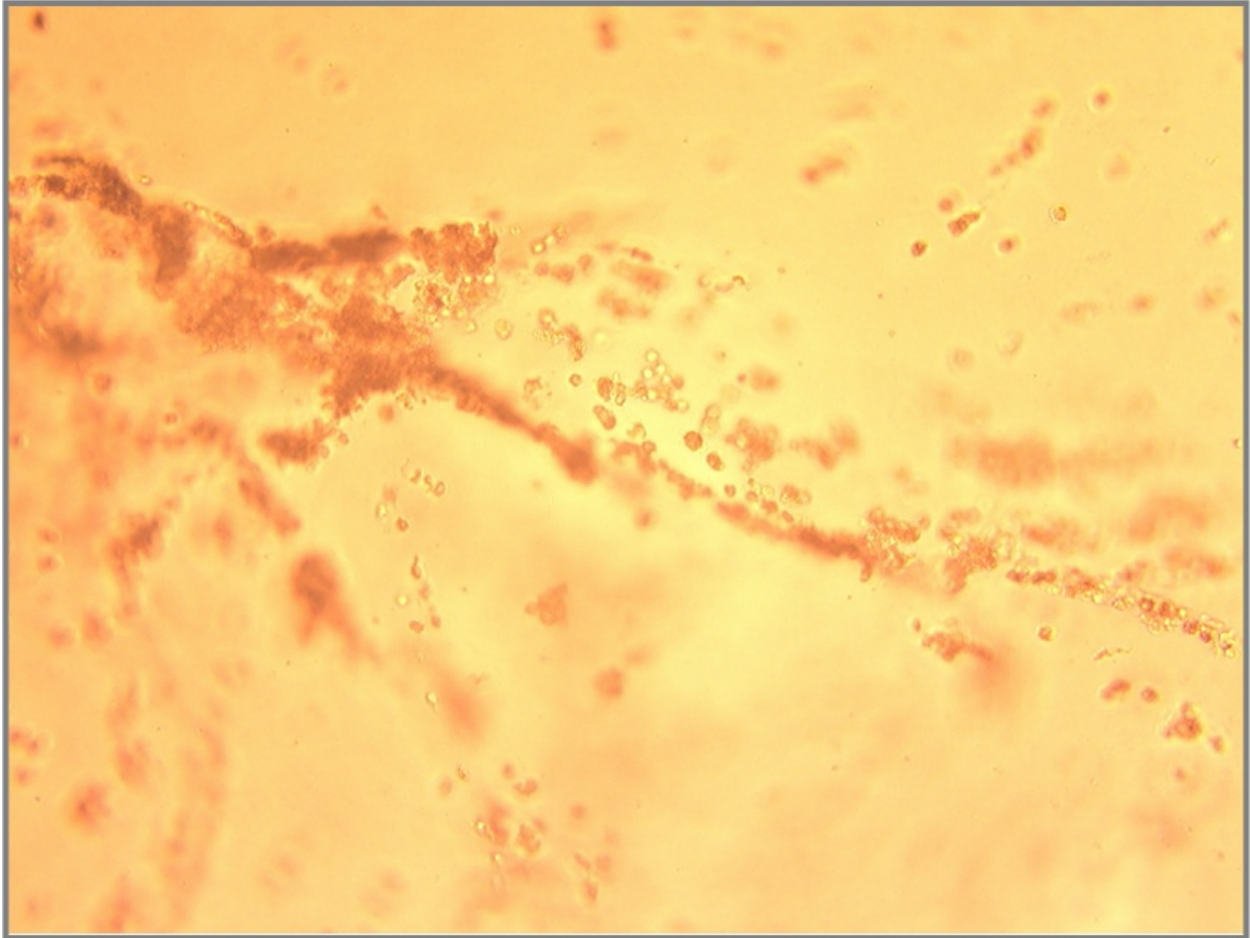
Supplemental 3
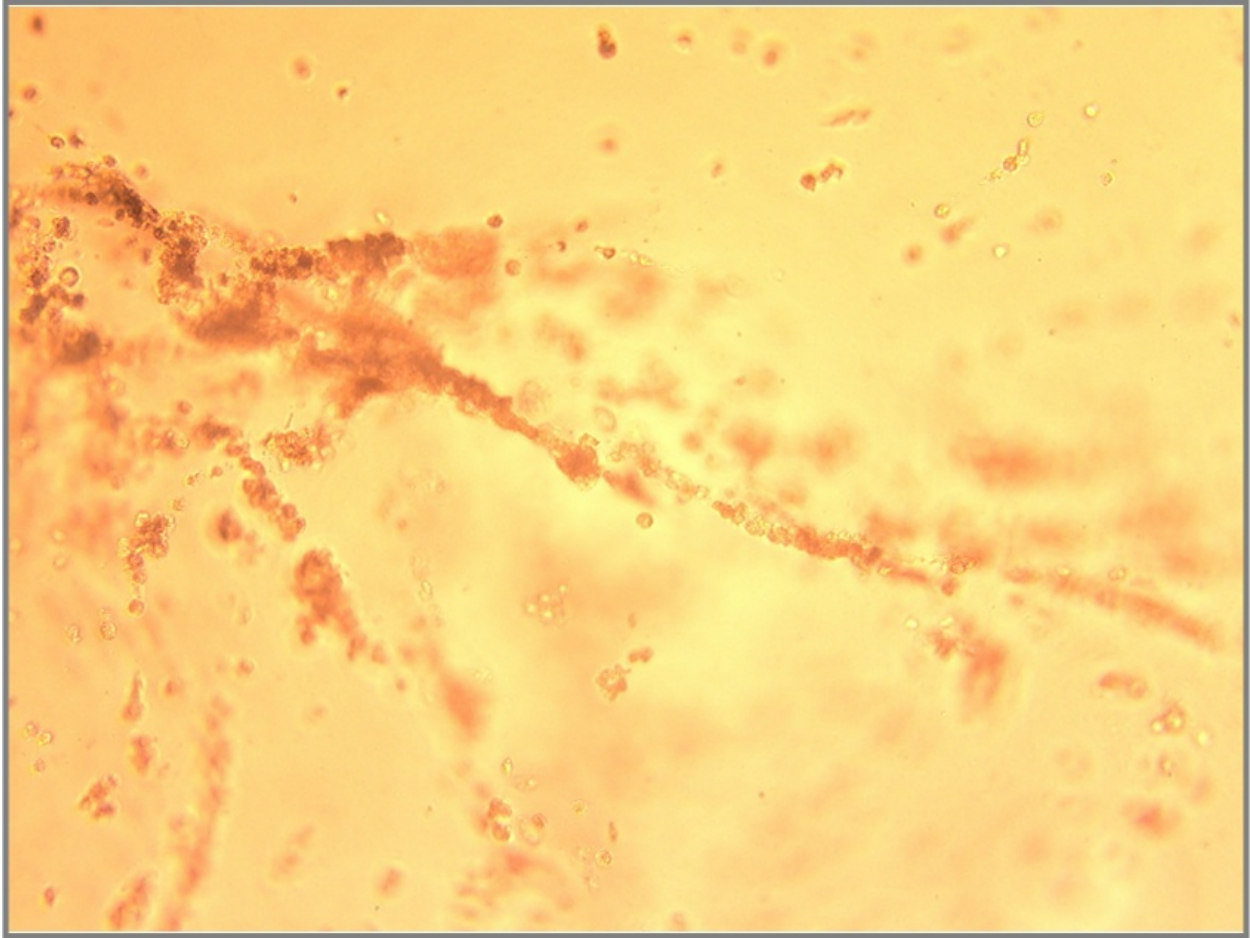
Supplemental 4
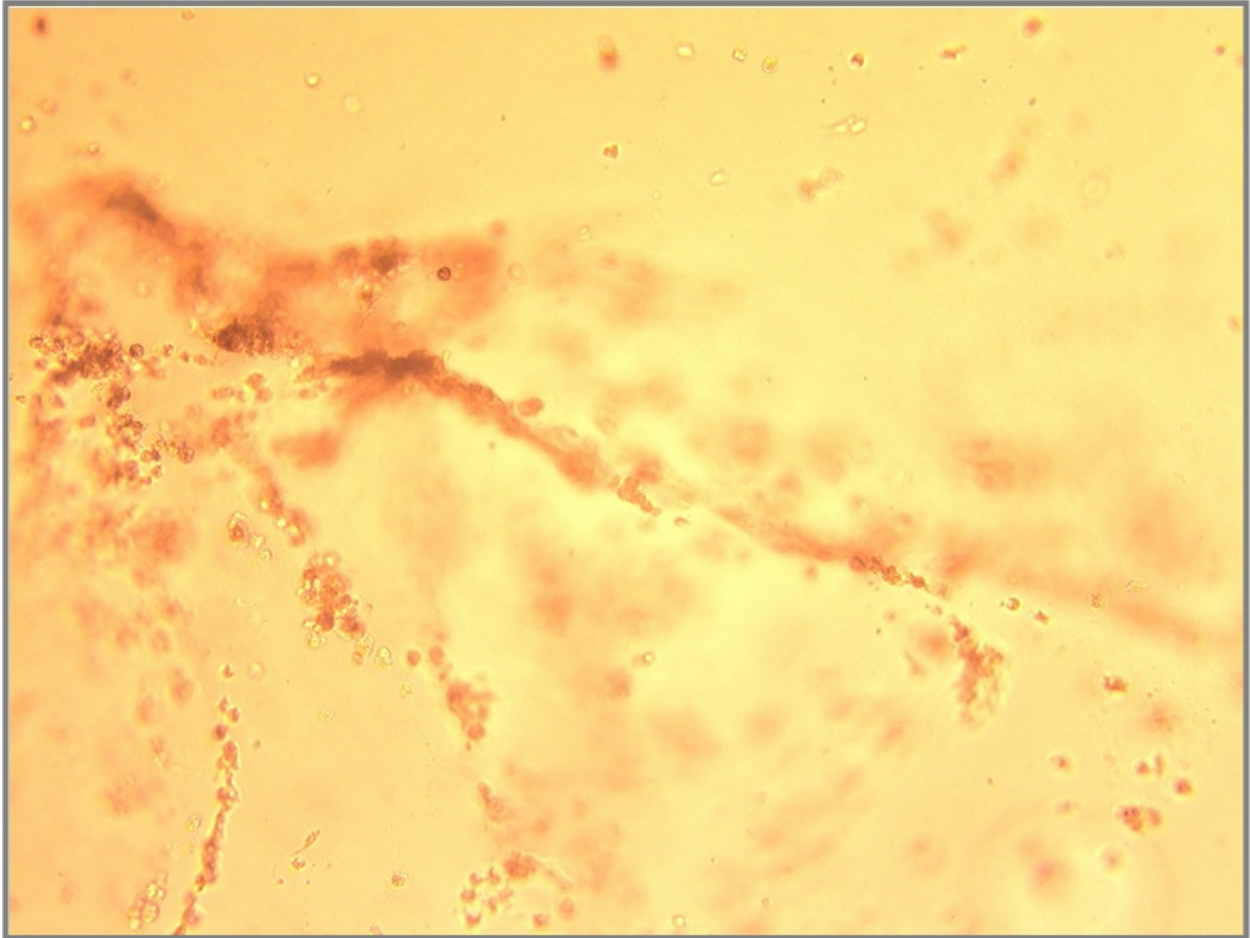
Chapter 3

TARGETING MIG-7 INHIBITS CARCINOMA CELL INVASION, PRIMARY TUMOR

GROWTH, AND STIMULATES KILLING OF BREAST CARCINOMA CELLS

Targeting Mig-7 inhibits carcinoma cell invasion, primary tumor growth, and stimulates killing of breast carcinoma cells

Aaron P. Petty[1], Stephen E. Wright[2-4], Kathleen A. Rewers-Felkins[2-3], Michelle A. Yenderrozos[5], Beth A. Vorderstrasse[5] and J. Suzanne Lindsey[1,5-8]

[1]School of Molecular Biosciences, Washington State University, Pullman, Washington,; [2]Department of Veterans Affairs Medical Center, Amarillo, Texas; Women's Health Research Institute, Departments of Internal Medicine, Microbiology & Immunology, and Cell Biology & Biochemistry, Texas Tech University Health Sciences Center, School of Medicine, Amarillo, Texas; [3]Harrington Cancer Center, Amarillo, Texas; [4]Department of Pharmaceutical Sciences, Texas Tech University Health Sciences Center School of Pharmacy, Amarillo, Texas; [5]Department of Pharmaceutical Sciences, College of Pharmacy; [6]Center for Reproductive Biology; [7]Cancer Prevention and Research Center, Washington State University, Pullman, Washington, [8]Recodagen Corporation, Seattle, Washington.

PBS, phosphate-buffered saline; IL-2, interleukin-2; TNF-α, tumor necrosis factor-alpha; IFN-γ, interferon-gamma; ELISA, enzyme-linked immunosorbent assay; PVDF, polyvinylidene fluoride; TBS, tris-buffered saline; HRP, horseradish peroxidase; DTI, defined trypsin inhibitor; DAB, 3,3'-diaminobenzidine; PI, propidium iodide.

Corresponding author: J. Suzanne Lindsey, Recodagen Corporation, 1616 Eastlake Ave. E, Seattle, WA 98102. Tel: 206-957-7350, E-mail address: slindsey@recodagen.com

Abstract

Migration inducing gene-7 (Mig-7) is expressed by tumor cells in circulation, in primary and in metastatic tumor sites as well as by occult tumor cells that mimic endothelial cells. Multiple tumor microenvironment factors, such as Epidermal and Hepatocyte growth factors, induce Mig-7 mRNA expression. Gain or loss of Mig-7 protein studies show that its expression leads to colon and endometrial carcinoma cell invasion. These data led us to hypothesize that targeting Mig-7 would decrease invasion and resulting disease progression. We first tested this hypothesis using an *in vitro* modified Boyden chamber chemoinvasion assay of endometrial carcinoma HEC1A cells treated with Mig-7 specific or control antibodies. Mig-7 antibody caused a >60% reduction in HEC1A cell invasion. In another approach to test this hypothesis, an *in vitro* analysis of peptide-stimulated human peripheral blood monocyte cells (MC) and their killing of MCF-7 breast carcinoma cells was used. Mig-7 peptide treatment increased MC TNF expression and killing of MCF-7 cells >2-fold over MUC-1 or control peptide treatments. Furthermore, in a xenograft nude mouse model, stably expressing Mig-7-specific short

interfering RNA (siRNA) resulted in significantly reduced Mig-7 protein levels and primary tumor growth, as well as phosphorylation of ERK1/2, Akt, and S6 kinase. In addition, membrane-type 1 matrix metalloproteinase (MT1-MMP) activity in Mig-7 siRNA expressing cells and in Mig-7 antibody-treated HEC1A cells decreased. Based on these collective data, Mig-7 expression is a potential candidate for future targeted cancer therapies.

Introduction

Cancer treatments targeting tumor-specific proteins are likely to result in decreased side effects. As a result, discovery and targeting of tumor cell-specific gene expressions would lead to more effective dosing and less toxicity. Furthermore, targeting tumor cell proteins that cause invasion, during which cells are resistant, would be even more important. We have discovered one such human protein, Migration inducting gene-7 (Mig-7), that is regulated by tumor microenvironment factor (1-4) .

Mig-7 protein is cysteine-rich and is primarily localized to the cell membrane fraction of carcinoma cells. Mig-7 expression, a result of receptor tyrosine kinase (RTK) activation, also requires αvβ5 integrin ligation that is known to be involved in RTK-activated tumor cell invasion and dissemination (1, 2, 5, 6). Antisense to Mig-7, but not sense, oligonucleotide treatment inhibits carcinoma cell scattering (1). In our studies to date, 87% of tumors from breast, endometrial, colon, lung, ovary, stomach kidney thyroid, cervix, small intestine, and prostate (n >200 patients), blood from cancer patients, and metastatic sites possess Mig-7 mRNA. Notable from these studies, Mig-7

mRNA is not detected in 25 different normal tissues (n=6 each tissue) or in blood from normal subjects (1, 3).

Consistent with Mig-7 expression causing invasion, its cDNA is 99% homologous to ESTs isolated from early invasive stage placenta (1). During placental development, trophoblast cells from the implanted blastocyst invade through the endometrium and one third of the myometrium. These plastic cells can also mimic endothelial cells to remodel the maternal spiral arteries; a process that provides sufficient blood flow for fetal growth and development. Thus, the only normal cells found to date that express Mig-7 are trophoblast cells (2) that behave like aggressive tumor cells (7-9). Stably transfected HT29 colon carcinoma cells with Mig-7 expression vector produce Mig-7 protein of the same size as endogenous Mig-7. Mig-7 overexpression induces invasion and vessel-like structure formation in three dimensional (3D) cultures (2). In addition, Mig-7 expression in these cells reduces their adhesion to laminin and increases laminin 5 γ2 chain promigratory fragments known to promote invasion and vessel-like structure formation by aggressive melanoma cells (10).

In vivo, tumor cells have been found to line the lumens of irregular vessels in the interior, more hypoxic region of multiple tumor types, including melanoma, ovarian carcinoma, Ewing sarcoma, and hepatocarcinoma (11-14). *In vitro*, aggressive melanoma cells have been found to form these vessel-like structures, a process termed vasculogenic mimicry (15) . In our nude mouse model of metastasis, both RL95 and HEC1A endometrial carcinoma cells that express Mig-7 localize to lymph node vessel-like structures formed by these invasive tumor cells (2). Numbers of these vessel-like structures correlate with levels of Mig-7 expression. Adhesion assays to various

components of the extracellular matrix suggest that a mechanism for Mig-7 in vessel formation by tumor cells is due, at least in part, to significantly lower adhesion to laminins, probably through facilitating cleavage of laminin 5 γ2 chain (2). These studies led us to hypothesize that targeting Mig-7 would decrease invasion and resulting disease progression (4).

In the present study, we showed that Mig-7 expression was specific to breast carcinoma and precancerous breast tissue and not to normal breast tissue. Several types of targeting were employed to test the above hypothesis. Targeting Mig-7 with an antibody to its first nine amino acids inhibited carcinoma cell invasion. In addition, peptides specific to Mig-7, but not control peptides, caused increased monocyte TNF expression and killing of breast carcinoma cells *in vitro*. *In vivo* studies showed that decreased Mig-7 expression impaired early tumor growth of endometrial cell xenografts in nude mice. Targeting or inhibition of Mig-7 expression did not affect cell growth or survival. Active states of membrane-bound metalloproteinase MT1-MMP (also known as MMP-14), ERK1/2, Akt, and S6 kinase were all reduced with Mig-7 targeting.

Methods

Cell cultures

Methods for transfection and cultures of HEC1A, RL95 endometrial carcinoma parental (1), RL95 stably transfected with siRNA expression vectors (2), and MCF-7 breast carcinoma (16) cells were previously described. Mig-7 sequence (Accession DQ080207) of the previously unpublished siRNA construct insert 4-2 as <u>antisense</u>-loop-<u>sense</u> is TCATTCA<u>CCTGCTATAGAC</u>TTCAAGAGA<u>GTCTATAGCAGG</u>-TGAATGA

90

(base pairs 1303 to 1321). Under Institutional Review Board approval, human isolated

monocyte cells (MC) were isolated and cultured at 2 X 10^6 cells/ml in AIM-V^R serum-free

lymphocyte medium (Gibco, Invitrogen, Carlsbad, CA) as previously described (16).

Modified Boyden chamber invasion assay

Chemoinvasion assays were performed as previously described (17). Briefly, transwell

filters (Costar, Corning, NY, 8 μm) were blocked in 1% BSA-DMEM/F12 for 30 minutes

and rinsed with phosphate-buffered saline (PBS). Matrigel (BD Biosciences, San Jose,

CA) was diluted in ice cold PBS to 1000 µg/mL to coat the lower side of each pre-chilled

transwell filter insert. After incubating the coated inserts at 37° C for one hour and

washing with PBS containing Ca^{2+} and Mg^{2+}, cells were detached using trypsin without

EDTA and neutralized with soybean trypsin inhibitor, centrifuged for 5 minutes at 1000

rpm (4° C), and washed one time in DMEM/F12. Cell count and viability were

determined using trypan blue exclusion and a hemacytometer. Cells were preincubated

with 10 µg/mL affinity-purified Mig-7 rabbit polyclonal antibody (2, 3) or control IgG

antibody for 15 minutes in a 37° C incubator. Rabbit IgG antibody served as control, as

previously described (18). Media containing the chemoattractant, hepatocyte growth

factor (HGF, R&D Systems Inc., Minneapolis, MN), was added to bottom wells at a

concentration of 20 ng/mL. Media without HGF containing 50,000 cells was added to

each top well. Cells were allowed to invade for 72 hours at 37° C in 5% CO_2, 95% air

humidified incubator. After invasion, filters were rinsed with PBS then fixed in Hema3

fixative (Fisher Scientific, Inc., Pittsburgh, PA) for at least 30 minutes. Non-invaded

cells in the upper chamber were removed with a cotton swab. Filters were dried and

stained with Hema3 (Fisher Diagnistics, Middletown, VA). Filters were mounted on slides with gridded coverslips to count invaded cells using a microscope (Electron Microscopy Science, Hatfield, PA) at 400X magnification with a count of 10 squares (0.6 x 0.6 mm each) per filter from each treatment. Percent invasion was calculated by extrapolating the average cell count for the entire filter surface area and dividing by initial cell number. Media from bottom wells was also analyzed for cells that potentially invaded through the Matrigel. All treatments were performed in triplicate and experiments were repeated three times.

Apoptosis Assay

Apoptosis was assessed by using the Vybrant Apoptosis Assay Kit #4 (Molecular Probes, Eugene, OR) and flow cytometry. For RL95 siRNA cells, 1×10^6 cells were plated in triplicate on 6-well ultra-low attachment plates (Corning, Inc., Corning, NY) for 18 hours prior to analysis. For HEC1A cells, 1×10^6 cells were plated in 24-well plates and treated with Mig-7 antibody or rabbit IgG (10 μg/ml each) for 72 hours prior to analysis. Cells were trypsinized and centrifuged to pellet followed by washing once in 1X PBS. After suspending in 250 μl of PBS, cells were transferred to 96-well plates. 1 μl of a 1:4 dilution of both YO-PRO-1 (100 μM) and propidium iodide (PI) (1 mg/ml) was added to cells and incubated on ice for 30 min. Cells were also left unstained or stained with YO-PRO-1 or PI alone for controls. Staining was analyzed using the FACSCalibur (Becton Dickinson, Bedford, MA) machine and Winlist for Mac 5.0® analysis software. Red fluorescence detection was used for PI staining and green fluorescence for YO-PRO-1 staining. Single-stained samples were used to perform

compensation and detected cells were gated to exclude large cell clumps and very small debris. YO-PRO-1 positive staining indicated apoptotic cells (lower oval). YO-PRO-1 and PI double staining indicated dead cells (upper oval). Each experiment was performed in triplicate.

Proliferation assay

Cell proliferation was assessed by using the PI nuclear staining dye and flow cytometry (19). HEC1A cells were counted and 5×10^5 cells were plated onto a 24-well plate and treated with IgG or Mig-7 antibodies as given above. For RL95 siRNA expressing cells, 5×10^5 cells were plated and grown for two days prior to collection. All cells were fixed in 1 ml of 70% ethanol overnight. After fixation, cells were centrifuged (470 x g, 5 min., 4° C) and the pellets washed once in 1X staining buffer (Dulbecco's PBS containing 2% FBS and 0.01% NaN_3). Cells were then treated with 1 mg/ml RNase A (Sigma, St. Louis, MO) in PBS at 37° C for 30 min. After removing the RNase A solution, 300 μl of staining buffer containing 20 μg PI was added to resuspended cells and incubated 30 min. at room temperature. PI was not added to one sample as a negative control. After 30 min., PI staining was analyzed using the FACSCalibur (Becton Dickinson, Bedford, MA). Levels of PI staining correlated to the different cell cycle phases, and the numbers of cells in the G2/M phase (highest PI expression) were compared as an indicator of proliferation. Cells were gated to exclude large cell clumps and small debris.

α2-Macroglobulin capture assay

This assay was performed as previously described (20).   Briefly, indicated cell lines were plated at confluency and treated as indicated in a 6-well plate on 1 mg/ml Matrigel for 18-20 hours before the assay.   Cells were then removed by scraping and each sample was split into two wells of a 24-well plate.   Purified human α2-macroglobulin (MP Biomedicals, Solon, OH) was added to three wells at a concentration of 1 mg/ml and samples were incubated at room temperature for 15 min.   Cells without α2-macroglobulin served as control.   Following incubation, 2% SDS lysis buffer, 60 mM Tris, 10% glycerol containing 2X protease inhibitors (Complete, Roche, Indianapolis, IN) was added at a 1:2 final dilution, and immunoblots performed, as detailed below.   Assay was performed in triplicate for each cell line and treatment, except for cells without α2 macroglobulin and RL95 parental cells.   Individual background levels for each lane were subtracted from the band of interest level then divided by respective tubulin level for densitometry calculations.

Protein phosphorylation analyses

For protein phosphorylation analyses, confluent RL95 siRNA-expressing cells were plated on a 1:10 dilution of Matrigel for 19 hours prior to harvest. Confluent cells were trypinized and pelleted at 4° C, 1000 rpm, 4 min. and washed three times in media, followed by three washes in cold TBS. Multiprotein phosphorylation analysis using antibodies and Luminex Bead-based immunoassays was performed by AssayGate, Inc. (Ijamsville, MD). Briefly, multiple analytes in a single cell lysate are determined quantitatively and simultaneously with Bio-Plex 200 Bead Reader System. Microparticles are dyed with differing concentrations of two fluorophores to generate

distinct bead sets. Each bead set is coated with capture antibody specific for one analyte. Captured analyte is detected using a biotinylated detection antibody and streptavidin-phycoerythrin (S-PE). The bead analyzer is a dual laser, flow-based, sorting and detection platform. One laser is bead-specific and determines which analyte is being detected. The other laser determines the magnitude of PE-derived signal, which is in direct proportion to the amount of analyte bound. Protein concentrations of samples are determined by 5-parameter logistic regression algorithm with analysis of the median fluorescence intensity readings of an 8-point protein standard curve. Once a regression equation is derived, the fluorescence intensity values of the standards are treated as unknowns and the concentration of each standard is calculated. A ratio of the calculated value to the expected value of this standard is determined. A ratio between 70 and 130% for each of standards indicated a good fit. Precision was evaluated by the coefficient of variation which equals the standard deviation divided by the mean (expressed as a percent, CV%) in the assays. All samples indicated a good level of precision.

Antibodies to phosphorylation sites analyzed included Ser^{473} for Akt, Thr^{202} /Tyr^{204} and Thr^{185} /Tyr^{187} for extracellular signal-regulated kinase 1/2 (ERK1/2), Thr^{246} for proline-rich Akt substrate of 40 kDa (PRAS40), Thr^{421}/Ser^{424} for S6 kinase, and Tyr^{1135} /Tyr^{1136} for insulin-like growth factor-1 receptor (IGF-1R). Antibodies to each protein were also used to detect total protein levels for normalization. Samples were tested in triplicate.

Immunoblotting

Cell lysates and immunoblots were performed as previously described (1, 2) with the following modifications. Cultured cells were lysed in 2% SDS, 60 mM Tris, 10% glycerol containing 2X protease inhibitors (Complete, Roche, Indianapolis, IN) and quantitated using RC/DC Protein Assay (Bio-Rad, Hercules, CA). Primary tumor tissue (100 mg) was homogenized in 1 ml of 2% SDS lysis buffer on ice, followed by incubation for 10 min. at 70° C. Tumor lysates were cleared by centrifugation for 10 min. at 14,000 x g, 4° C. Lysates were boiled for 5 min. in the presence of 100 mM DTT and 0.01% bromophenol blue. Equal amounts of protein were loaded onto a 12% polyacrylamide gel and run at constant 200 V for 30-40 min. Gels were semi-dry transferred to polyvinylidene fluoride (PVDF) membranes and blocked in tris-buffered saline (TBS)-Tween (0.05%) containing 5% dry milk for one hour at room temperature. Endogenous Mig-7 protein was detected using our affinity-purified Mig-7 antibody at 0.16 μg/ml in TBS-T. After extensive washings, horseradish peroxidase (HRP)-labeled secondary anti-rabbit IgG antibody (Zymed Laboratories, San Francisco, CA) was used to detect the Mig-7 antibody at 0.038 μg/ml in TBS-T. Mouse anti-β-tubulin (clone AA2, Upstate, Inc., Lake Placid, NY) was used at 0.2 μg/ml in TBS-T followed by extensive washing and incubation with HRP-labeled secondary anti-mouse IgG antibody (Cell Signalling, Danvers, MA). After stringent washings, Chemiluminescence Reagent (Amersham, Piscataway, NJ) allowed detection of HRP-labeled antibodies when exposed to film.

For α2-macroglobulin assay blots, lysates were not reduced or boiled before electrophoresis and transferring to nitrocellulose membrane. MT1-MMP (MMP-14) was detected using a goat anti-human MMP-14 antibody (R&D Systems, Inc.) at 0.1 μg/ml

and an HRP-labeled secondary anti-goat IgG antibody (Zymed Laboratories, San Francisco, CA) at 0.038 μg/ml.

Xenograft nude mouse studies

Nude mouse studies were performed under Institutional Animal Care and Use Committee approval as previously described with modifications (2, 3). Briefly, RL95 parental cells and cells stably transfected with siRNA expression vectors containing Mig-7 specific sequences 1-3, 3-1, or 4-2 were cultured as described previously (1, 2). Cells were lifted off the plate using 1X trypsin-EDTA (Gibco, Invitrogen), followed by inhibition of trypsin using Defined Trypsin Inhibitor (DTI) (Cascade Biologics, Portland, OR). Viable cells were counted using trypan blue exclusion and a hemocytometer. Parental RL95 and siRNA 1-3, 3-1, or 4-2 expressing cell lines were suspended in serum-containing media with 10 ng/ml EGF (Gibco, Invitrogen) and a 1:2 diluted Matrigel (BD Biosciences) and injected subcutaneously at $5x10^5$ each into the dorsal neck region of nu/nu athymic mice (National Cancer Institute, Bethesda, MD). The initial protein concentration of Matrigel was 10.3 mg/ml. Negative controls were mice injected with Matrigel alone (no cells). Five animals were injected per cell line. Tumor size was measured with a caliper every 2-3 days and volume was calculated using (length X width^2)/2 as previously described (21). Mice were euthanized after 4 weeks.

Immunohistochemistry

Breast core punch biopsies on tissue array slides were obtained from Cybrdi, Inc (Frederick, MD). Detection of Mig-7 protein was performed using Mig-7-specific affinity-

purified antibody produced in rabbits injected with KLH-conjugated Mig-7 peptide (MAASRCSGL) representing the first nine amino acids of Mig-7 protein, as previously described (2, 3). Briefly, 10% formalin fixed, paraffin embedded, 5 µm core tissue sections of normal breast or breast carcinomas as indicated were used. After deparaffinization with xylene for 10 minutes, rehydration through 100%, 95%, and 70% ethanol, antigen retrieval was performed for 2 seconds on ice in a microwave oven. Slides were washed two times in Dulbecco phosphate buffered saline (D-PBS) and then permeabilized with 0.01% digitonin (Sigma-Aldrich, St. Louis, MO) in PBS at room temperature for 30 minutes. After washing two times in PBS, slides were blocked in 10% horse serum (Gibco, Invitrogen) in D-PBS for 30 minutes at room temperature. Primary antibody (0.32µg/µl), affinity-purified polyclonal rabbit anti-human Mig-7, was diluted 1:50 and incubated on the tissue sections overnight at 4 ºC. Slides were washed two times in PBS then incubated for 20 minutes in 3% H_2O_2 in methanol. After washing two times in PBS, slides were incubated for 30 minutes in goat anti-rabbit IgG-horseradish peroxidase (HRP) in PBS containing 0.5% bovine serum albumin (BSA, Fisher Scientific). Slides were washed two times in PBS and then developed using 3,3'-diaminobenzidine (DAB) substrate (Vector Laboratories, Burlingame, CA) until brown specific staining was detected by microscopy (less than 3 minutes). After washing in water for 5 minutes, slides were counterstained in Hematoxylin QS (Vector Laboratories). Slides were dehydrated in two incubations for 3 minutes each of 75%, 95%, and absolute ethanol, air dried, and mounted with DPX mounting medium (BDH Laboratory Supplies, Poole, UK). Control was rabbit IgG instead of Mig-7 antibody.

Images were taken on a Nikon Microphot microscope with a Retiga 2000R digital CCD camera.

RNA isolation and RT-PCR

Total RNA from normal breast tissue and from breast carcinoma cell lines were purchased from Ambion, Inc. (Austin, TX). Isolation of total RNA from MCF-7 breast carcinoma cells, DNasing, and RT-PCR was performed as previously described (1-3).

Peptides

Control (MAA SRC SGL YIV RND TSG; YIV RND TSG LSG SQW VDS; LSG SQW VDS PLK SPC QVW) and Mig-7 (RVH MRA CSA GSA YLK QMK; GSA YLK QMK FCR MAA SLD; FCR MAA SLD KVK KTD RGE RG) peptides (Accession DQ080207) were synthesized by Biosource,Inc. Previously characterized MUC-1 peptide (GNN APA HGV NNA PDN RPA P) (16) was synthesized by American Peptide Co., Inc. Peptides, 95% pure, were evaluated by mass spectrometry and solubilized in media.

Stimulation of human monocyte cells and MCF-7 killing assays

Human peripheral blood MC isolation, culture, and stimulation were performed as previously described (16). Briefly, MCs were isolated from breast adenocarcinoma patients under Institutional Review Board (IRB) approval. Cells were cultured at 2 x 10^6 cells/ml in AIMV$^®$ serum-free lymphocyte medium (Gibco, Invitrogen) in a 37°C humidified 5% CO_2, 95% air atmosphere. IL-2 (Cetus, Inc., Emeryville, CA) was added twice per week at 100 IU/ml on days 0 and 4. Cells were stimulated with 1 µg/ml MUC-1 peptide alone or Mig-7 and MUC-1 peptides on days 0 and 7.   MCF-7 cells (5 X 10^3 per well) were plated into 96-well tissue culture plates. Effector peptide-stimulated MC were added to each well in two effector cell to target cell ratios (E:T) 10:1 and 5:1. Cell lysis was evaluated on day 8 of peptide stimulation using a tetrazolium salt XTT assay (Roche, Inc.) as previously described (22). Treatments were in replicates of 6 and each experiment was performed at least twice.

Formation of formazan in XTT assays indicates viable cells. Formazan formed by target (MCF-7 cells) alone, effector (MC) alone, or background (no cells) was

determined as the mean of six wells each. The percent specific lysis (%SL) was calculated as previously described (16):

$$\%SL = \frac{OD_{(target\text{-}medium)} - OD_{(experimental\ wells\text{-}well\ with\ corresponding\ number\ of\ effector)}}{OD_{(target\text{-}medium)}} \times 100$$

ELISA Cytokine Assay

Tumor necrosis factor-alpha (TNF-α) levels in media from each peptide treated monocyte cell culture were determined using the human BD OptEIA™ cytokine assay that is a solid phase sandwich Enzyme-Linked Immunosorbent Assay (ELISA) (BD Biosciences) , according to manufacturer's instructions.   Briefly, monocyte culture supernatant was added to TNF-α antibody coated wells and incubated for two hr. After washing and detection with an streptavidin-horseradish peroxidase conjugate mixed with a biotinylated anti-human TNF-α antibody with subsequent washing then 3,3',5,5'-tetramethylbenzidine substrate addition, reaction was stopped and amounts of TNF-α were determined by measuring absorbance at 450 nm with a spectrophotometer and comparison with a standard curve. Background of empty well were subtracted before statistical analyses. Experiments were performed in replicates of six for each peptide treated monocyte experiment.

Statistical Analysis

Statistical significance of the *in vitro* cytotoxicity assays and of cytokine assays were determined by the Mann-Whitney Rank Sum test. Data from invasion assay and nude mouse xenograft assay were statistically analyzed by One-Way ANOVA and Tukey-Kramer post test and considered significant at $p \leq 0.05$.

Results

Antibody to Mig-7 results in decreased invasion *in vitro.*

A means to quantitatively assess tumor cell invasion is the transwell chemoinvasion assay (17). In addition, HGF, the growth factor used to isolate Mig-7 (1), acts as a chemoattractant of HEC1A cells in transwell *in vitro* assays (23). Therefore, we used this cell line previously shown to express Mig-7 (1) and affinity-purified antibody to Mig-7 peptide representing the first nine amino acids of the full length protein to determine if this antibody could inhibit cell invasion.

Mig-7 antibody treatment of HEC1A cells significantly decreased the average percentage of invaded cells counted as described in Methods and Materials. When percentages of invaded cells were compared to control IgG antibody treated HEC1A cells, chemoinvasion toward HGF in the lower well was inhibited 70% (p value 0.0046) by Mig-7 antibody (Figure 1a). Treatment with rabbit IgG antibody did not significantly inhibit chemoinvasion when compared to HGF treatment alone. A lack of HGF treatment reduced invasion of HEC1A cells by >90% (Figure 1a). Flow cytometric analysis with the apoptotic dye YO-PRO-1 and propidium iodide (PI) showed no significant increase in apoptosis due to Mig-7 compared to IgG antibody treatment (Figure 1b). In addition, flow cytometric cell cycle analysis showed no significant decrease in cell proliferation of Mig-7 antibody-treated cells compared to untreated and control-treated cells (Figure 1c).

Antibody or expression of siRNA specific to Mig-7 decreases activity of MT1-MMP.

Mig-7 protein is membrane-bound and cysteine-rich. Because a free thiol group on one of the many cysteine residues in membrane bound Mig-7 could activate MT1-MMP via the "cysteine switch" (24, 25) in the absence of proteolytic activation, we used the α2-macroglobulin capture assay to test for MT1-MMP activation. We used this test instead of zymography because SDS, used in gel zymography, has been shown to activate the "cysteine switch" (26).

HEC1A cells treated with Mig-7 antibody showed a 54% decrease in the levels of activated MT1-MMP, as indicated by the upper, α2 macroglobulin captured band (~190 kD), compared to cells treated with IgG control. The lower unactivated band is 62 kD as indicated. Levels of activated MT1-MMP were determined by densitometry normalized with tubulin levels for each sample (Figure 2a).

Given that Mig-7 antibody treatment reduced levels of active MT1-MMP, we next tested whether stable Mig-7 knockdown in RL95 cells would inhibit MT1-MMP activation. In this study, we used previously characterized RL95 endometrial carcinoma cells stably expressing siRNA constructs 1-3 and 3-1 (2). Using the α2-macroglobulin capture assay, RL95 cells stably knocked down with siRNA 1-3 showed a 57% decrease in levels of active MT1-MMP compared to control cells transfected with siRNA 3-1A (Figure 2b). Analysis of these cell lines by flow cytometry for apoptosis and proliferation showed no significant differences between 1-3 and 3-1 cell lines (Figure 2c,d).

Expression of siRNA specific to Mig-7 decreases ERK1/2, Akt, and S6 kinase phosphorylation.

In order to further define potential mechanisms by which Mig-7 exerts its effects on invasion, a multiplex protein phosphorylation analysis was utilized to determine changes in signaling protein activation. Signaling proteins PRAS40, S6 kinase, ERK1/2, and Akt were analyzed, along with the receptor tyrosine kinase IGF-1R. Our results showed decreases of 10% ($p<0.05$), 40% ($p<0.01$), and 30% ($p<0.05$) in Akt (Ser^{473}), ERK1/2 (Thr^{202}/Tyr^{204}, Thr^{185}/Tyr^{187}), and S6 kinase (Thr^{421}/Ser^{424}) phosphorylation, respectively, in RL95 cells expressing siRNA 1-3 compared to siRNA 3-1 expressing cells (Figure 3a). No significant differences in phosphorylation between these two cell lines were detected for the remaining two proteins analyzed (Figure 3b).

Stimulation of human peripheral blood monocytes (MC) with peptides specific to Mig-7 increases levels of TNF and killing of MCF-7 breast carcinoma cells *in vitro.*

Cancer immunotherapies include *ex vivo* stimulation of cancer patients' immune cells with tumor antigens. We hypothesized that Mig-7 peptides could stimulate MC to increase their killing of breast carcinoma cells *in vitro*. To test this hypothesis, we utilized our previously described method of MC isolated from two different breast cancer patients and the MCF-7 breast carcinoma cell line (16, 27). Human MC were isolated under IRB approval as previously described (16). Our use of MCF-7 cells in the current

study was warranted both by the fact that this system is optimized with this cell line (16), and that they expressed Mig-7 mRNA and protein (Figure 4a).

Mig-7 peptides representing the +1 frameshifted protein sequence (28)(Accession DQ080207) or control peptides representing the sequence in the non-coding reading frame, i.e. the frame that did not produce protein (28), were used to determine sequences that contributed to enhanced MCF-7 killing by stimulate MC *in vitro*. In addition, these peptides included overlapping sequences to prevent the possible omission of a particular epitope. None of the peptides were significantly homologous to any sequence other than Mig-7 banked protein sequence or to translated cDNA sequences in databases available through the National Center for Biotechnology Information (NCBI). MUC-1 peptides served as internal controls because of their previous use and optimization in this assay (16, 27).

Stimulation with Mig-7 peptides significantly enhanced MC killing of MCF-7 cells by > 3-fold over MUC-1 peptide alone (0) or control (CTL) peptides. There was no significant difference between control peptides and MUC-1 peptide alone (Figure 4b). In Figure 4c, using a ratio of 10:1 MC:MCF-7 cells, unstimulated and MUC-1-stimulated MC were indistinguishable in levels of MCF-7 killing. In contrast, Mig-7 peptides significantly increased MC killing of MCF-7 cells > 2-fold over unstimulated and MUC-1-stimulated. At the 5:1 ratio, Mig-7 peptide stimulation of MC significantly enhanced their killing of MCF-7 cells 1.9-fold over MUC-1-peptide stimulation and at least 30-fold over no peptide stimulation (Figure 4c). Mig-7 peptide stimulation also significantly increased levels of MC-produced TNF-α >3-fold over control peptide-stimulated MC as determined by ELISA (Figure 4d).

Breast carcinoma tissue and cells express Mig-7

Mig-7 expression is detected in multiple types of tumor tissue and cells, but not in normal tissue and cells (1-3). However, normal breast tissue was absent in our previous studies. Here, we expand our analyses of Mig-7 specificity to breast pre-cancerous states and carcinomas compared to normal breast tissue and cells. Relative RT-PCR was used to analyze total RNA as previously described (1-3) from three breast carcinoma cell lines, T47D, MDA-MB453, DU4475, and from normal breast tissue from three subjects with no previous history of cancer. No amplification product specific to Mig-7 was detected in normal breast tissue RNA. However, all three breast carcinoma cell lines expressed Mig-7 mRNA (Figure 5a).

Immunohistochemistry was performed on 70 human breast tissue arrayed core samples of normal, adenosis, papillomatosis, and carcinoma. Our results showed that primarily carcinoma tissues (Figure 5b) stained positive for Mig-7, whereas normal breast tissues lacked specific Mig-7 staining (Figure 5c). No specific Mig-7 staining was detected with control rabbit IgG antibody in breast carcinoma tissue serial to that in Figure 5b (Figure 5d). A summary of the overall pathology report of Mig-7 staining for all 70 samples is as follows: normal, 0 positive, 3 negative; breast adenosis, 5 positive, 23 negative; breast papillomatosis, 0 positive, 3 negative; breast carcinoma, 19 positive, 17 negative. Pearson Chi-square analysis with 3 degrees of freedom to test goodness of Mig-7 fit for detection of breast carcinoma was statistically significant (p = 0.008).

Stable knockdown of Mig-7 expression reduces primary tumor growth *in vivo*.

106

In addition to invasion, Mig-7 appears to play a role in the formation of vessel-like structures by tumor cells both *in vitro* and *in vivo* (2). These data led us to test the effect of stable Mig-7 knockdown, through siRNA expression, on primary tumor growth *in vivo*.

Because we originally isolated Mig-7 from RL95 cells, we injected three RL95 endometrial carcinoma cell lines stably transfected with different siRNA expression plasmids, 1-3, 3-1, and 4-2 into nude mice and measured tumor growth compared to parental RL95 injection. We confirmed our previous results (2) that cells expressing siRNA 1-3 have reduced Mig-7 protein levels compared to parental and 3-1 expressing cells by Western blot analyses (Figure 6a). These cells showed a 43% decrease in Mig-7 levels compared to 3-1 expressing cells. In addition, we identified a previously uncharacterized siRNA construct, 4-2, which reduced Mig-7 protein levels by 30% compared to 3-1 expressing cells as well (Figure 6b). Mice injected with RL95 cells expressing siRNA 1-3 and 4-2 showed significant ($p < 0.05$) decreases of >60% and of 40-50%, respectively, in tumor volume 13 and 15 days after injection compared to mice injected with control cells expressing siRNA 3-1A (Figure 6b). Mice injected with Matrigel alone showed no tumor formation across the entire time period (data not shown). Western blot analyses of primary tumor lysates showed a 75% decrease in Mig-7 protein levels in tumors from mice injected with RL95 cells expressing siRNA 1-3 compared to tumors from mice injected with RL95 siRNA 3-1 expressing cells (Figure 6c).

107

Discussion

Using Mig-7 as a target decreased HEC1A endometrial carcinoma cell chemoinvasion and enhanced MC killing of MCF-7 breast carcinoma cells, as well as MC production of TNF-α *in vitro*. In addition, knockdown of Mig-7 using specific siRNA expression initially decreased RL95 cell tumor growth *in* vivo. These results suggest that Mig-7 may play a role in tumor growth and progression. Targeting molecules using both antibodies and siRNAs, which inhibit translation of RNA and downstream functions of overexpressed tumor cell proteins, may be possible therapies to decrease tumor progression (29-31). However, to date, none of the targets of these therapies are cancer-specific and, ultimately, *in vivo* toxicity affecting normal cells can occur. Because of its apparent specific expression in tumor cells (1-3), we speculate that targeting Mig-7 will allow higher, more effective doses that will not affect normal cells.

Anti-cancer antibody therapies are one of the newest in targeted approaches. For example, Herceptin® (Trastuzumab), an antibody therapy, targets HER2, an EGF receptor that is overexpressed in approximately 20% of breast cancer patients. In clinical trials of over 3,000 breast cancer patients positive for overexpression and after a median follow-up of 23 months, 13.7% of women treated with doxorubicin and cyclophosphamide then by docetaxel suffered recurrence or death, compared with 7.2% of women treated with doxorubicin and cyclophosphamide followed by docetaxel and trastuzumab (31). This finding is significant. However, due to cardiac toxicity, limitations in therapy include shorter duration or lower doses (31). These types of toxicities on normal cells could be avoided with tumor cell-specific targets. Mig-7

potentially represents one such target because, in studies to date, its expression is limited to cancer tissue and cells, as well as to cancer-like fetal trophoblast cells (1-3).

Our current immunohistochemical data further demonstrates the specificity of Mig-7 to cancer tissue, specifically to breast carcinoma tissue and not in normal breast tissue. Although the percentage of total breast carcinoma tissues staining for Mig-7 is 53%, this may be due to the fact that only a small core of the tumor tissue was taken for these analyses, and the invasive front of carcinoma cells may not be represented in some of these core samples. Our previous data, however, shows that 98% of cDNA from breast carcinoma tissue samples (n=50) contain moderate to high levels of Mig-7 (3). It is also intriguing that Mig-7 is expressed in human breast adenosis with hyperplasia, which is considered "pre-cancerous" tissue. We found similar pre-cancerous lesions positive for Mig-7 in endometrial tissue (3). Collectively, these data suggest that Mig-7 could potentially be targeted to inhibit cancer progression at early, as well as late, stage disease. In addition, Mig-7 is expressed in at least 87% (n=241) of all solid cancer types studied to date (3), in contrast to HER2 that is limited in expression (31).

Our current data demonstrate that antibody to Mig-7 peptide can inhibit invasion of carcinoma cells *in vitro*, suggesting that treatment with Mig-7 antibody *in vivo* may inhibit invasion and metastasis. Previous studies show that antibody to CXCR4, a chemokine receptor, inhibits invasion of carcinoma cells (32). In immunohistochemical analyses, this antibody detects Mig-7 protein localized to tumor cells lining vessel structures in metastasized lymph nodes. By immunoblot analyses, this antibody detects

109

endogenous Mig-7 at the same size as anti-FLAG antibody detects FLAG-tagged Mig-7 in stably transfected cells (2).

Interestingly, analysis of Collagen I degradation by HEC1A cells showed no difference between IgG and Mig-7 antibody-treated cells, suggesting that Mig-7 does not promote degradation of this particular matrix protein (data not shown). In contrast, Mig-7 does increase laminin 5-γ2 chain domain III fragments (2). Mig-7 is induced by several tumor microenvironment growth factors known to be involved in invasion and aggressive tumor cell behavior (2). These invading tumor cells are also resistant to current therapies (33). Thus, targeting Mig-7 would likely decrease aggressive tumor cell behavior that is caused by multiple growth factors.

Mig-7 protein is membrane-bound and cysteine-rich, and free thiol groups on cysteine residues have been shown to activate various matrix metalloproteinases, including the membrane-bound metalloproteinase MT1-MMP (MMP-14), via the "cysteine switch" mechanism (24, 25). Thus, we hypothesized that Mig-7 expression aids in MT1-MMP activation via its numerous cysteine residues. Our data have shown that inhibiting Mig-7 function and expression leads to decreased levels of active MT1-MMP, suggesting a possible mechanism by which Mig-7 is promoting invasion and tumor growth.

Analysis of protein phosphorylation in RL95 siRNA cell lines demonstrated decreased levels of phosphorylated ERK1/2, Akt, and S6 kinase in cells with reduced Mig-7, suggesting a potential downstream signaling cascade involved in Mig-7 effects. Other signaling molecules analyzed, IGF-1R and PRAS40, which are known to play roles in tumor growth and progression (5, 34), showed no decrease in phosphorylation,

further highlighting the potential for the ERK1/2, Akt, and S6 kinase signaling molecules being specifically involved in Mig-7 effects. Phosphorylation of IGF-1 receptor, whose activation is found to upregulate Mig-7 expression (unpublished data), was not changed upon reduction of Mig-7 levels, suggesting that Mig-7 is not acting directly on the receptor, but rather is acting by way of the downstream targets. Intriguingly, activation of ERK1/2 and Akt downstream of RTK signaling both results from and results in increased MT1-MMP activation (35-37), and is also linked to invasion downstream of RTK activation and αv integrin ligation (38-40), which induce endogenous Mig-7 (1, 2). Similarly, S6 kinase activation downstream of HGF and both ERK1/2 and Akt signaling has been shown to be important for tumor cell migration (41). These findings establish a potential connection between these signaling pathways as mechanisms of Mig-7 function and its effects on MT1-MMP activation.

Enhanced killing suggests that Mig-7 is a tumor antigen target capable of stimulating human MC and, thus, suggests that Mig-7 possesses tumor-specific epitopes recognized by human MC. In addition, these experiments show that Mig-7 peptides combined with MUC-1 are superior in stimulating MC to kill MCF-7 cells over MUC-1 peptide stimulation alone or with control peptides. Furthermore, one mechanism involved is the enhanced production of TNF-α by Mig-7 peptide treatment, a MC cytokine known to cause tumor cell death (42). This is likely the mechanism of cell killing in our assay because MCF-7 cells are responsive to TNF-α (43). Interestingly, other cases have been found in which frameshifted proteins produce new, cryptic, tumor-specific epitopes (44). These epitopes can potentially allow tumor cells to evade detection by the immune system. Since Mig-7 is apparently frameshifted to the +1

reading frame (28)(Accession DQ080207), it may contain cryptic epitopes. These data suggest that Mig-7 peptides could be used *ex vivo* to enhance the efficacy of antigen-presenting cells *in vivo*. In light of the recent and virtually 100% efficacy of vaccine to human papilloma virus strains that prevent cervical cancer (45), it is tempting to speculate that inoculating with peptides specific to Mig-7 may serve as a cancer vaccine.

Expression of Mig-7 leads to invasion and vessel-like structure formation in 3D cultures (2). In the present study, we also demonstrated that inhibition of Mig-7 expression by stable expression of Mig-7 specific siRNAs reduced tumor growth *in vivo*, suggesting its involvement in tumor growth as well. Interestingly, a significant decrease in tumor growth was observed between 11 and 18 days after injection and this tumor growth trend correlated to Mig-7 protein levels determined by immunoblot analysis. Immunoblot data also demonstrate that Mig-7 protein is decreased in the primary tumors from mice injected with RL95 siRNA 1-3-expressing cells compared to tumors from siRNA 3-1-expressing cells collected at day 28 after injection. However, the relative reduction in Mig-7 protein between tumors from mice injected with 1-3 expressing cells and 3-1 expressing tumors was larger than the relative reduction shown in these cells *in vitro*. This may be due to the inherent difference between the *in vitro* and *in vivo* settings and the different effects this may have on the cells. This data confirmed that decreased selection and loss of Mig-7 knockdown is not responsible for increased tumor sizes at later time points. The reduction in tumor growth observed may be due to inhibition of vessel formation by aggressive tumor cells, called vasculogenic mimicry (46, 47). Tumors formed in mice injected with RL95 cells expressing normal

levels of Mig-7 expression may contribute to the formation of these vessel-like structures to aid in tumor growth, while normal angiogenesis further accelerates tumor growth. RL95 cells containing reduced Mig-7 levels may initially have a reduced capacity to form these structures, making angiogenesis the primary source of nutrients and slowing tumor growth. However, vessel-like structures were not seen in these primary tumors by histology (data not shown).

Another possible explanation stems from a recent study utilizing knockdown of the E-cadherin repressor Snail1 in breast carcinoma cells which demonstrated a link between invasion and primary tumor growth (48). Knockdown of Snail1 inhibited transition to the invasive phenotype and invasion *in vitro*, while also suppressing tumor growth *in vivo*. Based on this data, and because Mig-7 is also linked to invasion *in vitro*, it is possible that reduction of Mig-7 in RL95 cells slows primary tumor growth by inhibition of local invasion of tumor cells. This local invasion would facilitate tumor growth until the size of the tumor exceeds its blood supply. Thus, targeting Mig-7 may inhibit primary tumor growth as a direct result of local invasion inhibition.

Vasculogenic mimicry and aggressive invasion are highly correlated with poor prognosis and outcome (12, 46). Furthermore, when cancer cells are invading or circulating they are resistant to apoptosis and current therapies (33). Thus, targeting a gene expression involved in invasion, especially one specific to tumor cells, such as Mig-7, could lead to more effective treatments with less recurrence due to residual invading or circulating cancer cells that were not killed by standard therapies. These proof-of-principle results suggest that inhibition of Mig-7 expression or function can inhibit carcinoma cell invasion and possibly disease progression *in vivo*.

References

(1) Crouch S, Spidel CS, Lindsey JS. HGF and ligation of $\alpha v \beta 5$ integrin induce a novel, cancer cell-specific gene expression required for cell scattering. Experimental Cell Research 2004;292:274-87.

(2) Petty AP, Garman KL, Winn VD, Spidel CM, Lindsey JS. Overexpression of carcinoma and embryonic cytotrophoblast cell-specific Mig-7 induces invasion and vessel-like structure formation. Am J Pathol 2007;170:1763-80.

(3) Phillips TM, Lindsey JS. Carcinoma cell-specific Mig-7: A new potential marker for circulating and migrating cancer cells. Oncology Reports 2005;13:37-44.

(4) Robertson GP. Mig-7 linked to vasculogenic mimicry. The American Journal of Pathology 2007;170:1454-6.

(5) Brooks PC, Klemke RL, Schon S, Lewis JM, Schwartz MA, Cheresh DA. Insulin-like growth factor receptor cooperates with integrin alpha v beta 5 to promote tumor cell dissemination in vivo. Journal of Clinical Investigation 1997;99:1390-8.

(6) Klemke RL, Yebra M, Bayna EM, Cheresh DA. Receptor tyrosine kinase signaling required for integrin alpha v beta 5-directed cell motility but not adhesion on vitronectin. Journal of Cell Biology 1994;127:859-66.

(7) Beard J. Embryological aspects and etiology of carcinoma. The Lancet 1902;1:1758-61.

(8) Red-Horse K, Zhou Y, Genbacev O, et al. Trophoblast differentiation during embryo implantation and formation of the maternal-fetal interface. Journal of Clinical Investigation 2004;114:744-54.

(9) Soundararajan R, Rao AJ. Trophoblast 'pseudo-tumorigenesis': Significance and contributory factors. Reproductive Biology and Endocrinology 2004;2:15.

(10) Seftor REB, Seftor EA, Koshikawa N, et al. Cooperative interactions of Laminin 5 γ2 Chain, Matrix Metalloproteinase-2, and Membrane Type-1 Matrix/Metalloproteinase are required for mimicry of embryonic vasculogenesis by aggressive melanoma. Cancer Res 2001;61:6322-7.

(11) Maniotis AJ, Folberg R, Hess A, et al. Vascular channel formation by human melanoma cells in vivo and in vitro: Vasculogenic mimicry. Am J Pathol 1999;155:739-52.

(12) Sood AK, Seftor EA, Fletcher MS, et al. Molecular determinants of ovarian cancer plasticity. Am J Pathol 2001;158:1279-88.

(13) Sun B, Zhang S, Zhang D, et al. Vasculogenic mimicry is associated with high tumor grade, invasion and metastasis, and short survival in patients with hepatocellular carcinoma. Oncology Reports 2006;16:693-8.

(14) van der Schaft DWJ, Hillen F, Pauwels P, et al. Tumor cell plasticity in Ewing sarcoma, an alternative circulatory system stimulated by hypoxia. Cancer Res 2005;65:11520-8.

(15) Hendrix MJC, Seftor EA, Kirschmann DA, Quaranta V, Seftor REB. Remodeling of the microenvironment by aggressive melanoma tumor cells. Ann NY Acad Sci 2003;995:151-61.

(16) Wright SE, Kilinski L, Talib S, et al. Cytotoxic T lymphocytes from humans with adenocarcinomas stimulated by native MUC1 mucin and a mucin peptide mutated at a glycosylation site. Journal of Immunotherapy 2000;23:2-10.
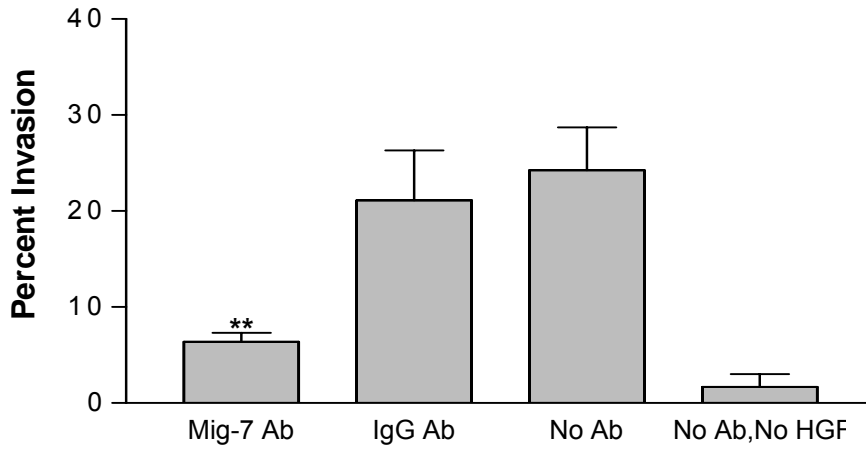
(17) Hendrix MJC, Seftor EA, Seftor REB. Comparison of tumor cell invasion assays: human amnion versus reconstituted basement membrane barriers. Invasion & Metastasis 1989;9:278-97.

(18) Yang AD, Camp ER, Fan F, et al. Vascular Endothelial Growth Factor Receptor-1 Activation Mediates Epithelial to Mesenchymal Transition in Human Pancreatic Carcinoma Cells. Cancer Res 2006;66:46-51.

(19) Noguchi P. Use of flow cytometry for DNA analysis. Current Protocols in Immunology.New York: Green Publishing Associates and Wiley-Interscience; 1991. p. 5.7.1-5.7.4.

(20) Windsor LJ, Bodden MK, Birkedal-Hansen B, Engler JA, Birkedal-Hansen H. Mutational analysis of residues in and around the active site of human fibroblast-type collagenase. J Biol Chem 1994;269:26201-7.

(21) Williams NS, Burgett AWG, Atkins AS, Wang X, Harran PG, McKnight SL. Therapeutic anticancer efficacy of a synthetic diazonamide analog in the absence of overt toxicity. PNAS 2007;104:2074-9.

(22) Roehm NW, Rodgers GH, Hatfield SM, Glasebrook AL. An improved colorimetric assay for cell proliferation and viability utilizing the tetrazolium salt XTT. Journal of Immunological Methods 1991;142:257-65.

(23) Bae-Jump V, Segreti EM, Vandermolen D, Kauma S. Hepatocyte growth factor (HGF) induces invasion of endometrial carcinoma cell lines in vitro. Gynecologic Oncology 1999;73:265-72.

(24) Bescond A, Augier T, Chareyre C, Garcon D, Hornebeck W, Charpiot P. Influence of Homocysteine on Matrix Metalloproteinase-2: Activation and Activity. Biochemical and Biophysical Research Communications 1999;263:498-503.

(25) Wart HEV, Birkedal-Hansen H. The Cysteine Switch: A Principle of Regulation of Metalloproteinase Activity with Potential Applicability to the Entire Matrix Metalloproteinase Gene Family. PNAS 1990;87:5578-82.

(26) Birkedal-Hansen H, Taylor RE. Detergent-activation of latent collagenase and resolution of its component molecules. Biochemical and Biophysical Research Communications 1982;107:1173-8.

(27) Wright SE, Rewers-Felkins KA, Quinlin IS, et al. Adoptive immunotherapy of mucin1 expressing adenocarcinomas with mucin1 stimulated human peripheral blood mononuclear cells. International Journal of Molecular Medicine 2002;9:401-4.

(28) Petty AP, Dick CL, Lindsey JS. Translation of an atypical human cDNA requires fidelity of a purine-pyrimidine repeat region and recoding. GENE In Press. 2008.

116

(29) Pai SI, Lin YY, Macaes B, Meneshian A, Hung CF, Wu TC. Prospects of RNA interference therapy for cancer. Gene Ther 2005;13:464-77.

(30) Pushparaj PN, Melendez AJ. Short Interfering RNA (siRNA) as a novel therapeutic. Clinical and Experimental Pharmacology and Physiology 2006;33:504-10.

(31) Tuma RS. Trastuzumab Faces Trials, Clinical and Otherwise. J Natl Cancer Inst 2006;98:296-8.

(32) Müller A, Homey B, Soto H, et al. Involvement of chemokine receptors in breast cancer metastasis. Nature 2001;410:50-6.

(33) Condeelis J, Singer RH, Segall JE. The great escape: When cancer cells hijack the genes for chemotaxis and motility. Annual Review of Cell and Developmental Biology 2005;21:695-718.

(34) Madhunapantula SV, Sharma A, Robertson GP. PRAS40 Deregulates Apoptosis in Malignant Melanoma. Cancer Res 2007;67:3626-36.

(35) Lehti K, Allen E, Birkedal-Hansen H, et al. An MT1-MMP-PDGF receptor-{beta} axis regulates mural cell investment of the microvasculature. Genes Dev 2005;19:979-91.

(36) Takino T, Miyamori H, Watanabe Y, Yoshioka K, Seiki M, Sato H. Membrane Type 1 Matrix Metalloproteinase Regulates Collagen-Dependent Mitogen-Activated Protein/Extracellular Signal-Related Kinase Activation and Cell Migration. Cancer Res 2004;64:1044-9.

(37) Tsubaki M, Matsuoka H, Yamamoto C, et al. The protein kinase C inhibitor, H7, inhibits tumor cell invasion and metastasis in mouse melanoma via suppression of ERK1/2. Clinical and Experimental Metastasis 2007;24:431-8.

(38) Hollier BG, Kricker JA, Van Lonkhuyzen DR, Leavesley DI, Upton Z. Substrate-Bound Insulin-Like Growth Factor (IGF)-I-IGF Binding Protein-Vitronectin-Stimulated Breast Cell Migration Is Enhanced by Coactivation of the Phosphatidylinositide 3-Kinase/AKT Pathway by {alpha}v-Integrins and the IGF-I Receptor. Endocrinology 2008;149:1075-90.

(39) Matsuo M, Sakurai H, Ueno Y, Ohtani O, Saiki I. Activation of MEK/ERK and PI3K/Akt pathways by fibronectin requires integrin alphav-mediated ADAM activity in hepatocellular carcinoma: A novel functional target for gefitinib. Cancer Science 2006;97:155-62.

(40) Zhou HY, Pon YL, Wong AST. Synergistic Effects of Epidermal Growth Factor and Hepatocyte Growth Factor on Human Ovarian Cancer Cell Invasion and Migration: Role of Extracellular Signal-Regulated Kinase 1/2 and p38 Mitogen-Activated Protein Kinase. Endocrinology 2007;148:5195-208.
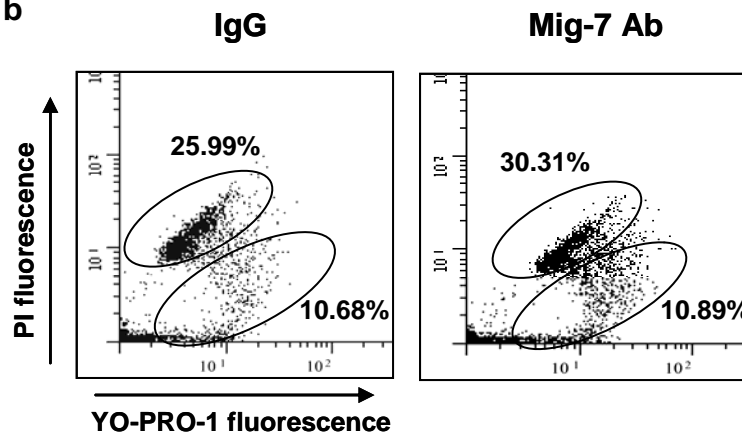
(41) Wong AST, Roskelley CD, Pelech S, Miller D, Leung PCK, Auersperg N. Progressive changes in Met-dependent signaling in a human ovarian surface epithelial model of malignant transformation. Experimental Cell Research 2004;299:248-56.

(42) Bonta IL, Ben Efraim S. Interactions between inflammatory mediators in expression of antitumor cytostatic activity of macrophages. Immunology Letters 1990;25:295-301.

(43) Xiang J, Moyana T, Qi Y. Genetic engineering of a recombinant fusion possessing anti-tumor F(ab')2 and tumor necrosis factor. Journal of Biotechnology 1997;53:3-12.

(44) Ho O, Green WR. Alternative Translational Products and Cryptic T Cell Epitopes: Expecting the Unexpected. J Immunol 2006;177:8283-9.

(45) Hildesheim A, de Gonzalez AB. Etiology and Prevention of Cervical Adenocarcinomas. J Natl Cancer Inst 2006;98:292-3.

(46) Folberg R, Hendrix MJC, Maniotis AJ. Vasculogenic mimicry and tumor angiogenesis. Am J Pathol 2000;156:361-81.

(47) Sood AK, Fletcher MS, Hendrix MJ. The embryonic-like properties of aggressive human tumor cells. Journal of the Society for Gynecologic Investigation 2002;9:2-9.

(48) Olmeda D, Moreno-Bueno G, Flores JM, Fabra A, Portillo F, Cano A. SNAI1 Is Required for Tumor Growth and Lymph Node Metastasis of Human Breast Carcinoma MDA-MB-231 Cells. Cancer Res 2007;67:11721-31.

Figure 1. Mig-7 specific antibody decreases HEC1A endometrial carcinoma chemoinvasion. **(a)** Mig-7 affinity-purified antibody, but not IgG rabbit isotype antibody, significantly decreased chemoinvasion of HEC1A cells into Matrigel toward HGF (p<0.01). Ab = antibody, w/HGF = bottom wells contained 20 ng/ml HGF. Results shown are after 72 hours of invasion. Results are representative of three independent experiments performed in triplicate**.** Bars represent SEM. **(b)** Representative flow cytometry graphs of control IgG and Mig-7 antibody-treated HEC1A cells stained with YO-PRO-1 and propidium iodide (PI). YO-PRO-1 positive detected (lower oval) are apoptotic cells and double positive detected (upper oval) indicated dead cells. Mean percentages of three samples are shown. **(c)** Representative flow cytometry graphs of control IgG and Mig-7 antibody-treated HEC1A cells stained with PI. In each graph, left peak indicates cells in G1 cell cycle phase and right peak indicates cells in G2/M phase. Mean percentages of three samples are shown. Experiments were repeated once with similar results.
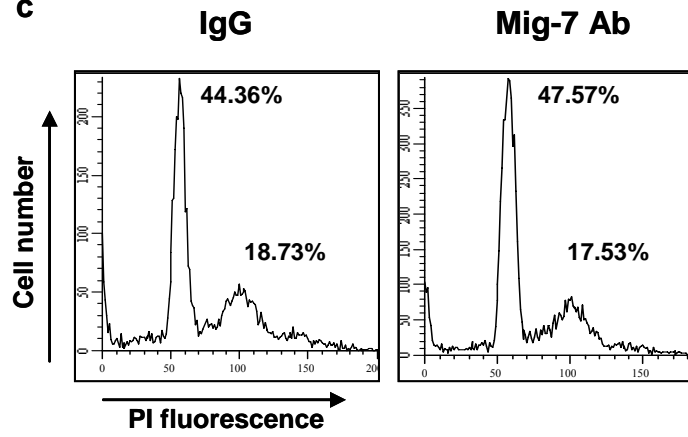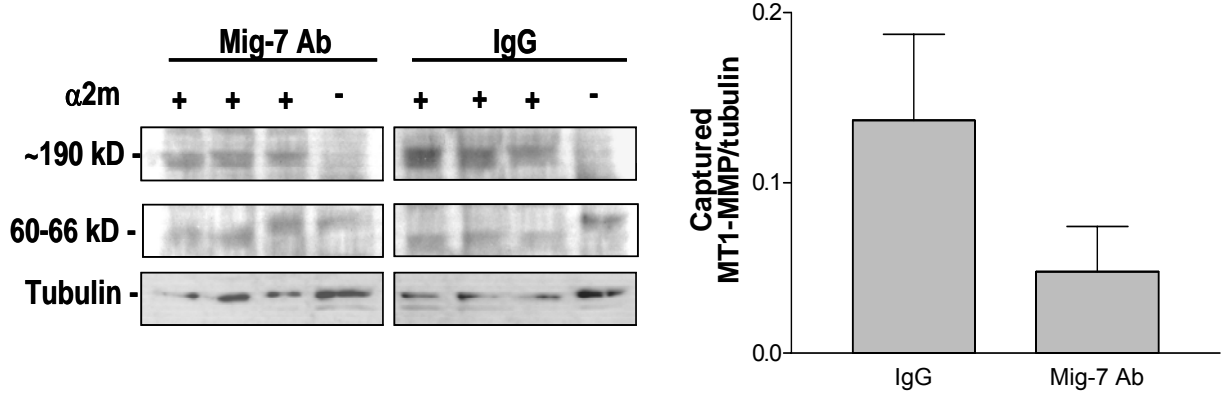
a

b

IgG Mig-7 Ab

25.99%

10.68%

30.31%

10.89%

PI fluorescence

YO-PRO-1 fluorescence

c

IgG Mig-7 Ab

44.36%

18.73%

47.57%
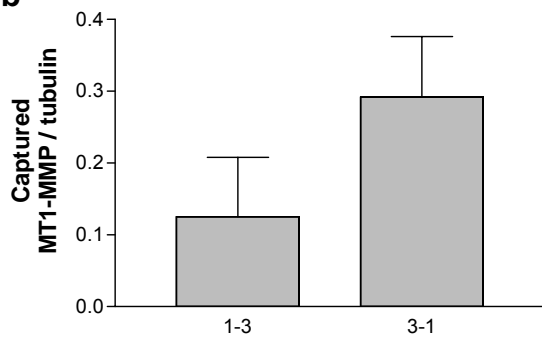
17.53%

Cell number

PI fluorescence

Figure 2. Antibody or expression of siRNA specific to Mig-7 decreases activity of MT1-MMP. **(a)** Representative immunoblot and densitometry results for α2-macroglobulin capture assay of HEC1A cells treated with IgG or Mig-7 antibody. Mig-7 antibody treatment decreased MT1-MMP activity by 54% compared to IgG treatment. Densitometry data are for the upper, captured MT1-MMP band in each lane normalized to its respective tubulin band. Bars represent SEM. **(b)** Densitometry analysis of the upper, captured MT1-MMP band from α2-macroglobulin capture assay in lysates from RL95 cells stably transfected with siRNA 1-3 and 3-1. Results are normalized to β-tubulin. RL95 cells expressing siRNA 1-3 showed a 57% decrease in MT1-MMP activity compared to 3-1 expressing cells. Bars represent SEM. **(c)** Representative flow cytometry graphs of RL95 siRNA 1-3 and 3-1 stably transfected cells stained with YO-PRO-1 and propidium iodide (PI). YO-PRO-1 positive staining (lower oval) indicated apoptotic cells and double positive staining (upper oval) indicated dead cells. Mean percentages of three samples are shown. **(d)** Representative flow cytometry graphs of RL95 siRNA 1-3 and 3-1 stably transfected cells stained with propidium iodide for cell cycle analysis. Left peak indicates cells in G1 phase, and right peak indicates cells in G2/M phase. Mean percentages of three samples are shown.
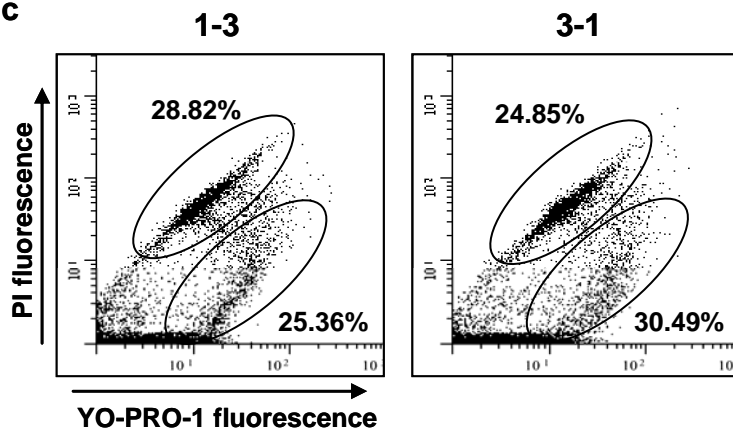
a

Mig-7 Ab   IgG

α2m   + + + -   + + + -

~190 kD -

60-66 kD -

Tubulin -

b

c

1-3   3-1

28.82%   24.85%

25.36%   30.49%

PI fluorescence

YO-PRO-1 fluorescence

122

d
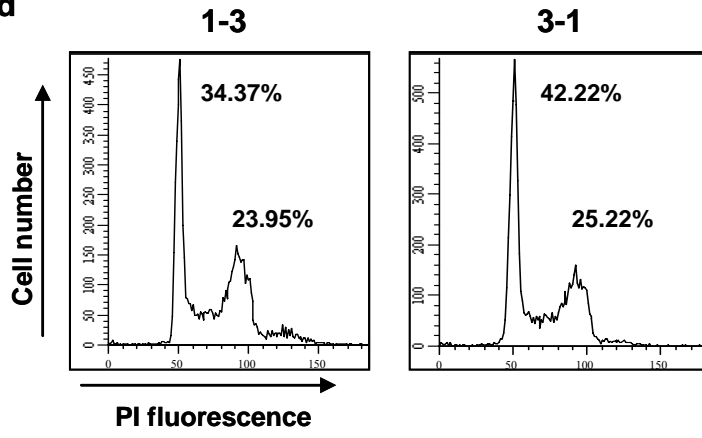
Figure 3. Expression of siRNA specific to Mig-7 decreases ERK1/2, Akt, and S6 kinase phosphorylation. **(a)** Normalized fluorescence intensity from analysis of phosphorylated ERK1/2, Akt, and S6 kinase in RL95 siRNA 1-3 and 3-1 stably transfected cells. Cells were plated and prepared as given in Materials and Methods. 1-3 expressing cells showed a 40% decrease ($p<0.01$) in ERK1/2 activation, a 10% decrease ($p<0.05$) in Akt activation, and a 30% decrease in S6 kinase activation ($p<0.05$) compared to 3-1 expressing cells. **(b)** Normalized fluorescence intensities from analysis of phosphorylated PRAS40 and IGF-1R. All results were normalized to total protein fluorescence intensities. All experiments were performed in triplicate.

a

ERK1/2

Akt

S6K

b

PRAS40

IGF-1R

125
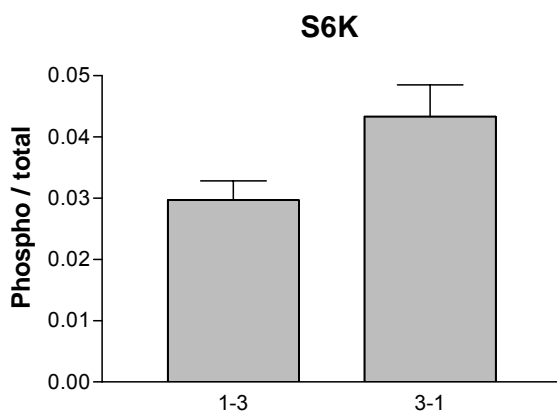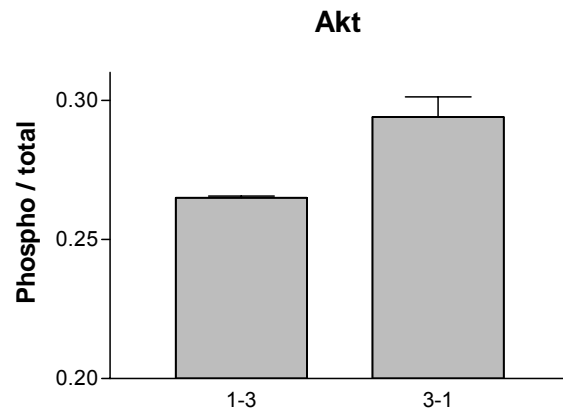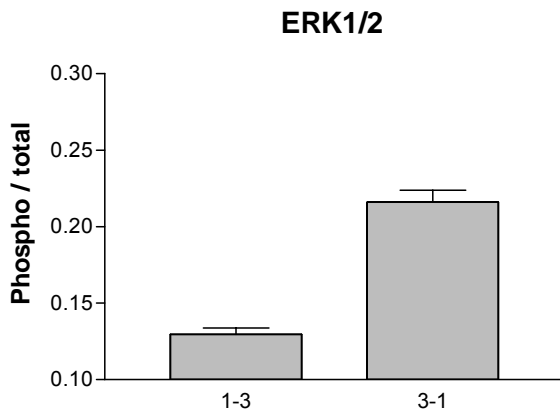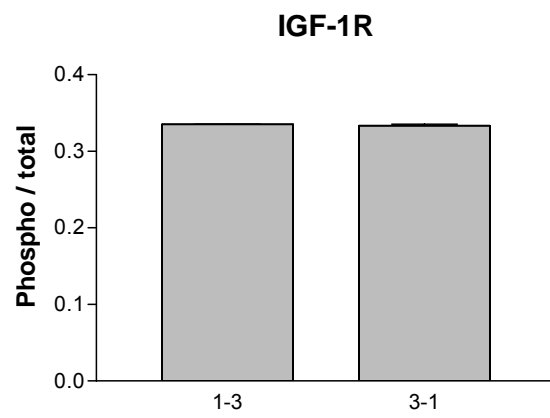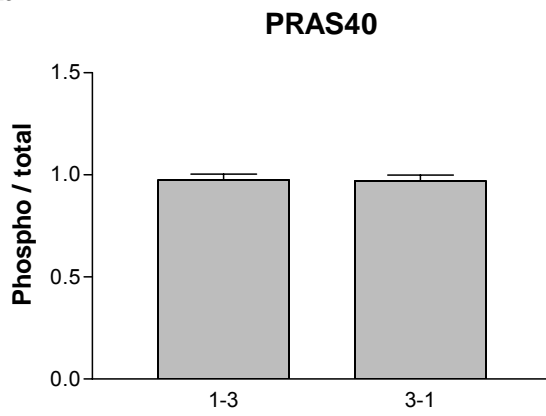
Figure 4. Mig-7 peptides enhance human monocyte killing of MCF-7 breast carcinoma cells. **(a)** MCF-7 cells expressed Mig-7 mRNA by RT-PCR and protein by immunoblot analyses. Experiments were repeated twice. **(b)** Human MC cells stimulated with IL-2 and either no peptide (0), pooled control peptides (CTL), or pooled Mig-7 peptides (sequences given in Methods) and their respective levels of MCF-7 cell lysis as described in Methods and Materials. Note that Mig-7 peptides significantly (p = 0.001) enhanced MC killing of MCF7 carcinoma cells. Experiments have been repeated 3 times in replicates of 6 for each treatment group. MCs were isolated from two different individuals. **(c)** Cytotoxic response of human isolated MC after peptide stimulation using indicated ratios of immune cells (MC) to MCF-7 cells. ─●─ represents no peptide group, ─■─ represents MUC-1 peptide treated MC group and ─▲─ represents MUC-1 plus Mig-7 peptides treated group. Bars indicate ± S.E. Experiments were repeated twice with replicates of six for each treatment group. **(d)** TNF-α production by human isolated MC after indicated peptide stimulation. TNF-α production was measured by ELISA assay as described in Methods and Materials after MC were cultured for 8 days with MUC-1 peptide, control peptides, or with Mig-7 peptides. Assays were performed in triplicate.
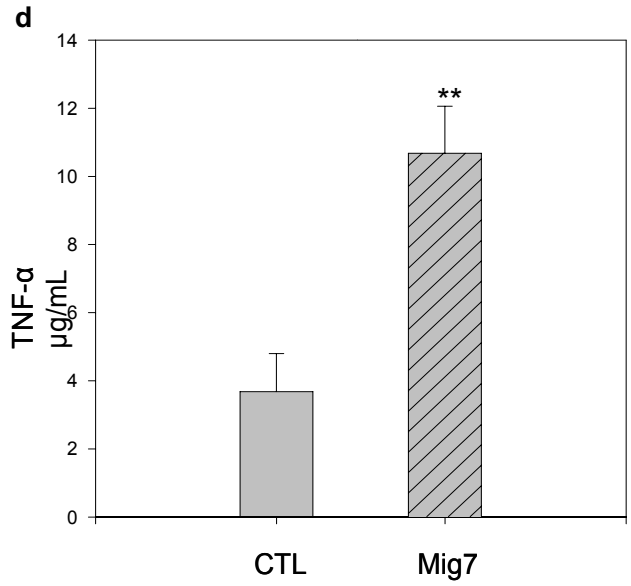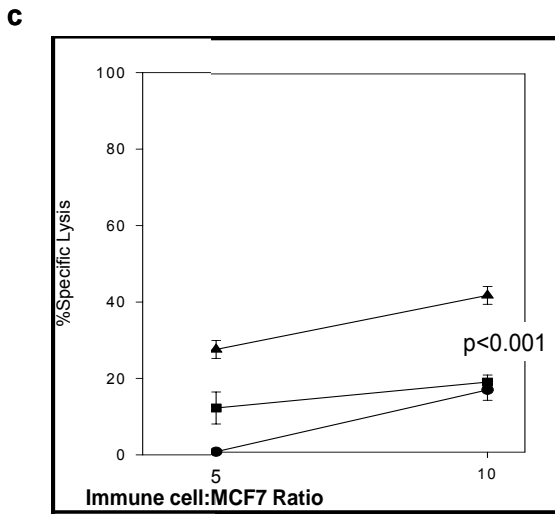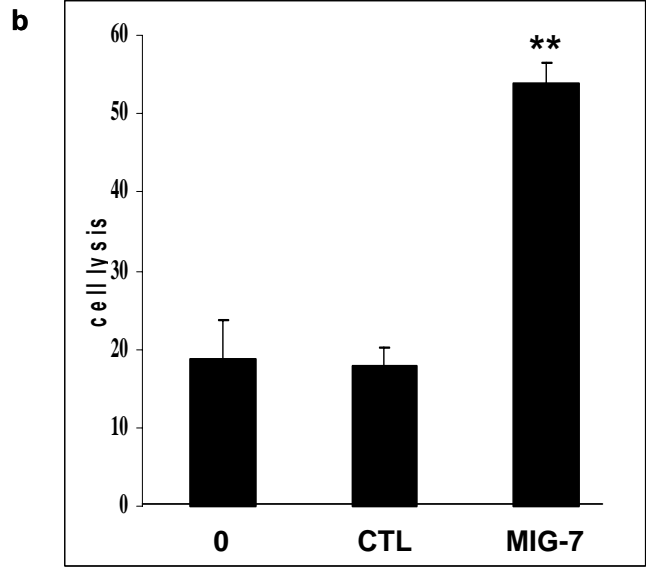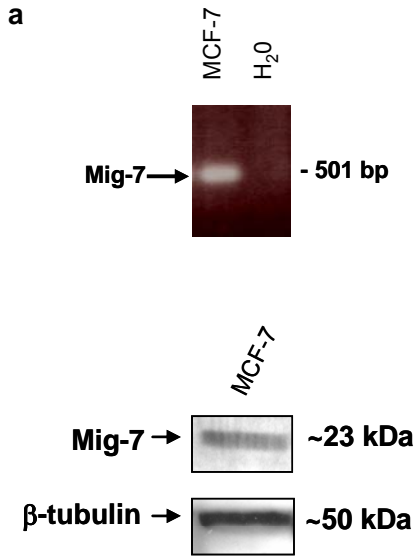
Figure 5. Mig-7 expression is specific to breast carcinoma tissue and cells. **(a)** Representative Mig-7 specific RT-PCR of three breast carcinoma cell lines (T47D, MDA-MB453, DU4475) and normal breast tissue from three subjects without previous history of cancer. Representative images of Mig-7 antibody IHC on breast tissue array from Cybrdi, Inc. as described in Materials and Methods. Core samples from **(b)** breast carcinoma. Arrows point to positive Mig-7 staining. **(c)** Normal breast tissue IHC with Mig-7 antibody. **(d)** Representative image of rabbit IgG instead of Mig-7 as primary antibody IHC of breast carcinoma tissue section (serial to that shown in b) that served as negative control. Hematoxylin was used to counterstain. Note a lack of specific staining in d compared to b. Images were taken with 10X objective on a Nikon microscope (100X total magnification) and inserts with 40X objective (400X total magnification). Scale bars indicate 100 μm for 100X images and 20 μm for inserts.

a

	ladder	T-47D	MDA-MB453	DU4475	normal

501 bp   Mig-7

324 bp   18s

b

c

d
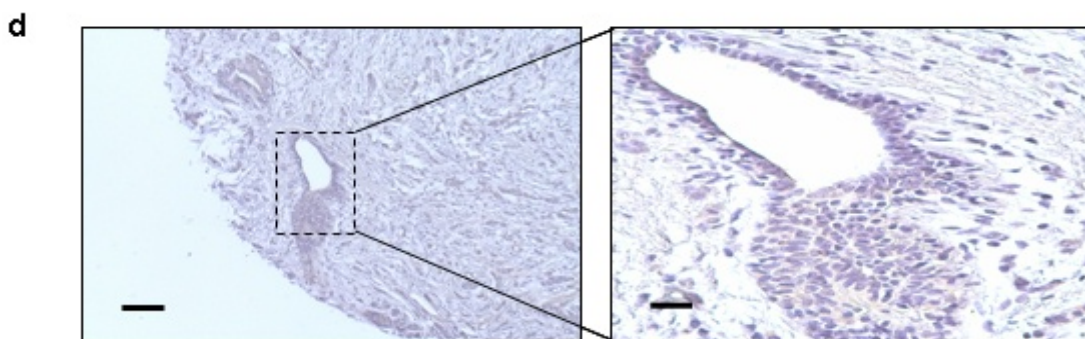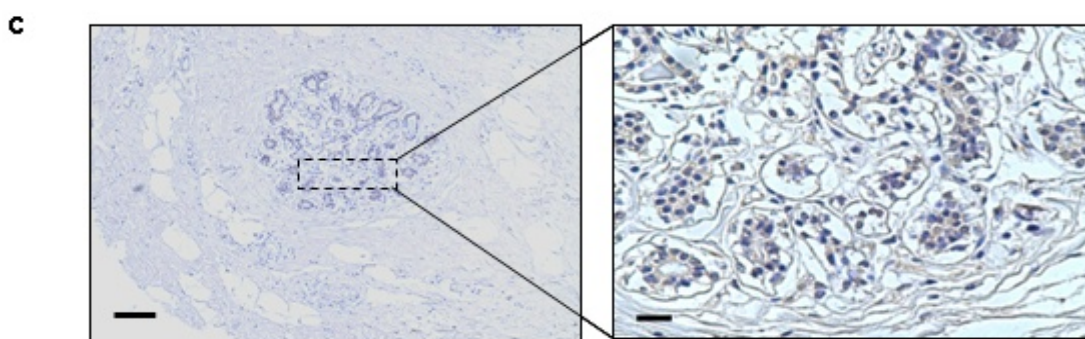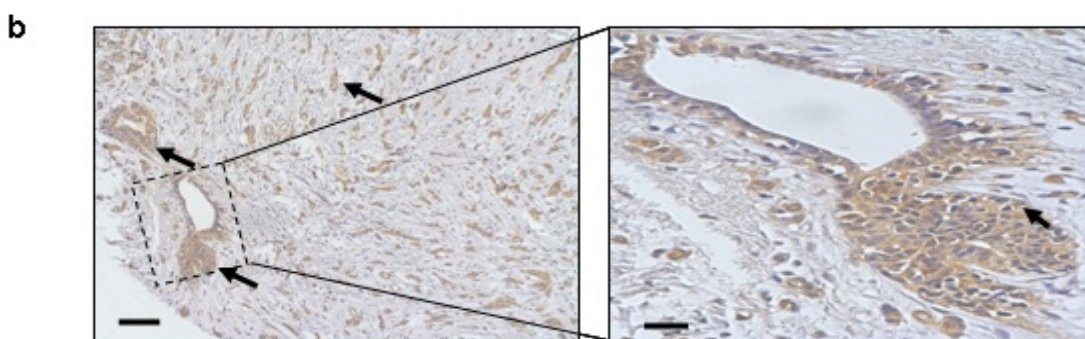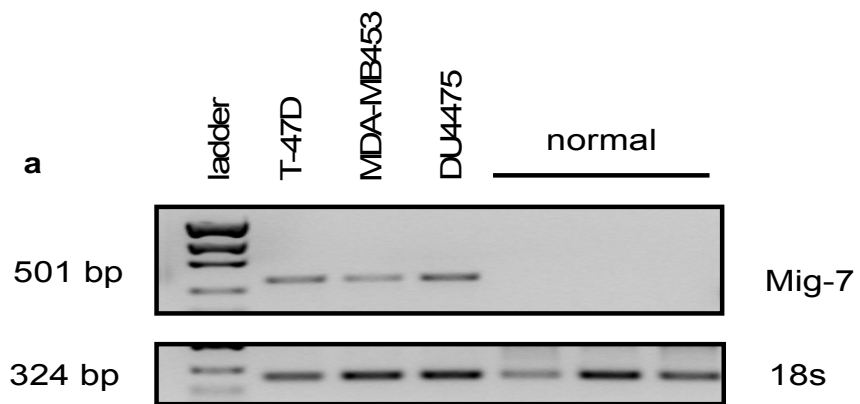
Figure 6. Stable knockdown of Mig-7 expression in RL95 cells decreases primary tumor growth in nude mice. **(a)** Representative immunoblot and densitometry of RL95 parental and Mig-7-specific siRNA stably transfected clones 1-3A, 2-3B, 3-1A, 4-2A, and 4-2B cell lines. Cells were grown for 4 days before harvest. Reprobing with β–tubulin was performed to demonstrate equal loading. Mig-7 levels were reduced in 1-3 and 4-2 expressing cells by 43% and 30%, respectively, compared to 3-1 expressing cells. **(b)** Representative graph showing the tumor volume (mm^3) measured 11, 13, 15, 18, and 23 days after injection of RL95 parental cells or cells stably transfected with siRNA constructs 1-3, 3-1, or 4-2 into nude mice, as given in Materials and Methods. Cells expressing siRNAs 1-3 and 4-2 showed a 60% and 40-50% ($p<0.05$) decrease in tumor volume, respectively, at days 13 and 15. Bars represent SEM. Experiment was performed in triplicate, n=5 mice for each treatment group, with similar results. Sequences of specific siRNAs were shown previously (5) and in Methods. **(c)** Densitometry analysis of Mig-7 western blot of primary tumor tissue lysates from RL95 parental, siRNA 1-3, and siRNA 3-1 cell-injected mice. Results were normalized to levels of β-tubulin. Tumor lysates from 1-3 expressing cell-injected mice showed a 75% decrease in Mig-7 protein levels compared to 3-1 expressing tumor lysates.

a

Mig-7 → ~23 kDa

Tubulin → ~50 kDa

b

c

1° tumors

131
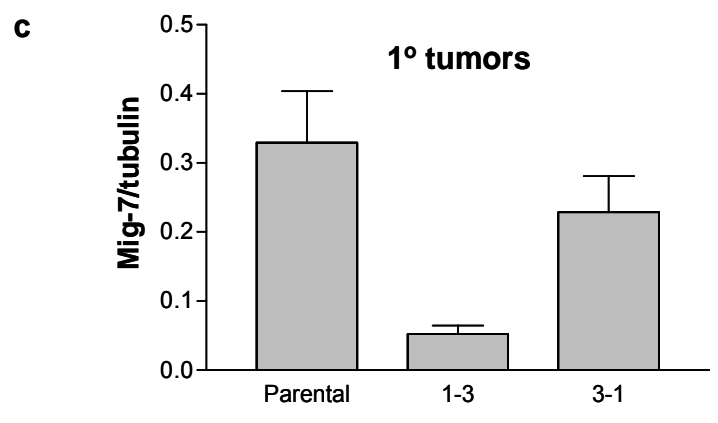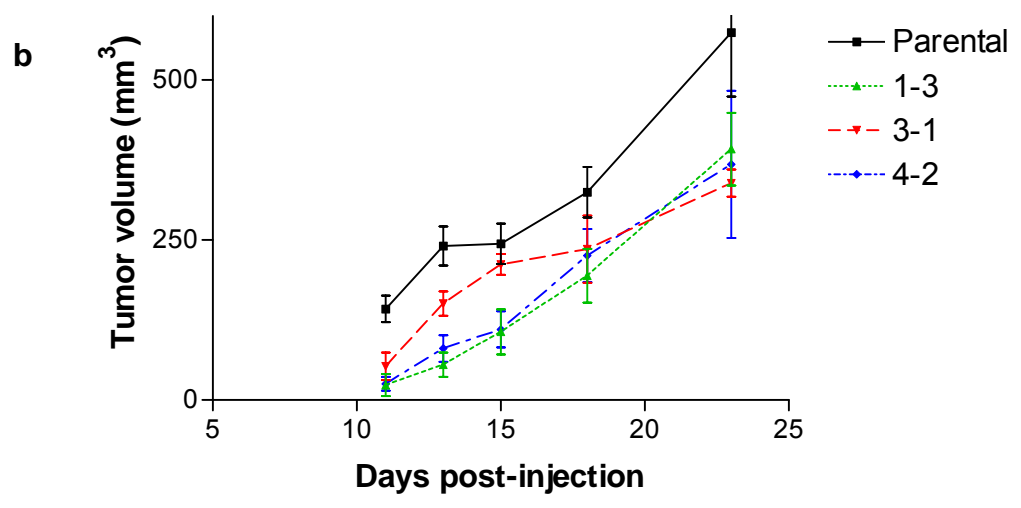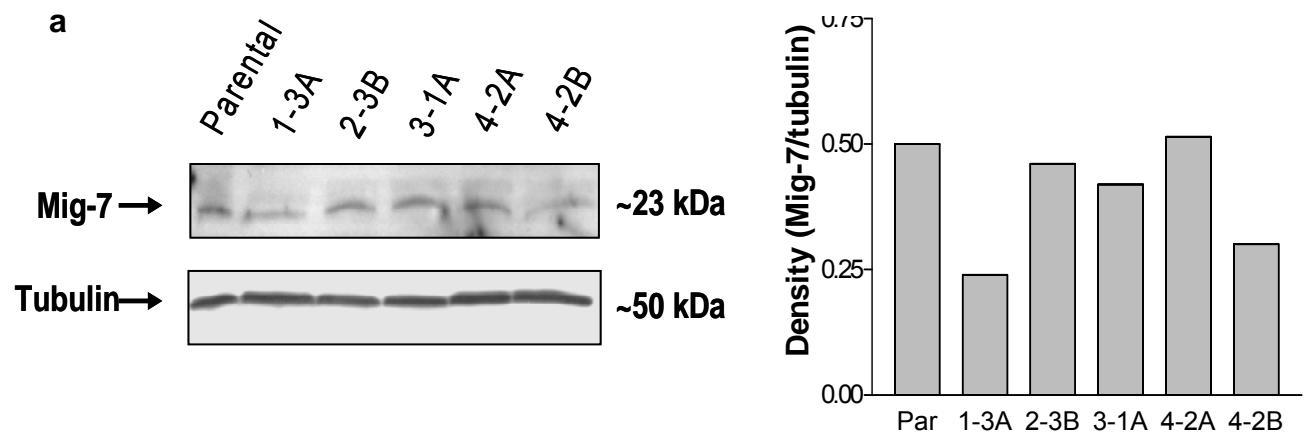
Chapter 4

CONCLUSIONS AND FUTURE DIRECTIONS

4.1 Mig-7 and cancer cell invasion

The current studies have demonstrated that Mig-7 plays a role in cancer cell sensing of the microenvironment and resulting invasion, as well as the process of vasculogenic mimicry.   Previous studies to date show that Mig-7 is expressed primarily in tumor cells of various types, including breast, ovarian, colon, endometrial, lung, and oral squamous carcinomas [80,82,83].   However, Mig-7 cDNA also shows significant homology to expressed sequence tags (ESTs) from 10-week placenta [80], suggesting that this normal tissue also may express Mig-7. Embryonic cytotrophoblast cells (CTBs) from this tissue are similar to invasive cancer cells [24,25] because they invade maternal decidua and remodel the spiral arteries during placenta development, with peak invasion and remodeling occurring between 14 and 22 weeks of gestation [25,84]. The current studies demonstrated that Mig-7 is expressed by invasive CTBs.   Mig-7 mRNA and protein is expressed in early first and second trimester (14-22 weeks), but is decreased or absent in third trimester and term placental tissue.   In addition, Mig-7 mRNA was upregulated 6 to 15-fold in embryonic CTBs plated on growth factor-containing Matrigel, which results in recapitulation of the invasive basal plate CTB phenotype [26].   Increased Mig-7 protein was also detected in these cells and colocalized with basal plate CTB cytokeratin-7 staining by immunohistochemistry.

The expression of Mig-7 in both cancer cells and CTBs suggested that it was somehow linked to invasion. To begin testing the involvement of Mig-7 expression in

the invasive process, FLAG-Mig-7 was overexpressed in HT29 colon carcinoma cells. An invasive phenotype of FLAG-Mig-7 cells was observed in 2-D Matrigel cultures, but no difference was seen in cultures on plastic. Similarly, detectable promigratory laminin 5 γ2 domain III (DIII) fragments formed only when HT29 Mig-7-overexpressing cells were plated on growth factor-containing Matrigel. Formation of these fragments apparently allows increased migration and invasion by making cells less adhesive to their basement membranes, in addition to upregulation of MMP-2 [28,52]. Overexpression of Mig-7 in HT29 cells caused decreased adhesiveness of these cells to various laminins, suggesting that this is a potential mechanism by which Mig-7 is causing invasion. Interestingly, laminin matrix, but not other basement membrane components, is also important for vessel formation by human umbilical endothelial cells (HUVEC) derived from the fetus [85].

RL95 cells with reduced levels of Mig-7 demonstrated more clonal growth when plated in 3-D growth factor-containing Matrigel, as opposed to the more disseminated phenotype exhibited by parental and control siRNA cells. Consistent with HT29 results, these cells showed no noticeable differences in phenotype when plated in 2-D on tissue culture dish plastic. Previous plating of RL95 parental cells on growth factor-containing Matrigel in 2-D also showed increased levels of Laminin 5 γ2 chain fragments, which are known to be important in invasion, cell motility, and tumor progression [28,30,86], compared to plating on growth factor-reduced Matrigel. The fragment detected by immunoblotting and by IHC is the domain III (DIII) segment, which is known to contain EGF-like repeats and stimulate the EGF receptor to increase MMP-2 expression, further chain cleavage, and cell motility [28,52]. These results demonstrate that adoption of

the invasive phenotype depends not only on Mig-7 expression, but also on the local microenvironment of the tumor. Matrigel contains multiple growth factors present in the tumor microenvironment *in vivo* and better mimics the local environment in which the tumor cells are normally present. In addition, culturing cells in 3-D simulates the *in vivo* context better than plating in 2-D [87-91]. Thus, Mig-7 seems to play a role in allowing the cells to better sense the surrounding microenvironment and may be interacting with MT1-MMP and/or integrins to cause cryptic sites to be revealed and binding to them, respectively, causing this different sensing.

Furthermore, transwell chemoinvasion assays with HEC1A endometrial carcinoma cells treated with a polyclonal Mig-7-specific antibody inhibits invasion by 70-75%, suggesting Mig-7 is important for invasion of these cells *in vitro*. This assay is correlative to invasive potential *in vivo* [92]. HEC1As invaded lymph nodes and formed higher numbers of vessel-like "hot-spots" compared to RL95 cells. These data are consistent with levels of Mig-7 expressed by each cell line and their respective invasive potential [75,81].

Invasion of cancer cells involves cleavage of the laminin 5 γ2 chain into promigratory fragments [28-30], and the metalloproteinases MMP-2 and MT1-MMP have been shown to directly or indirectly cleave the γ2 chain [49-51]. These proteases exist in a membrane complex with TIMP-2 that is required for their activation [46-48], and disruption of the interaction between the cysteine residue in the prodomain and the Zn^{+2} ion in the catalytic domain by multiple mechanisms activates these enzymes [33,34]. Since Mig-7 protein possesses ~10% cysteine residues in the first 91 amino acids, we hypothesized that these cysteine residues are able to interact with and disrupt

134

this bond on MT1-MMP via the "cysteine switch" mechanism [40,93], resulting in its increased activation and the increased cleavage of laminin 5-γ2 chain previously shown in Mig-7 expressing cells. Data in these studies show that reducing Mig-7 expression by ~70% in RL95 cells resulted in a 57% reduction in the levels of activated MT1-MMP (MMP-14). This data was supported by a similar 54% reduction in active MT1-MMP in HEC1A cells in which invasion was reduced 70% by Mig-7 specific antibody treatment. These results suggest that Mig-7 may be involved in activation of MT1-MMP, resulting in laminin 5 γ2 chain cleavage and invasion. Further studies are required to determine how Mig-7 alters MT1-MMP activity.

Recent analysis of protein phosphorylation in RL95 siRNA expressing cell lines showed a decrease in ERK1/2, Akt, and S6 kinase phosphorylation in siRNA expressing cells with 70% less Mig-7 compared to control siRNA expressing cells. Phosphorylation of other signaling molecules involved in tumor progression [94,95] was also examined and no differences were seen. Activation of ERK1/2 is a result of interaction between the laminin 5 γ2 chain DIII fragment with the EGF receptor, resulting in increased MMP-2 expression, γ2 chain cleavage, and invasion [52]. In addition, ERK1/2 and Akt activation has been linked to both MT1-MMP activation and invasion downstream of RTK activation [96-98]. Interestingly, growth factors which are known to upregulate Mig-7 expression have been shown to activate both ERK1/2 and Akt in coordination with αv integrin activation [99-101]. S6 kinase activation downstream of HGF and both Erk1/2 and Akt signaling has also been shown to be involved in tumor cell migration [102]. Thus, upregulation of Mig-7 expression by these growth factors and αvβ5 integrin may indirectly cause MT1-MMP activation by aiding in coordinate activation of these

135

pathways.   These data may represent a potential link between the increased MT1-MMP activation and invasion exhibited by Mig-7-expressing cells.   Taken together, these data demonstrate that Mig-7 may play a role in tumor cell invasion, which could be due to increased MT1-MMP, ERK1/2, Akt, and S6 kinase activation.

4.2 Mig-7 and Vasculogenic Mimicry

Tumor growth and metastasis rely on invasion [103] and the support of an adequate blood supply [104,105]. Recent studies have uncovered a process, termed vasculogenic mimicry, in which tumor cells can form vessel-like structures both *in vitro* and *in vivo* that can serve as conduits for blood and nutrients [9]. This process has been well characterized in various cutaneous melanoma cell lines, which differ in their ability to form these structures. Formation of these vessel-like structures only occurs in aggressively invasive melanoma cells, linking the invasive phenotype with this process. In the current studies, five melanoma cell lines were analyzed for their expression of Mig-7 protein. The 23 kD Mig-7 protein is only detected in the aggressively invasive cell lines (MUM-2B, C918, C8161) capable of vasculogenic mimicry. The non-invasive cell lines (MUM-2C, A375P) lacked detectable Mig-7 protein.

Three-dimensional cell culture analysis with HT29 cells that overexpress FLAG-Mig-7 was performed to further analyze the involvement of Mig-7 in tumor cell invasion. These cells not only showed a more invasive phenotype compared to vector alone cells, but also formed long cord-like structures. Formation of these structures in 3-D culture has previously been seen with other cells capable of vessel formation [106,107]. Thus,

Mig-7 expression in non-expressing cells seems to allow these cells to invade and form vessel-like structures *in vitro*.

Further studies in the lab also demonstrated that Mig-7 protein localized primarily to vessel-like structures in lymph nodes from mice injected subcutaneously with RL95 and HEC1A endometrial carcinoma cells. These vessel-like structures also stained positive for laminin 5 γ2 chain DIII fragments, Factor VIII-associated antigen, and VE-Cadherin. The DIII fragments and VE-Cadherin are known to be involved in vasculogenic mimicry [67,69], and Factor VIII-associated antigen is a common endothelial marker that is involved in platelet, as well as tumor cell, adhesion to vessel walls [108,109]. This demonstration of Mig-7 colocalization to vessel-like structures implies a potential correlation between Mig-7 expression in aggressive carcinoma cells and the process of vasculogenic mimicry.

Interestingly, the frequency of Mig-7 staining around these structures correlated to level of invasiveness of these cells. RL95 cells are known to be less invasive than HEC1A cells [75], and mice injected with RL95 cells showed 4-fold fewer vessel-like structure "hot spots" in these lymph nodes, again highlighting the correlation between invasive capacity and vasculogenic mimicry. In addition, aggressive melanoma cells were able to form vessel-like structures in 3-D cultures of Collagen I, as previously demonstrated [9,64,71], but RL95 cells could not effectively recapitulate this phenotype (data not shown). Again, the possible explanation for this is the fact that RL95 cells have a much lower invasive capacity that does not allow vessel-like structure formation *in vitro*. It is also possible that RL95 cells have a larger requirement for laminins, rather than collagen I, in culture for their invasive behavior, such as is the case with HUVEC

137

cells [85]. Collectively, these data suggest that Mig-7 may play a role in the process of vasculogenic mimicry. However, further studies will need to be performed to further link Mig-7 to this process.

4.3 Mig-7 and primary tumor growth

In vivo results with RL95 Mig-7 siRNA-expressing cell lines demonstrated that Mig-7 knockdown by 30% in 4-2 expressing cells and 43% in 1-3 expressing cells compared to control 3-1 expressing cells appears to slow the initial primary tumor growth in nude mice by 40-50% and by 60%, respectively. This suggests that Mig-7 may play a role in facilitating tumor growth *in vivo*. One potential reason for the decreased tumor growth observed is that knockdown of Mig-7 in RL95 cells results in a decrease in vessel-like structure formation by these cells. Initially, before angiogenesis has been stimulated, the cells may rely on vasculogenic mimicry alone. Thus, the reduced capacity of Mig-7 knockdown cells for vasculogenic mimicry results in a concomitant decrease in the availability of blood and nutrients for the primary tumor, slowing its growth.

Additionally, other studies with inhibition of the E-cadherin repressor Snail1 by siRNA expression have demonstrated a potential link between local invasion of tumor cells and primary tumor growth [103]. In these studies, decreased Snail1 resulted in repression of the invasive phenotype and primary tumor growth.   Based on these data, it is possible that Mig-7 knockdown in RL95 cells expressing siRNA 1-3 decreases their local invasion, as seen *in vitro*, directly resulting in decreased primary tumor size. The

studies by Olmeda et al also demonstrated increased apoptosis and necrosis in primary tumors from Snail1 knockdown cells. Although our *in vitro* studies with RL95 siRNA-expressing cells showed no changes in apoptosis, perhaps the *in vivo* environment stimulates apoptosis to a greater extent in Mig-7 knockdown cells compared to control siRNA-expressing cells. Increased necrosis *in vivo* may also be an important factor, as this was not analyzed *in vitro*. More studies will need to be carried out on these tissues to determine the actual cause of the decreased primary tumor growth observed.   .

Interestingly, tumor growth is only slowed from the first day that tumors could be palpated to 18 days post-injection. Following this timepoint, growth of tumors from mice injected with cells containing lower Mig-7 levels seemed to overtake that of control siRNA-expressing cells with normal Mig-7 levels. Analysis of expression of Mig-7 protein in these tumors at 28 days post-injection showed that cells expressing siRNA 1-3 still maintained a similar level of Mig-7 reduction compared to 3-1-expressing cells *in vivo.* This demonstrates that decreased selection of the siRNA-expressing cells is not likely causing this effect. However, another explanation for this trend may be that the cells with normal Mig-7 levels may have reached a point at which they have begun to invade and metastasize out of the primary site. This increased metastasis of these cells would lead to a decrease in the apparent growth of the primary tumor. Thus, at the point which cells with reduced Mig-7 have begun to invade locally and increase growth, the control cells are invading away from the tumor and decreasing growth. Intriguingly, RL95 parental cells apparently lack the plateau phase of growth seen in control siRNA-expressing cells. Perhaps the parental cells are invading both locally and into the blood or lymphatics to the same extent, resulting in no noticeable slowing of tumor growth.

Alternatively, control siRNA cells may be located closer to blood or lymphatic vessels, which could result in increased intravasation. Another potential explanation is that the H1 RNA polymerase III promoter that drives siRNA expression may be depleting factors necessary for expression of other genes important for normal cell growth and functions.

Our studies to date have demonstrated a potential link between Mig-7 expression in a number of carcinoma cells, as well as melanoma cells, and invasion, as well as the process of vasculogenic mimicry. The specific studies with RL95 cells containing reduced levels of Mig-7 have demonstrated this potential link between its expression in these cells and their invasive capacity, as well as their ability to aid in primary tumor growth. Analysis of Mig-7 expression in melanoma cells further supports this link. Linking Mig-7 to invasion and vasculogenic mimicry would potentially allow better targeting of these processes to inhibit disease progression and improve patient outcome.

4.4 Future Directions

While the current studies have further supported a link between expression of novel Mig-7 in cancer cells and invasion and tumor progression, further studies still need to be done to better establish whether Mig-7 plays a role in vasculogenic mimicry in RL95 cells. Although Mig-7 expression has been linked to invasion and primary tumor growth in RL95 cells, more studies will need to be carried out to better establish the effect of altered Mig-7 expression in these cells on vessel-like structure formation *in vivo*. These studies would allow better demonstration of a direct link between Mig-7 expression and vasculogenic mimicry. Studies with altered Mig-7 expression in

melanoma cells would also serve as another system for analyzing Mig-7 effects on this process. Because non-invasive melanoma cells apparently lack Mig-7, overexpression of our FLAG-Mig-7 construct in these cells could be utilized, and the resulting effects on structure formation both *in vitro* and *in vivo* characterized. Similarly, the current Mig-7 siRNA constructs could be transfected into aggressive melanoma cells which express Mig-7 to decrease its expression and the resulting effects on vessel-like structure formation characterized. These cells would be much more informative as they have been previously well-characterized and show a marked difference in their phenotypes.

The current studies have also demonstrated increased activation of membrane type-1 MMP as a potential mechanism by which Mig-7 affects invasion and vasculogenic mimicry. More thorough studies will need to be carried out to begin to better characterize the exact mechanisms and downstream signaling involved in Mig-7 functional effects. Because ERK1/2 and Akt phosphorylation appears to be affected by Mig-7 expression, further analysis of the phosphorylation of these proteins and downstream signaling resulting from altered Mig-7 expression would further define these mechanisms.

References

1. A.F.Chambers, A.C.Groom, I.C.MacDonald (2002). Metastasis: Dissemination and growth of cancer cells in metastatic sites. *Nat Rev Cancer* **2**, 563-572.

2. L.A.Liotta, E.C.Kohn (2001). The microenvironment of the tumour-host interface. *Nature* **411**, 375-379.

3. H.Hugo, M.L.Acklund, T.Blick, M.G.Lawrence, J.A.Clements, E.D.Williams, E.W.Thompson (2007). Epithelial-mesenchymal and mesenchymal-epithelial transitions in carcinoma progression. *Journal of Cellular Physiology* **213**, 374-383.

4. J.P.Thiery (2002). Epithelial-mesenchymal transitions in tumour progression. *Nat Rev Cancer* **2**, 442-454.

5. C.Scheel, T.Onder, A.Karnoub, R.A.Weinberg, J.E.Talmadge (2007). Adaptation versus Selection: The Origins of Metastatic Behavior. *Cancer Res* **67**, 11476-11480.

6. J.E.Talmadge (2007). Clonal Selection of Metastasis within the Life History of a Tumor. *Cancer Res* **67**, 11471-11475.

7. F.Li, B.Tiede, J.Massague, Y.Kang (2007). Beyond tumorigenesis: cancer stem cells in metastasis. *Cell Res* **17**, 3-14.

8. D.C.Radisky, P.A.Kenny, M.J.Bissell (2007). Fibrosis and cancer: Do myofibroblasts come also from epithelial cells via EMT? *Journal of Cellular Biochemistry.* **101**, 830-839.

9. A.J.Maniotis, R.Folberg, A.Hess, E.A.Seftor, L.M.G.Gardner, J.Pe'er, J.M.Trent, P.S.Meltzer, M.J.C.Hendrix (1999). Vascular Channel Formation by Human Melanoma Cells in Vivo and in Vitro: Vasculogenic Mimicry. *Am J Pathol* **155**, 739-752.

10. W.Birchmeier, V.Brinkmann, C.Niemann, S.Meiners, S.DiCesare, H.Naundorf, M.Sachs (1997). Role of HGF/SF and c-Met in morphogenesis and metastasis of epithelial cells. *Ciba Foundation Symposium* **212**, 230-246.

11. S.Byers, M.Park, C.Sommers, S.Seslar (1994). Breast carcinoma: a collective disorder. *Breast Cancer Research & Treatment* **31**, 203-215.

12. C.C.Fehlner-Gardiner, H.Cao, L.Jackson-Boeters, T.Nakamura, B.E.Elliott, S.Uniyal, B.M.Chan (1999). Characterization of a functional relationship between hepatocyte growth factor and mouse bone marrow-derived mast cells. *Differentiation* **65**, 27-42.

13. A.S.T.Wong, P.C.K.Leung, N.Auersperg (2000). Hepatocyte growth factor promotes *in vitro* scattering and morphogenesis of human cervical carcinoma cells. *Gynecologic Oncology* **78**, 158-165.

14. S.Jodele, L.Blavier, J.Yoon, Y.DeClerck (2006). Modifying the soil to affect the seed: role of stromal-derived matrix metalloproteinases in cancer progression. *Cancer and Metastasis Reviews* **25**, 35-43.

15. F.G.Giancotti, E.Ruoslahti (1999). Integrin signaling. *Science* **285**, 1028-1032.

16. W.Guo, F.G.Giancotti (2004). Integrin signalling during tumour progression. *Nat Rev Mol Cell Biol* **5**, 816-826.

17. J.D.Hood, D.A.Cheresh (2002). Role of integrins in cell invasion and migration. *Nat Rev Cancer* **2**, 91-100.

18. P.E.Hughes, M.W.Renshaw, M.Pfaff, J.Forsyth, V.M.Keivens, M.A.Schwartz, M.H.Ginsberg (1997). Suppression of Integrin Activation: A Novel Function of a Ras/Raf-Initiated MAP Kinase Pathway. *Cell* **88**, 521-530.

19. L.A.Maile, Y.Imai, J.B.Clarke, D.R.Clemmons (2002). Insulin-like Growth Factor I Increases alpha Vbeta 3 Affinity by Increasing the Amount of Integrin-associated Protein That Is Associated with Non-raft Domains of the Cellular Membrane. *J.Biol.Chem.* **277**, 1800-1805.

20. P.R.Somanath, E.S.Kandel, N.Hay, T.V.Byzova (2007). Akt1 Signaling Regulates Integrin Activation, Matrix Recognition, and Fibronectin Assembly. *J.Biol.Chem.* **282**, 22964-22976.

21. Z.Zhang, K.Vuori, H.G.Wang, J.C.Reed, E.Ruoslahti (1996). Integrin Activation by R-ras. *Cell* **85**, 61-69.

22. M.A.Wozniak, K.Modzelewska, L.Kwong, P.J.Keely (2004). Focal adhesion regulation of cell behavior. *Biochimica et Biophysica Acta (BBA) - Molecular Cell Research* **1692**, 103-119.

23. C.ffrench-Constant, H.Colognato (2004). Integrins: versatile integrators of extracellular signals. *Trends in Cell Biology* **14**, 678-686.

24. J.Beard (1902). Embryological aspects and etiology of carcinoma. *The Lancet* **1**, 1758-1761.

25. R.Soundararajan, A.J.Rao (2004). Trophoblast 'pseudo-tumorigenesis': Significance and contributory factors. *Reproductive Biology and Endocrinology* **2**, 15.

26. K.Red-Horse, Y.Zhou, O.Genbacev, A.Prakobphol, R.Foulk, M.T.McMaster, S.J.Fisher (2004). Trophoblast differentiation during embryo implantation and

formation of the maternal-fetal interface. *Journal of Clinical Investigation* **114**, 744-754.

27. Y.Zhou, S.J.Fisher, M.Janatpour, O.Genbacev, E.Dejana, M.Wheelock, C.H.Damsky (1997). Human cytotrophoblasts adopt a vascular phenotype as they differentiate. *Journal of Clinical Investigation* **99**, 2139-2151.

28. E.Hintermann, V.Quaranta (2004). Epithelial cell motility on laminin-5: regulation by matrix assembly, proteolysis, integrins and erbB receptors. *Matrix Biology* **23**, 75-85.

29. W.Hornebeck, F.X.Maquart (2003). Proteolyzed matrix as a template for the regulation of tumor progression. *Biomedecine & Pharmacotherapy* **57**, 223-230.

30. E.Pirila, A.Sharabi, T.Salo, V.Quaranta, H.Tu, R.Heljasvaara, N.Koshikawa, T.Sorsa, P.Maisi (2003). Matrix metalloproteinases process the laminin-5 [gamma]2-chain and regulate epithelial cell migration. *Biochemical and Biophysical Research Communications* **303**, 1012-1017.

31. J.Xu, D.Rodriguez, E.Petitclerc, J.J.Kim, M.Hangai, S.M.Yuen, G.E.Davis, P.C.Brooks (2001). Proteolytic exposure of a cryptic site within collagen type IV is required for angiogenesis and tumor growth in vivo. *J.Cell Biol.* **154**, 1069-1080.

32. M.Egeblad, Z.Werb (2002). New functions for the matrix metalloproteinases in cancer progression. *Nat Rev Cancer* **2**, 161-174.

33. M.D.Sternlicht, Z.Werb (2001). How matrix metalloproteinases regulate cell behavior. *Annual Review of Cell and Developmental Biology* **17**, 463-516.

34. E.B.Springman, E.L.Angleton, H.Birkedal-Hansen, H.E.V.Wart (1990). Multiple Modes of Activation of Latent Human Fibroblast Collagenase: Evidence for the Role of a Cys73 Active-Site Zinc Complex in Latency and a "Cysteine Switch" Mechanism for Activation. *PNAS* **87**, 364-368.

35. G.P.Stricklin, J.J.Jeffrey, W.T.Roswit, A.Z.Eisen (1983). Human skin fibroblast procollagenase: mechanisms of activation by organomercurials and trypsin. *Biochemistry* **22**, 61-68.

36. H.Birkedal-Hansen, R.E.Taylor (1982). Detergent-activation of latent collagenase and resolution of its component molecules. *Biochemical and Biophysical Research Communications* **107**, 1173-1178.

37. S.J.Weiss, G.Peppin, X.Ortiz, C.Ragsdale, S.T.Test (1985). Oxidative autoactivation of latent collagenase by human neutrophils. *Science* **227**, 747-749.

38. H.W.Macartney, H.Ischesche (1983). The Collagenase Inhibitor from Human Polymorphonuclear Leukocytes. *European Journal of Biochemistry* **130**, 79-83.

39. G.Murphy, U.Bretz, M.Baggiolini, J.J.Reynolds (1980). The latent collagenase and gelatinase of human polymorphonuclear neutrophil leucocytes. *Biochem.J.* **192**, 517-525.

40. A.Bescond, T.Augier, C.Chareyre, D.Garcon, W.Hornebeck, P.Charpiot (1999). Influence of Homocysteine on Matrix Metalloproteinase-2: Activation and Activity. *Biochemical and Biophysical Research Communications* **263**, 498-503.

41. Q.Yu, I.Stamenkovic (2000). Cell surface-localized matrix metalloproteinase-9 proteolytically activates TGF-beta and promotes tumor invasion and angiogenesis. *Genes Dev.* **14**, 163-176.

42. G.Davies, W.G.Jiang, M.D.Mason (2001). Matrilysin mediates extracellular cleavage of E-cadherin from prostate cancer cells: a key mechanism in hepatocyte growth factor/scatter factor-induced cell-cell dissociation and *in vitro* invasion. *Clin Cancer Res* **7**, 3289-3297.

43. T.Maretzky, K.Reiss, A.Ludwig, J.Buchholz, F.Scholz, E.Proksch, B.de Strooper, D.Hartmann, P.Saftig (2005). ADAM10 mediates E-cadherin shedding and regulates epithelial cell-cell adhesion, migration, and {beta}-catenin translocation. *PNAS* **102**, 9182-9187.

44. J.M.Mei, G.L.Borchert, S.P.Donald, J.M.Phang (2002). Matrix metalloproteinase(s) mediate(s) NO-induced dissociation of {beta}-catenin from membrane bound E-cadherin and formation of nuclear {beta}-catenin/LEF-1 complex. *Carcinogenesis* **23**, 2119-2122.

45. F.Fukai, M.Ohtaki, N.Fujii, H.Yajima, T.Ishii, K.Miyazaki, T.Katayama (1995). Release of Biological Activities from Quiescent Fibronectin by a Conformational Change and Limited Proteolysis by Matrix Metalloproteinases. *Biochemistry* **34**, 11453-11459.

46. G.S.Butler, M.J.Butler, S.J.Atkinson, H.Will, T.Tamura, S.S.van Westrum, T.Crabbe, J.Clements, M.P.d'Ortho, G.Murphy (1998). The TIMP2 Membrane Type 1áMetalloproteinase "Receptor" Regulates the Concentration and Efficient Activation of Progelatinase A. A KINETIC STUDY. *J.Biol.Chem.* **273**, 871-880.

47. T.Kinoshita, H.Sato, A.Okada, E.Ohuchi, K.Imai, Y.Okada, M.Seiki (1998). TIMP-2 Promotes Activation of Progelatinase A by Membrane-type 1áMatrix Metalloproteinase Immobilized on Agarose Beads. *J.Biol.Chem.* **273**, 16098-16103.

48. M.A.Lafleur, A.M.Tester, E.W.Thompson (2003). Selective involvement of TIMP-2 in the second activational cleavage of pro-MMP-2: refinement of the pro-MMP-2 activation mechanism. *FEBS Letters* **553**, 457-463.

49. G.Giannelli, J.Falk-Marzillier, O.Schiraldi, W.G.Stetler-Stevenson, V.Quaranta (1997). Induction of Cell Migration by Matrix Metalloprotease-2 Cleavage of Laminin-5. *Science* **277**, 225-228.

50. N.Koshikawa, G.Giannelli, V.Cirulli, K.Miyazaki, V.Quaranta (2000). Role of Cell Surface Metalloprotease MT1-MMP in Epithelial Cell Migration over Laminin-5. *J.Cell Biol.* **148**, 615-624.

51. N.Koshikawa, T.Minegishi, A.Sharabi, V.Quaranta, M.Seiki (2005). Membrane-type Matrix Metalloproteinase-1 (MT1-MMP) is a processing enzyme for human laminin {gamma}2 chain. *J.Biol.Chem.* **280**, 88-93.

52. S.Schenk, E.Hintermann, M.Bilban, N.Koshikawa, C.Hojilla, R.Khokha, V.Quaranta (2003). Binding to EGF receptor of a laminin-5 EGF-like fragment liberated during MMP-dependent mammary gland involution. *J.Cell Biol.* **161**, 197-209.

53. N.Ferrara (2000). Vascular endothelial growth factor and the regulation of angiogenesis. *Recent Progress in Hormone Research* **55**, 15-36.

54. M.Grano, F.Galimi, G.Zambonin, S.Colucci, E.Cottone, A.Z.Zallone, P.M.Comoglio (1996). Hepatocyte growth factor is a coupling factor for osteoclasts and osteoblasts in vitro. *Proceedings of the National Academy of Science* **93**, 7644-7648.

55. R.van der Voort, R.M.J.Keehnen, L.Smit, M.Groenink, S.T.Pals (1997). Paracrine regulation of germinal center B cell adhesion through the c-Met-Hepatocyte growth factor/scatter factor pathway. *Journal of Experimental Medicine* **185**, 2121-2131.

56. L.Watanabe, M.Hirose, X.E.Wang, O.Kobayashi, A.Nagahara, T.Murai, R.Iwazaki, H.Miwa, A.Miyazaki, N.Sato (2000). Epithelial-mesenchymal interaction in gastric mucosal restoration. *Journal of Gastroenterology* **35**, 65-68.

57. R.Folberg, M.J.C.Hendrix, A.J.Maniotis (2000). Vasculogenic mimicry and tumor angiogenesis. *Am J Pathol* **156**, 361-381.

58. A.K.Sood, E.A.Seftor, M.S.Fletcher, L.M.G.Gardner, P.M.Heidger, R.E.Buller, R.E.B.Seftor, M.J.C.Hendrix (2001). Molecular determinants of ovarian cancer plasticity. *Am J Pathol* **158**, 1279-1288.

59. B.Sun, S.Zhang, D.Zhang, J.Du, H.Guo, X.Zhao, W.Zhang, X.Hao (2006). Vasculogenic mimicry is associated with high tumor grade, invasion and metastasis, and short survival in patients with hepatocellular carcinoma. *Oncology Reports* **16**, 693-698.

60. D.W.J.van der Schaft, F.Hillen, P.Pauwels, D.A.Kirschmann, K.Castermans, M.G.A.oude Egbrink, M.G.B.Tran, R.Sciot, E.Hauben, P.C.W.Hogendoorn,

O.Delattre, P.H.Maxwell, M.J.C.Hendrix, A.W.Griffioen (2005). Tumor cell plasticity in Ewing sarcoma, an alternative circulatory system stimulated by hypoxia. *Cancer Res* **65**, 11520-11528.

61. M.J.C.Hendrix, E.A.Seftor, D.A.Kirschmann, V.Quaranta, R.E.B.Seftor (2003). Remodeling of the microenvironment by aggressive melanoma tumor cells. *Ann NY Acad Sci* **995**, 151-161.

62. D.W.J.van der Schaft, R.E.B.Seftor, E.A.Seftor, A.R.Hess, L.M.Gruman, D.A.Kirschmann, Y.Yokoyama, A.W.Griffioen, M.J.C.Hendrix (2004). Effects of angiogenesis inhibitors on vascular network formation by human endothelial and melanoma cells. *J Natl Cancer Inst* **96**, 1473-1477.

63. J.Condeelis, R.H.Singer, J.E.Segall (2005). The great escape: When cancer cells hijack the genes for chemotaxis and motility. *Annual Review of Cell and Developmental Biology* **21**, 695-718.

64. E.A.Seftor, P.S.Meltzer, D.A.Kirschmann, N.V.Margaryan, R.E.B.Seftor, M.J.C.Hendrix (2006). The epigenetic reprogramming of poorly aggressive melanoma cells by a metastatic microenvironment. *Journal of Cellular and Molecular Medicine* **10**, 174-196.

65. E.Seftor, P.Meltzer, D.Kirschmann, J.Pe'er, A.Maniotis, J.Trent, R.Folberg, M.Hendrix (2002). Molecular determinants of human uveal melanoma invasion and metastasis. *Clinical and Experimental Metastasis* **19**, 233-246.

66. H.Hashizume, P.Baluk, S.Morikawa, J.W.McLean, G.Thurston, S.Roberge, R.K.Jain, D.M.McDonald (2000). Openings between defective endothelial cells explain tumor vessel leakiness. *Am J Pathol* **156**, 1363-1380.

67. R.E.B.Seftor, E.A.Seftor, N.Koshikawa, P.S.Meltzer, L.M.G.Gardner, M.Bilban, W.G.Stetler-Stevenson, V.Quaranta, M.J.C.Hendrix (2001). Cooperative interactions of Laminin 5 γ2 Chain, Matrix Metalloproteinase-2, and Membrane Type-1 Matrix/Metalloproteinase are required for mimicry of embryonic vasculogenesis by aggressive melanoma. *Cancer Res* **61**, 6322-6327.

68. A.R.Hess, E.A.Seftor, L.M.G.Gardner, K.Carles-Kinch, G.B.Schneider, R.E.B.Seftor, M.S.Kinch, M.J.C.Hendrix (2001). Molecular regulation of tumor cell vasculogenic mimicry by tyrosine phosphorylation: Role of epithelial cell kinase (Eck/EphA2). *Cancer Res* **61**, 3250-3255.

69. M.J.C.Hendrix, E.A.Seftor, P.S.Meltzer, L.M.G.Gardner, A.R.Hess, D.A.Kirschmann, G.C.Schatteman, R.E.B.Seftor (2001). Expression and functional significance of VE-cadherin in aggressive human melanoma cells: Role in vasculogenic mimicry. *PNAS* **98**, 8018-8023.

70. A.R.Hess, E.A.Seftor, L.M.Gruman, M.S.Kinch, R.E.B.Seftor, M.J.C.Hendrix. VE-Cadherin Regulates EphA2 in Melanoma Cells Through a Novel Signaling

Mechanism: Implications for Vasculogenic Mimicry (2006). *Cancer Biology and Therapy* **5**, 228-233.

71. A.R.Hess, L.-M.Postovit, N.V.Margaryan, E.A.Seftor, G.B.Schneider, R.E.B.Seftor, B.J.Nickoloff, M.J.C.Hendrix (2005). Focal Adhesion Kinase promotes the aggressive melanoma phenotype. *Cancer Res* **65**, 9851-9860.

72. A.R.Hess, E.A.Seftor, R.E.B.Seftor, M.J.C.Hendrix (2003). Phosphoinositide 3-kinase regulates membrane type 1-Matrix Metalloproteinase (MMP) and MMP-2 activity during melanoma cell vasculogenic mimicry. *Cancer Res* **63**, 4757-4762.

73. V.Givant-Horwitz, B.Davidson, R.Reich (2005). Laminin-induced signaling in tumor cells. *Cancer Letters* **223**, 1-10.

74. R.Katso, K.Okkenhaug, K.Ahmadi, S.White, J.Timms, M.D.Waterfield (2001). Cellular function of phosphoinositide 3-kinases: Implications for development, immunity, homeostasis, and cancer. *Annual Review of Cell and Developmental Biology* **17**, 615-675.

75. V.Bae-Jump, E.M.Segreti, D.Vandermolen, S.Kauma (1999). Hepatocyte growth factor (HGF) induces invasion of endometrial carcinoma cell lines in vitro. *Gynecologic Oncology* **73**, 265-272.

76. W.G.Jiang, S.Hiscox (1997). Hepatocyte growth factor/scatter factor, a cytokine playing multiple and converse roles. *Histology & Histopathology* **12**, 537-555.

77. G.F.Vande Woude, M.Jeffers, J.Cortner, G.Alvord, I.Tsarfaty, J.Resau (1997). Met-HGF/SF: tumorigenesis, invasion and metastasis. *Ciba Foundation Symposium* **212**, 119-130.

78. L.Beviglia, R.H.Kramer (1999). HGF induces FAK activation and integrin-mediated adhesion in MTLn3 breast carcinoma cells. *International Journal of Cancer* **83**, 640-649.

79. L.Trusolino, S.Cavassa, P.Angelini, M.Ando, A.Bertotti, P.M.Comoglio, C.Boccaccio (2000). HGF/scatter factor selectively promotes cell invasion by increasing integrin avidity. *FASEB Journal* **14**, 1629-1640.

80. S.Crouch, C.S.Spidel, J.S.Lindsey (2004). HGF and ligation of $\alpha v \beta 5$ integrin induce a novel, cancer cell-specific gene expression required for cell scattering. *Experimental Cell Research* **292**, 274-287.

81. A.P.Petty, K.L.Garman, V.D.Winn, C.M.Spidel, J.S.Lindsey (2007). Overexpression of carcinoma and embryonic cytotrophoblast cell-specific Mig-7 induces invasion and vessel-like structure formation. *Am J Pathol* **170**, 1763-1780.

82. T.M.Phillips, J.S.Lindsey (2005). Carcinoma cell-specific Mig-7: A new potential marker for circulating and migrating cancer cells. *Oncology Reports* **13**, 37-44.

83. A.P.Petty, S.E.Wright, K.A.Rewers-Felkins, M.A.Yenderrozos, B.A.Vorderstrasse, J.S.Lindsey (2008). Targeting Mig-7 inhibits carcinoma cell invasion, primary tumor growth, and stimulates killing of breast carcinoma cells. *Molecular Cancer Therapeutics* Submitted.

84. S.J.Fisher, T.Y.Cui, L.Zhang, L.Hartman, K.Grahl, G.Y.Zhang, J.Tarpey, C.H.Damsky (1989). Adhesive and degradative properties of human placental cytotrophoblast cells in vitro. *J.Cell Biol.* **109**, 891-902.

85. Y.Kubota, H.K.Kleinman, G.R.Martin, T.J.Lawley (1988). Role of laminin and basement membrane in the morphological differentiation of human endothelial cells into capillary-like structures. *J.Cell Biol.* **107**, 1589-1598.

86. C.Pyke, J.Romer, P.Kallunki, L.R.Lund, F.Ralfkiaer, K.Dano, K.Tryggvason (1994). The gamma 2 chain of kalinin/laminin 5 is preferentially expressed in invading malignant cells in human cancers. *The American Journal of Pathology* **145**, 782-791.

87. E.Cukierman, R.Pankov, D.R.Stevens, K.M.Yamada (2001). Taking cell-matrix adhesions to the third dimension. *Science* **294**, 1708-1712.

88. J.Debnath, J.S.Brugge (2005). Modeling glandular epithelial cancers in three-dimensional cultures. *Nat Rev Cancer* **5**, 675-688.

89. D.E.Discher, P.Janmey, Y.-L.Wang (2005). Tissue cells feel and respond to the stiffness of their substrate. *Science* **310**, 1139-1143.

90. J.Walker-Daniels, A.R.Hess, M.J.C.Hendrix, M.S.Kinch (2003). Differential regulation of EphA2 in normal and malignant cells. *Am J Pathol* **162**, 1037-1042.

91. V.M.Weaver, A.H.Fischer, O.W.Peterson, M.J.Bissell (1996). The importance of the microenvironment in breast cancer progression: recapitulation of mammary tumorigenesis using a unique human mammary epithelial cell model and a three-dimensional culture assay. *Biochemistry and Cell Biology* **74**, 833-851.

92. A.Albini, R.Benelli, D.M.Noonan, C.Brigati (2004). The "chemoinvasion assay": a tool to study tumor and endothelial cell invasion of basement membranes. *International Journal of Developmental Biology* **48**, 563-571.

93. H.E.V.Wart, H.Birkedal-Hansen (1990). The Cysteine Switch: A Principle of Regulation of Metalloproteinase Activity with Potential Applicability to the Entire Matrix Metalloproteinase Gene Family. *PNAS* **87**, 5578-5582.

94. P.C.Brooks, R.L.Klemke, S.Schon, J.M.Lewis, M.A.Schwartz, D.A.Cheresh (1997). Insulin-like growth factor receptor cooperates with integrin alpha v beta 5 to promote tumor cell dissemination in vivo. *Journal of Clinical Investigation* **99**, 1390-1398.

95. S.V.Madhunapantula, A.Sharma, G.P.Robertson (2007). PRAS40 Deregulates Apoptosis in Malignant Melanoma. *Cancer Res* **67**, 3626-3636.

96. K.Lehti, E.Allen, H.Birkedal-Hansen, K.Holmbeck, Y.Miyake, T.H.Chun, S.J.Weiss (2005). An MT1-MMP-PDGF receptor-{beta} axis regulates mural cell investment of the microvasculature. *Genes Dev.* **19**, 979-991.

97. M.Tsubaki, H.Matsuoka, C.Yamamoto, C.Kato, M.Ogaki, T.Satou, T.Itoh, T.Kusunoki, Y.Tanimori, S.Nishida (2007). The protein kinase C inhibitor, H7, inhibits tumor cell invasion and metastasis in mouse melanoma via suppression of ERK1/2. *Clinical and Experimental Metastasis* **24**, 431-438.

98. H.Y.Zhou, Y.L.Pon, A.S.T.Wong (2007). Synergistic Effects of Epidermal Growth Factor and Hepatocyte Growth Factor on Human Ovarian Cancer Cell Invasion and Migration: Role of Extracellular Signal-Regulated Kinase 1/2 and p38 Mitogen-Activated Protein Kinase. *Endocrinology* **148**, 5195-5208.

99. B.G.Hollier, J.A.Kricker, D.R.Van Lonkhuyzen, D.I.Leavesley, Z.Upton (2008). Substrate-Bound Insulin-Like Growth Factor (IGF)-I-IGF Binding Protein-Vitronectin-Stimulated Breast Cell Migration Is Enhanced by Coactivation of the Phosphatidylinositide 3-Kinase/AKT Pathway by {alpha}v-Integrins and the IGF-I Receptor. *Endocrinology* **149**, 1075-1090.

100. M.Matsuo, H.Sakurai, Y.Ueno, O.Ohtani, I.Saiki (2006). Activation of MEK/ERK and PI3K/Akt pathways by fibronectin requires integrin alphav-mediated ADAM activity in hepatocellular carcinoma: A novel functional target for gefitinib. *Cancer Science* **97**, 155-162.

101. M.R.Shen, Y.M.Hsu, K.F.Hsu, Y.F.Chen, M.J.Tang, C.Y.Chou (2006). Insulin-like growth factor 1 is a potent stimulator of cervical cancer cell invasiveness and proliferation that is modulated by {alpha}v{beta}3 integrin signaling. *Carcinogenesis* **27**, 962-971.

102. A.S.T.Wong, C.D.Roskelley, S.Pelech, D.Miller, P.C.K.Leung, N.Auersperg (2004). Progressive changes in Met-dependent signaling in a human ovarian surface epithelial model of malignant transformation. *Experimental Cell Research* **299**, 248-256.

103. D.Olmeda, G.Moreno-Bueno, J.M.Flores, A.Fabra, F.Portillo, A.Cano (2007). SNAI1 Is Required for Tumor Growth and Lymph Node Metastasis of Human Breast Carcinoma MDA-MB-231 Cells. *Cancer Res* **67**, 11721-11731.

104. P.Carmeliet, R.K.Jain (2000). Angiogenesis in cancer and other diseases. *Nature* **407**, 249-257.

105. J.Folkman (1971). Tumor angiogenesis: Therapeutic implications. *New England Journal of Medicine* **285**, 1182-1186.

106. R.Folberg, Z.Arbieva, J.Moses, A.Hayee, T.Sandal, S.Kadkol, A.Y.Lin, K.Valyi-Nagy, S.Setty, L.Leach, P.Chevez-Barrios, P.Larsen, D.Majumdar, J.Pe'er, A.J.Maniotis (2006). Tumor cell plasticity in uveal melanoma: Microenvironment directed dampening of the invasive and metastatic genotype and phenotype accompanies the generation of vasculogenic mimicry patterns. *Am J Pathol* **169**, 1376-1389.

107. I.N.M.A.Segura, A.N.T.O.Serrano, G.G.De Buitrago, M.A.Gonzalez, J.L.Abad, C.R.I.S.Claveria, L.U.C.I.Gomez, A.N.T.O.Bernad, A.Martinez, H.H.Riese (2002). Inhibition of programmed cell death impairs in vitro vascular-like structure formation and reduces in vivo angiogenesis. *FASEB J.* **16**, 833-841.

108. M.Morganti, A.Carpi, B.mo-Takyi, A.Sagripanti, A.Nicolini, R.Giardino, C.Mittermayer (2000). Von Willebrand's factor mediates the adherence of human tumoral cells to human endothelial cells and ticlopidine interferes with this effect. *Biomedecine & Pharmacotherapy* **54**, 431-436.

109. Z.M.Ruggeri. Von Willebrand Factor: Looking back and looking forward (2007). *Thrombosis and Haemostasis* **98**, 55-62.